



GLO2328

OXBOW GEOTHERMAL

December 29, 1987

Mr. Gudmundur Bodvarsson  
Earth Science Division  
Lawrence Berkeley Lab. #1  
Cyclotron Road Bldg. 50 E  
University of Calif.  
Berkeley, Calif. 94720

Dear Bo:

Please find enclosed one copy of the step-rate injection testing reports for Dixie Valley wells 45-5, 65-18, 32-18, and 52-18. I have also included an Executive Summary of these test results. The last item enclosed is a copy of all of the geochemistry tables from the six-well test report. All pages have been stamped confidential.

Sincerely,

Dick Benoit  
Dick Benoit

Joel

These data should be circulated among INEL, LLNL and Stanford and then returned to me! Please note that at present the only INEL and LLNL have reached agreement with Oxbow regarding a confidentiality agreement. Please do not forward the data to Stanford until they have also signed one. Same goes for LLNL

Thank Bo

P.S. Rodi ~~usht~~ should know what they need, and make sure to keep the package complete!



O X B O W G E O T H E R M A L

October 30, 1987

Mr. Gudmundur Bodvarsson  
Staff Scientist  
Earth Sciences Division  
Bldg. 90 Room 1092  
Lawrence Berkeley Laboratory  
University of California  
Berkeley, Calif. 94720

Dear Bo:

Please find enclosed the following confidential information for background information for the proposed tracer testing program at Dixie Valley.

1. Pages 10 through 131 of the 1986 Dixie Valley Reservoir Assessment Report -- This should provide adequate background data on the geology, hydrology, individual wells, chemistry, and some reservoir parameters. Material not included from the Reservoir Assessment deals primarily with interpretation as to size and longevity of the reservoir. Of course you already have the complete numerical modeling parameters from this report.

2. Summaries of the productive fracture locations on wells SWL-1, 27-33, and 45-33. These 3 are summaries because there are little or no electrical logs available to precisely locate the fractures.

Reports from wells 52-18, 65-18, 32-18, 76-7, 74-7, and 84-7 are included. These reports contain some logs which are in short supply and I would appreciate it if these are returned when you are finished with them. These reports and summaries cover 8 of the 10 production and injection wells. Reports on 73-7 and 45-5 have not yet been written. I hope to get these done in November.

3. Chemical analyses from well 45-5 in the summer of 1987 and a brief summary on the flow test, sampling and logging. These samples appear to be reliable.

Next week I will try to get additional information from well 45-5 and the six-well test report to you.

Sincerely,

*Dick Benoit*

Dick Benoit

STRICTLY

Log of Data Received from Oxbow

Benoit letter to Bodvarsson dated Oct. 30, 1987

✓ Benoit letter to Bodvarsson dated Dec. 29, 1987

✓ Reservoir assessment report (pages 10 - 131, no chapter 8 or appendices)

✓ Summaries of productive fracture locations  
wells Lamb-1 (1 p.), 27-33 (2 p.), and 45-33 (1p.)

Drillhole data in blue folders

Well 52-18

Benoit logging results June 13, 1986

Borehole compensated sonic log

Induction log

compensated neutron-formation density

Baroid drilling log

Pruett spinner survey

NO  
3-28

Well 65-18

Benoit logging results June 2, 1986

Spinner log

2" sonic

5" sonic

NO  
3-28

Well 32-18

Production logging results (electric logging)

spinner flolog

2" sonic

5" density (with gamma and caliper)

BHC Acoustilog / gamma ray

Differential temperature log

Drilling log

NO  
3-28

Well 76-7

Benoit production logging May 27, 1986

2" sonic gamma

5" sonic

spinner log

temperature log

drilling log

drilling log RD #1

NO  
3-28

Well 74-7

Benoit production logging report May 28, 1986

2" sonic

spinner log

5" sonic

drilling log

NO  
3-28

Well 84-7

Benoit production logging April 25, 1986

Compensated formation density log

compensated neutron-formation density

caliper log

differential temperature log (12-28-85)

spinner log

spinner (without log heading)

differential temperature (1-8-80)

3-28

- ✓ Chemical analysis from summer of 1987, well 45-5
- ✓ Summary flow test, sampling and logging for well 45-5
- Step-rate injection testing reports  
for wells 45-5, 65-18, 32-18, and 52-18
- ✓ Executive summary of 1987 step rate injection testing
- ✓ Geochemical tables from 6-well test report

## 2. INTRODUCTION

### 2.1 Project Description.

Oxbow Geothermal Corporation is developing a 50 megawatt (MW) net geothermal electrical generating facility in Dixie Valley, Nevada. The Dixie Valley geothermal field and power plant site are located along the northwest margin of Dixie Valley at the foot of the Stillwater Range, in northeastern Churchill County. The Dixie Valley project site lies 110 miles northeast of Reno and is reached from U. S. Highway 50 via 60 miles of paved and graded road (Fig. 2.1).

The electricity generated by the Dixie Valley geothermal project will be sold to Southern California Edison (SCE) at the SCE substation in Bishop, California (Fig. 2.1). Electricity from the project will be wheeled by a 230 kilovolt (kV) radial transmission line extending a distance of 217 miles from the project site to the SCE substation. The project is scheduled to go on-line in early 1988 at a total cost, including field development, power plant construction, and transmission line construction of \$165 million. A detailed description of the economics, budget, organization, and schedule of the Dixie Valley project is presented in the Oxbow project prospectus entitled "Dixie Valley Development" (March, 1986).

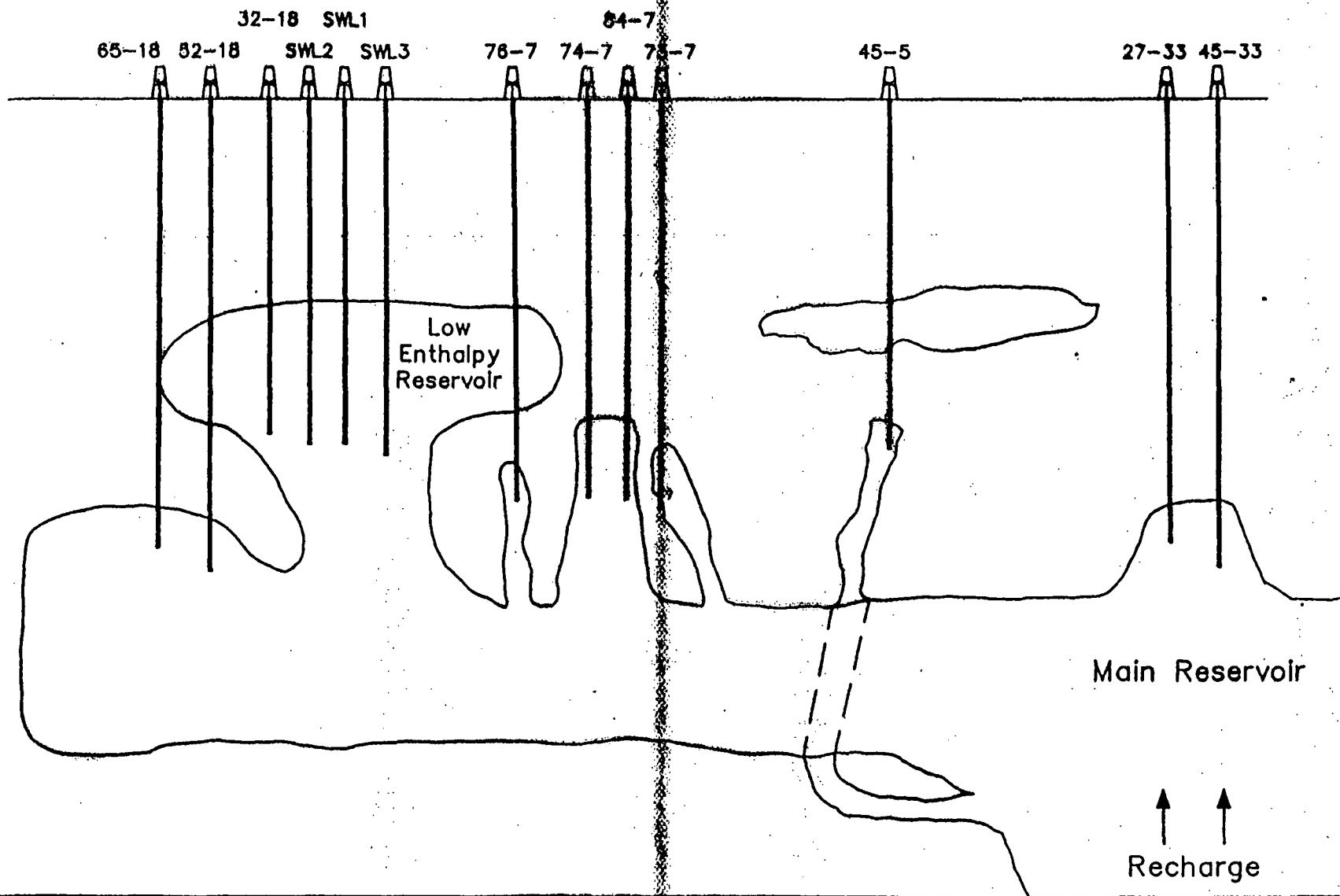
To date 16 wells have been drilled within or near the Dixie Valley geothermal reservoir ranging in depth from 7500 feet to over 12,500 feet. Two other wells, 45-14 and 66-21, are located to the southwest of the area shown on Figure 2.2. The producing wells are divided geographically into three clusters (Fig. 2.2) which are distributed along a northeast trend parallel to the strike of the Stillwater range-front fault. The southwestern cluster is referred to as the Section 18 wells, the central cluster as the Section 7 wells and the northeastern cluster as the Section 33 wells. This nomenclature is used throughout this document. The wells have encountered a liquid-dominated reservoir below a depth of 7000 feet and extending to depths below 10273 feet which is the deepest production encountered in the field to date. The downhole flowing temperatures in the field range from 400 deg.F to 480 deg.F with the Section 7 and Section 33 wells producing a higher temperature fluid than the Section 18 wells.

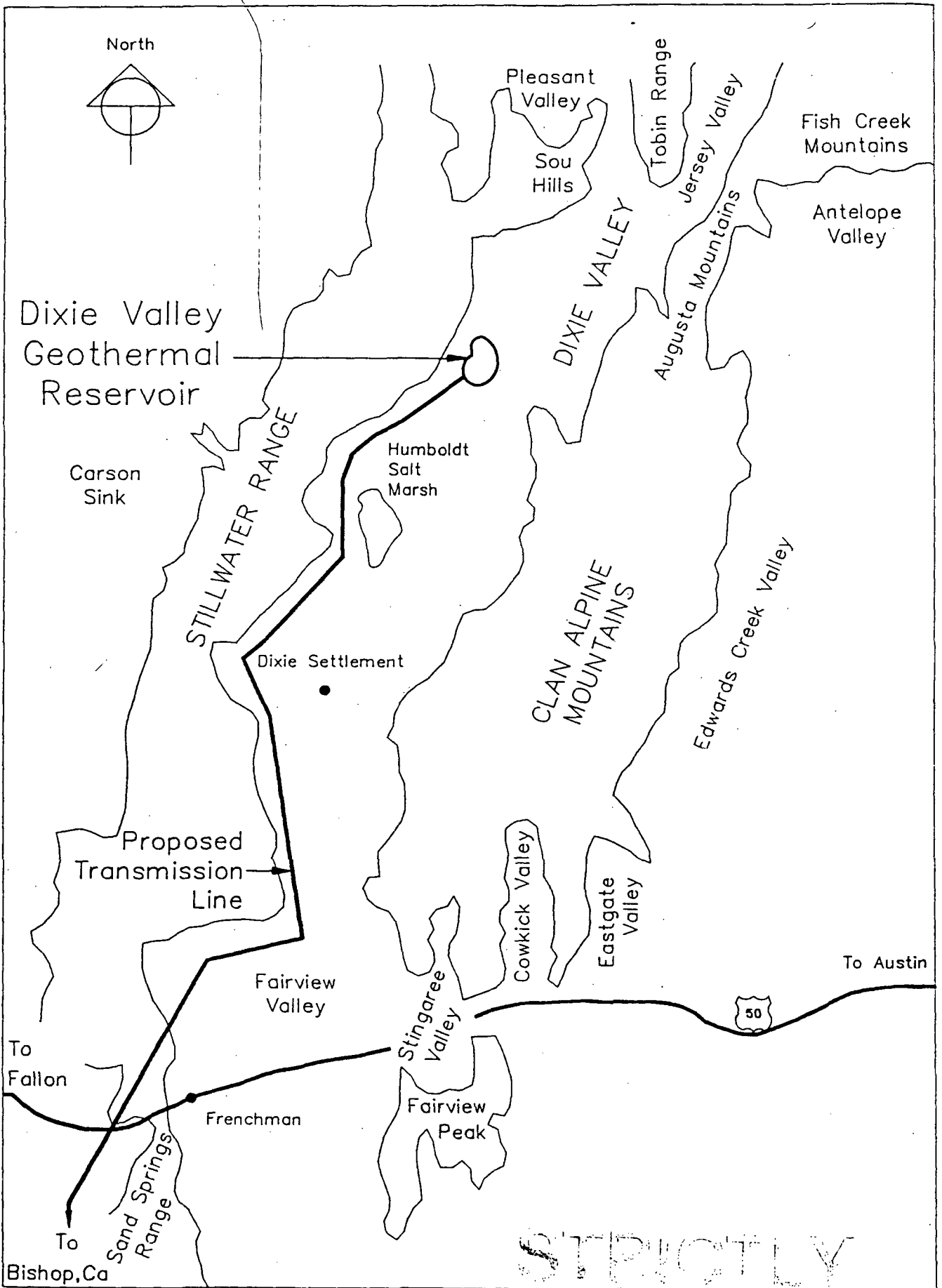
The wells are generally prolific producers with production rates varying from 300,000 to 1.7 million lbs/hr. The most prolific wells have mass flow rates equivalent to an electric power output of over 20 MWe each. The initial flow capability

STRICTLY

CONFIDENTIAL

# Schematic Reservoir Model





OXBOW

STRICTLY

Figure 2.1

of all existing wells at a wellhead pressure of 100 psig is approximately 7.5 million lbs/hr. This total flow rate is sufficient to produce 100 MWe using a dual flash power cycle.

## 2.2 Purpose of the Reservoir Assessment.

The purpose of this reservoir assessment is to provide a prediction of reservoir and individual well behavior over the 30-year life of the proposed 50 MW net power plant based on the best geologic and reservoir engineering data available. The 50 MW net power plant will require a continuous geothermal fluid mass flow of approximately 4.3 million lbs/hour. Sound management, design, and financing decisions for the project are dependent on an accurate assessment of the capacity of the geothermal reservoir to supply the required mass flow at sufficient pressure and temperature for power plant operation over the life of the project. This document presents a quantitative assessment of the productive capability of the Dixie Valley geothermal reservoir. The primary results of the assessment are:

1. To prepare a comprehensive geological, geochemical, and hydrological model of the Dixie Valley geothermal reservoir and surrounding area.
2. To determine the existing and future production characteristics of the individual wells.
3. To determine the probable pressure and temperature depletion characteristics of the Dixie Valley geothermal reservoir for the first 50 MW net power plant.
4. To determine the effect of reinjection on reservoir behavior and to determine which among the various reinjection options will provide optimum pressure support.
5. To provide a preliminary estimate of the rate of infill drilling required to maintain full plant capacity during the thirty year life of the first 50 MW plant.
6. To provide an assessment of silica and calcium carbonate scaling potential in production and reinjection wells and in surface equipment.
7. To provide an assessment of risk of damage to production and injection wells due to seismic activity.



8. To outline possible reinjection strategies that will lead to full reinjection in a period of less than three years from power plant startup.

### 2.3 Scope of the Reservoir Assessment.

The Dixie Valley geothermal reservoir as discussed in this document is defined by the region contained within the 4 deg.F/100' thermal gradient anomaly (Fig. 2.2). Deep production drilling within this region has confirmed that the near-surface thermal anomaly correlates closely with an active hydrothermal system with temperatures exceeding 400 deg.F as shallow as 5,700 feet.

A large body of geotechnical data relating to the Dixie Valley Field has been accumulated by Oxbow and by developers preceding Oxbow, primarily SUNEDCO and Trans-Pacific Geothermal Inc. (TGI). The Oxbow geologic staff assimilated this large data set into a comprehensive geologic model of the geothermal reservoir. The geologic model was then converted into a computerized numerical reservoir model by assigning observed hydrologic characteristics of the reservoir derived from extensive well and interference testing to the various lithologic and structural entities which make up the reservoir.

A detailed description of the work plan used to synthesize the geotechnical data base into the conceptual reservoir model is given in Appendix A: "Scope of Work, Dixie Valley Geothermal Reservoir Model".

The following geotechnical data sets were used to create the conceptual reservoir model:

1. Subsurface Geology: All lithologic and structural data available from production drilling, surface mapping, and seismic reflection profiles were integrated into a geologic model of the reservoir. Well logs and drilling logs were used to identify production zones, dips, and formation changes.
2. Static Pressure and Temperature: Static pressure and temperature profiles were obtained for all available deep wells in the area to establish the natural thermal and hydrologic state of the reservoir and surrounding area.
3. Brine Chemistry and Hydrology: Fluid chemistry from production wells, hot springs, perennial streams, and

shallow aquifers was examined to determine reservoir recharge zones, mixing zones, and discharge zones. Flow patterns within the reservoir were established by matching natural state hydrologic data with fluid chemistry patterns. Isotope geochemistry of reservoir fluids and gases and surrounding hot spring and non-thermal surface waters was used to identify possible local and regional sources of recharge. Bench testing of production fluid, caliper logging of well bores, and observation of surface brine handling equipment after long flow periods provided information regarding silica and calcium carbonate scaling.

4. Seismic Reflection Profile Reprocessing: Seismic reflection profiles provided by SUNEDCO were reprocessed to enhance resolution of structure adjacent to the range-front fault in production zones.
5. Tectonic Activity and Fracturing within the Reservoir: The nature of ongoing tectonic activity that is creating permeability in the reservoir was examined using low sun angle aerial photography and first motion studies of local seismic events.
6. Assessment of Seismic Hazard: Operating histories of geothermal fields throughout the world were reviewed for the purpose of indentifying the number and nature of seismic events that have caused mechanical or hydrologic damage to production and injection wells. These histories were related to observed Dixie Valley seismicity to assess the probability of damage to Dixie Valley wells by seismic activity.

Summaries and interpretations resulting from the examination of each of the geotechnical data sets are presented in Chapters 3, 4, 5, and 6.

Well and reservoir testing procedures and results from tests performed by Oxbow and others are described in Chapter 7. Included for each well are test results, flow characteristics, and casing design. Reservoir pressure response during production and shut-in are also presented. These data are used to produce an analytical model of the reservoir based on an idealized reservoir configuration. Future behavior of individual wells is predicted by use of a computer simulation of wellbore flow characteristics as reservoir pressure and enthalpy decline during the 30 year production history of the field. This analytical model is used as a simplified check of

the far more complex numerical model described in Chapter 8.

The conceptual reservoir model derived from the geologic data sets and reservoir test data are synthesized in Chapter 8 to produce the computer generated numerical reservoir model. This computer model provides a simulation of reservoir behavior under various conditions of production and reinjection.

The accuracy of the predictions provided by the simulation is dependent on the accuracy of the underlying geotechnical data used to create the conceptual model and the duration of reservoir testing.

#### 2.4 Contributors.

The following investigators contributed to the reservoir assessment.

Dick Benoit - Execution of well and reservoir testing, electric log interpretation, measurement of scaling, chief editor.

Mr. Benoit (M.S. geology) has been involved in the geological aspects of geothermal development for 13 years, primarily in the Basin and Range province in Nevada. He played a key role in the discovery and development of the Desert Peak geothermal field. He has also either worked with or evaluated almost every other high-temperature geothermal reservoir in the Basin and Range province.

Gudmundur Bodvarsson - Numerical reservoir modeling

Mr. Bodvarsson (Ph. D. reservoir engineering) has been involved in geothermal reservoir engineering and modeling for 9 years. He is currently a staff scientist with the Lawrence Berkeley Laboratory specializing in numerical modeling and reservoir engineering in fractured porous media. He has modeled and evaluated geothermal reservoirs throughout the world and has published numerous articles in professional journals.

Bill Desormier - Execution of well and reservoir testing and compilation of data bases.

Mr. Desormier (M. S. geology) has been involved in the geological aspects of geothermal development for 11

years. He played a key role in the discovery of the Steamboat Springs and Humboldt House geothermal reservoirs in western Nevada. Most of his geothermal experience is in the Basin and Range province.

Chris Doughty - Numerical reservoir modeling  
Ms. Doughty (B. S. engineering physics) is a staff scientist with the Lawrence Berkeley Laboratory involved in mathematical modeling of geothermal reservoirs. She has an extensive list of professional publications to her credit.

Roger Harrison - Reservoir engineering including design of reservoir test and analytical analysis of results.

Mr. Harrison (M. E.) has 12 years of experience in all aspects of geothermal drilling and reservoir and production engineering at most of the major geothermal resources in the United States and many of the high-temperature resources around the world. He has been associated with the Dixie Valley reservoir since 1983.

Stu Johnson - Geochemistry of reservoir fluids.

Mr. Johnson (M. S. geology) has been involved in both geology and geochemistry in both geothermal exploration and development for 13 1/2 years. He has evaluated many of the high-temperature geothermal areas in the Basin and Range province. His most extensive experience is at the Roosevelt geothermal field in Utah.

Tsvi Meidav - Assessment of seismic hazard.

Mr. Meidav (Ph. D. geophysics) has been involved in geothermal exploration and development for 19 years in academic, administrative, and developer roles. He has published numerous articles on geothermal areas throughout the United States and the world.

David Okaya - Seismic reflection profile reprocessing.  
Mr. Okaya (Ph. D. geophysics) is a guest scientist at the Lawrence Berkeley Laboratory and a research associate professor at the University of Southern California.. He specializes in seismic reflection processing and interpretation of crustal structures. He has published

papers on faulting and seismic profiling at Dixie Valley.

Bill Peppin - Structural interpretation of local seismic events.

Mr. Peppin (Ph. D. seismology) is a research seismologist at the University of Nevada. He has authored numerous seismological papers including an analysis of seismicity at the Geysers in California.

Bill Teplow - Design of the reservoir assessment program, development of the structural and conceptual geological models.

Mr. Teplow (B. A. geology) has been involved in geological aspects of geothermal exploration and development for 5 1/2 years and has 4 years of experience in Dixie Valley. He was responsible for locating the two Section 33 wells while working for Trans-Pacific Geothermal Inc. In addition, he played a key role in the discovery of the high-temperature Fish Lake Valley geothermal prospect in Nevada.

Al Waibel - Reservoir lithology, stratigraphy, and hydrothermal mineralization.

Mr. Waibel (B. S. anthropology) has been involved in geological aspects of geothermal exploration for 13 years and has worked extensively in Dixie Valley for over 6 years. In addition he has experience in many areas in the western United States, Mexico, and Africa.

Bob Whitney - Aerial photo interpretation of surface faulting.

Mr. Whitney (Ph. D. expected 1987 in geology) has been involved with numerous structural and seismic evaluations throughout the United States and in Argentina. In addition he has previous structural experience in Dixie Valley as part of the Mackay Mineral Research Institute study in 1980.

Doug Willier - Graphics Design

Mr. Willier (M.S. Public Administration) has over 6 years of experience in energy and related fields.

Frank Yeamans - Hydrology

Mr. Yeamans (M. S. Water Resources) has been involved in hydrologic aspects of geothermal exploration and development for 7 years. He has worked extensively on geothermal systems in the Basin and Range province, including Steamboat Springs, Desert Peak, and Roosevelt.

### 3. GEOLOGY

#### 3.1 Regional Geology

The regional geology of west-central Nevada including Dixie Valley has been described by Willden and Speed (1974). The local geology has been extensively studied by Speed (1976). The complex structural history is described in the MMRI (1980) Geothermal Reservoir Assessment Case Study. The major geologic features of the region are shown in Figure 3.1 which is a simplified NW-SE cross section of west-central Nevada passing through the Dixie Valley geothermal reservoir. The major stratigraphic and structural features seen in the cross section can be summarized as follows.

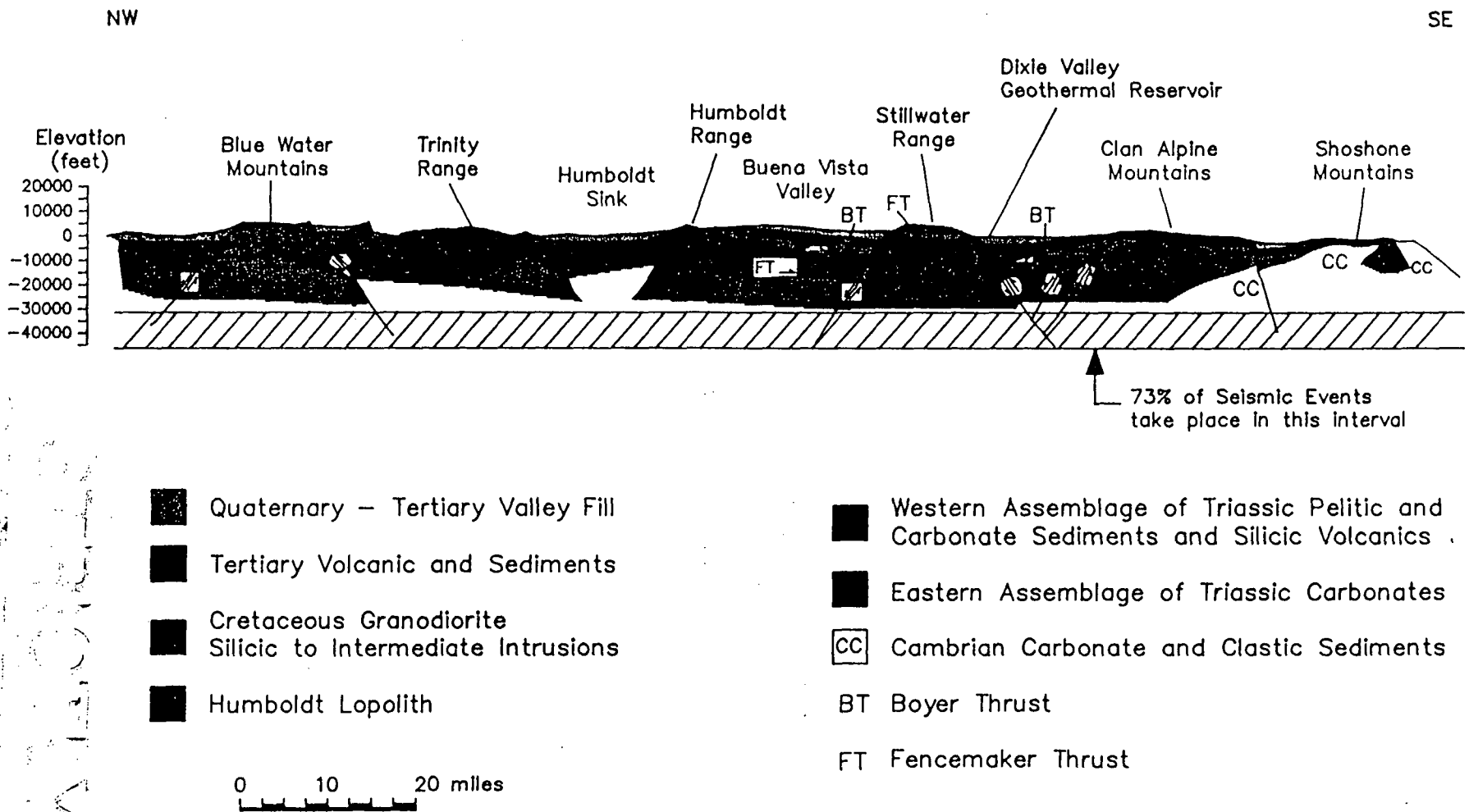
1. The deepest sedimentary rocks underlying the Dixie Valley region are probably carbonate and silicic clastic sediments, characteristic of the eastern Nevada shelf facies, ranging in age from Cambrian to Triassic. These units have not yet been encountered in the Dixie Valley wells, due to the great thickness of the overlying Triassic-Jurassic marine sediments, but are exposed to the east of Dixie Valley in the Clan Alpine and Shoshone Mountains.

2. A sheet of Triassic marine sediments and silicic volcanics ranging in thickness from 10,000 to 40,000 feet blankets most of west-central Nevada. This sheet has been thrust over the Cambrian-Triassic section along the Fencemaker thrust fault from the west. Dixie Valley is located near the leading edge of the thrust so this unit pinches out within the deep part of the Dixie Valley graben at the northern end of the production well field in the vicinity of well 45-33. The Triassic marine sediments are dominated by siltstone and shale with less than 30 percent interbedded carbonates and sandstone.

3. A Jurassic oceanic crust complex consisting of gabbros, diorites, and basalts intruding marine clastic and carbonate sediments overlies the Triassic section over an area of several hundred square miles in and surrounding Dixie Valley. This complex, which is termed the Humboldt Lopolith, has a thickness of up to 4000 feet near its center and thins gradually toward the margins. The complex is thrust over the Triassic marine sediments along the Boyer Thrust.

STRICTLY  
CONFIDENTIAL

# Simplified Geologic Cross Section West Central Nevada





4. The imbricated Paleozoic-Mesozoic marine sedimentary and oceanic crustal thrust sheets were intruded by Cretaceous intermediate to silicic magmas similar to those of the Sierra Nevada batholith. These intrusions are exposed in isolated outcrops throughout the region and have been encountered in the deeper wells in Dixie Valley that penetrate into the Stillwater Range block. These intrusives probably become more abundant at depth than is apparent from the extent of surface outcrops.

5. During middle to late Tertiary time several thousand feet of silicic, intermediate, and basaltic volcanic and volcanoclastic rocks were deposited over most of the region. These volcanic events occurred prior to and during incipient Basin and Range extension and block faulting.

6. East-west crustal extension of up to 30 percent during the last 8 million years has resulted in the formation of the horst and graben structural features which currently dominate the regional geomorphology. Northeast-trending horst block mountain ranges are separated from the graben blocks by range-front faults with dips of 50 to 60 degrees. Earthquake focal points along these faults indicate that brittle fracturing takes place to a maximum depth of approximately 49,000 (Fig. 3.1). Most seismic events occur in the depth interval between 33,000 and 49,000 feet. Basins created by this extensional faulting have accumulated up to 10,000 feet of late Tertiary and Quaternary lacustrine, volcanoclastic, and alluvial deposits.

### 3.2 Geology of the Dixie Valley Geothermal Reservoir

#### 3.2.1 Introduction

This description of the geology of the Dixie Valley geothermal reservoir has been excerpted from a comprehensive report prepared for Oxbow by Al Waibel.

The stratigraphy, in the order encountered in the majority of the drill holes, includes basin filling sediments (Qal), silicic tuff-rich sediments (Tts), Miocene basalt (Tb), Miocene sediments (Ts), Oligocene silicic volcanics (Tsv), Jurassic oceanic crust (Js & Jpg), Jurassic marine sediments (Jms), Cretaceous granodiorite (Kgd), and Triassic marine sediments (Trc). The letter designations are those employed in the drill hole lithologies shown in Figure 3.2 and geologic cross sections shown in subsequent Figures.

The distribution of hydrothermal aquifers in the geothermal drill holes is also shown in Figure 3.2. The location of

these currently or recently active aquifers has been determined from secondary mineralization and the effects of the host rock interacting with geothermal fluid and gas. Analyses by the Argonne National Labs suggest that the geothermal system may have been active for as much as 150,000 to 300,000 years.

The structural history of the area now occupied by the geothermal field is complex. Jurassic oceanic crustal rocks have been thrust over carbonaceous marine sediments of Triassic age. Siliceous and mafic rocks of Tertiary age unconformably overlie the pre-Tertiary rocks. North-striking normal faulting occurred in this area in the Miocene, followed by a superimposed NNE striking set of normal faults. The Dixie Valley graben and the Stillwater Range are artifacts of the most recent episode of faulting. Highly fractured areas hosting geothermal production appear to have best developed in tensional zones resulting from strike-slip and normal faulting along the two generations of normal faults.

### 3.2.2 Lithology

#### Triassic Marine Sedimentary Rocks (Trc)

These are the deepest and oldest rocks encountered by a few of the wells in Dixie Valley. They are primarily calcareous carbonaceous shale, siltstone, and silty carbonates. The carbonaceous marine sediments are correlative to the Favret Formation, a lower member of the Star Peak Group. Geological and geochemical evidence indicates that the Favret Fm. is the primary reservoir at Dixie Valley; i.e., the fluid recovered from the deep production wells apparently reached thermal and chemical equilibrium within this unit and then has moved rather rapidly to the producing intervals.

Mechanically the Triassic sediments will deform rather than fracture when subjected to strain. Dolomite bearing horizons form secondary serpentine during deformation. These characteristics make this formation an unlikely host for geothermal production. However, it is not necessary for this unit to be capable of giving up large volumes of fluid in short times. As a geothermal reservoir rock it is necessary to have substantial storage capacity and the ability to slowly release fluids into small fractures over time. The large producing fractures are found overlying

these Triassic sediments in much more competent igneous rocks.

The Favret Fm. is rich in hydrocarbons and is apparently undergoing metamorphism which is liberating gases such as CH<sub>4</sub>, H<sub>2</sub>S, N<sub>2</sub>, NH<sub>3</sub>, and CO<sub>2</sub>. Chemical reactions involving these gases, particularly CH<sub>4</sub> and H<sub>2</sub>S, control rock-water-gas reactions in the shallower production portion of the geothermal system.

#### Jurassic Formations (Jms Js Jpg)

From a production viewpoint, the Jurassic rocks are the most important rocks in the Dixie Valley field as it is these formations which contain most of the large productive fractures. Wells 74-7, 73-7, and 84-7 produce from the Jurassic oceanic crust (Js and Jpg) as do the deeper productive wells in Section 18 (52-18 and 65-18). Wells 27-33 and 45-33 produce from the Jurassic marine sediments.

#### Jurassic Marine Sediments (Jms)

Jurassic shallow marine sediments overlie the Triassic marine sediments and are separated from each other by the Fencemaker thrust fault. Compositionally these sediments consist of carbonate, quartzite, and minor conglomerate. Willden and Speed (1974) refer to these sediments as the Boyer Ranch Formation. Thrusting of the Jurassic oceanic crust clearly involved the Boyer Ranch Formation. Portions of the sediments can be observed in the Stillwater Range as overlying, overridden by, and mechanically incorporated into the allochthonous oceanic crust.

The quartz arenite portion of the Boyer Ranch Formation is a well-lithified, competent rock that tends to host open permeability along fault planes. However, outcrop evidence suggests that it is not prone to extensive fracture propagation. The rock is composed largely of lithified quartz grains and should be chemically and mineralogically stable in the geothermal system. The only extensive occurrences of this quartz arenite in the geothermal wells are in 27-33 and 45-33 where it forms the foot wall of a fault.

#### Jurassic Oceanic Crust (Js & Jpg)

The Jurassic oceanic crust section consists primarily of mafic igneous rocks that have undergone extensive sodium

metasomatism. The dominant rock types vary from spillites, basalts, keratophyres, and trondhjemites to albitites, plagiogranites, and gabbro. Locally, lenses of sedimentary rock, most commonly siltstone, are observed within the igneous series.

Willden and Speed (1974) and Speed (1976) describe the Jurassic igneous rock as a locally intruding lopolith. Autochthonous thrusting has been associated with the intrusion of the lopolith. Al Waibel and others, however, have concluded that the entire Jurassic igneous section is most probably an allochthonous fragment of oceanic crust, thrust over Triassic marine shelf and slope sediments. The most obvious points leading to this reinterpretation include pervasive sodium metasomatization, pervasive secondary calcite, and abundant lamellar plates, lenses, and nappes markedly disrupting specific lithologic and stratigraphic continuity. The "lopolith" is remarkably similar to igneous portions of ophiolites observed in many places throughout the world.

The large blocks of spilite, keratophyre, and trondhjemite rock tend to be very brittle and are capable of maintaining good fracture permeability. The albitite and plagiogranite are somewhat less prone to host good fracture permeability. The prevailing mineral assemblage, albite, calcite, chloritized hornblende, chloritized biotite, and chloritized augite, tends to be stable in the chemical and thermal environment of the currently active geothermal system.

The mineral suite is not mechanically stable in the cataclastic environment of thrust faulting, shear planes, and nappes. The mafic minerals are usually altered to serpentine and chlorite; the albite tends to be broken up into small angular fragments and the calcite tends to recrystallize as a matrix mineral. The resulting effect is lenses of mechanically unstable rock within the more competent formation. While these lenses have the potential of hosting permeability, the permeability does not always have good communication with major geothermal production, and the formation tends to slough when produced. The serpentinized zones in two of the legs of well 82-5 are the result of thrust related alteration.

#### Cretaceous Granodiorite (Kgd)

A quartz monzonite to granodiorite intrusive pluton has been penetrated in several of the deeper wells in Dixie Valley. The mineralogy of the rock is distinctly different from the igneous rocks of the Jurassic oceanic crust. Where least

STRICTLY  
CONFIDENTIAL

altered this rock consists of quartz, plagioclase, biotite, muscovite, hornblende, and minor K-feldspar. Where altered the mineralogy is albite, chlorite, K-feldspar, epidote, and calcite. The mafic minerals usually are slightly chloritized.

The genetic and structural relationship of this silicic intrusive to other igneous rocks in the area is not totally clear. It is typically observed as the foot wall in fault contact with Jurassic rock. In the first leg of well SWL-2 it is in fault contact with Miocene basalt. At no place in the Jurassic rocks cropping out in the Stillwater Range is rock this potassic observed. The mineralogy and texture more closely resemble intrusives cropping out along the west side of the Stillwater Range in the New York Canyon area that have been dated as late Cretaceous. This would place the intrusive event after the allochthonous thrust faulting and would explain the apparent thin fingers or layers of granodiorite within thrust fault zones as intrusive sills.

While granitic rocks in other reservoirs in the Basin and Range province have excellent productive intervals no commercial production has been developed from the granodiorite in the Dixie Valley geothermal field. The rock is mechanically competent and should fracture when under stress. Fracture permeability would tend to seal in the unaltered granodiorite as calcic plagioclase altered to albite and calcite. The albite-chlorite-epidote-K-feldspar altered granodiorite would be in chemical/mechanical equilibrium with geothermal fluids. Fracture permeability is more stable here, though the rock at this grade of alteration is usually observed in fault zones containing mechanically incompetent fault gouge. Perhaps fracturing has simply not occurred in the footwall of the Stillwater fault where the granodiorite is located or the fault gouge does not allow any fracturing stresses to be transmitted into the granodiorite.

#### Oligocene Silicic Volcanics (Tsv)

Oligocene silicic volcanic tuffs in excess of 4000 feet thick dominate the Clan Alpine Range to the east of the Dixie Valley geothermal field, and are a few hundred feet thick in the Stillwater Range just west of the geothermal field. These volcanics are only rarely encountered in the geothermal drill holes, however. In most of the geothermal wells in Dixie Valley the Oligocene volcanic section has been faulted out (e.g., 65-18 and 84-7) by basin-bounding normal faults. The single good example of these silicic tuffs in the wells is observed in 74-7, where a 180 foot

section of predominantly welded biotite-quartz-sanidine tuff is overlain by Miocene sediments.

Welded portions of the Oligocene silicic tuffs are brittle and generally fracture when subjected to strain. Poorly welded and cemented aspects of the tuff sequence are generally soft and undergo plastic deformation rather than structural failure when subjected to strain. Fracture permeability within Oligocene silicic volcanics may or may not be significantly affected by interaction with the current geothermal system depending upon the individual rock type.

#### Miocene Sediments (Ts)

The Miocene lacustrine sedimentary section conformably overlies the silicic volcanic tuffs of late Oligocene age. The formation is composed of intercalated volcanoclastic sediments, carbonaceous siltstone, and silicic volcanoclastic tuff. The section is usually observed in a truncated form in many of the drill holes in Dixie Valley due to normal faulting. The thickest sections observed in drill holes are seen in 27-33 (1040 ft) and in 45-33 (1300 ft).

The upper portion of the sediments consists of intercalated volcanoclastic sediments and carbonaceous siltstone. The volcanoclastic sediments appear to be derived predominantly from silicic volcanics and tuffs. The lower portion of the sedimentary section is composed of reworked silicic tuffaceous sediments with only minor carbonaceous siltstone horizons. The basal boundary of this sedimentary unit is not distinct. In well 74-7 a downward progression is observed from reworked silicic tuffs to possibly primary devitrified silicic tuff to primary welded Oligocene silicic tuff.

Clays represent the dominant mineralogy in this sedimentary section. As a result, tectonic strain tends to cause plastic deformation rather than brittle failure and rock breakage.

Rock-water-gas interaction between the sediments and the geothermal system is limited due to the low potential for porosity and permeability.

#### Miocene Basalt (Tb)

After the Jurassic rocks the Miocene basalt is the second major producing formation. Wells 76-7, 32-18, SWL-1 and

SWL-3 produce from this unit. Of these wells only 76-7 is regarded as a high enthalpy well.

The Miocene basalt overlies Miocene lacustrine sediments and is overlain by as much as 6000 to 7000 feet of basin filling sediments in the area of the geothermal field. These basalts crop out as high as 8000 feet elevation in the Stillwater Range which indicates an offset on the Stillwater fault of 12,000 feet since these basalts were deposited. A K-Ar date from a sample from the Stillwater Range analyzed for SUNEDCO in 1981 shows an age of  $8.5 \pm .4$  million years. The basalt section as observed in geothermal drill holes is often abbreviated due to normal faulting. Observed thicknesses in the drill holes range from less than 300 ft (45-33) to greater than 1900 ft (65-18).

Two distinct alteration mineral suites are observed in the Miocene basalt section in drill holes. The effects of weathering are plainly visible in portions of the basalt chips recovered during drilling. Other portions of the basalt show a later overprinting of alteration resulting from interaction with geothermal fluid and gas with a low oxygen activity. Precipitation of quartz, chlorite, and occasionally epidote into open fractures indicates that this later alteration is likely associated with conductive cooling geothermal fluids. No mineral-chemical evidence for mixing of geothermal and nongeothermal water in the basalt is found in any of the drill holes.

#### Basin Filling Sediments (Qal & Tts)

Subsequent to the eruption of the Miocene basalts, horst and graben tensional structural features developed in the area of the Stillwater Range and Dixie Valley. Sediments accumulated in the grabens, unconformably overlying the Miocene basalt flows. The current Dixie Valley basin is asymmetrical with the deepest portions occurring in the northwest margin along the Stillwater Range. In the wells 74-7 and 76-7 the basin filling sediments are in excess of 7000 feet thick. Seismic data suggest that toward the center and along the eastern portion of Dixie Valley these sediments are no more than 2000 to 3000 feet thick.

The composition of the fill which makes up the basin sediments is somewhat variable from place to place. Toward the center and along the eastern portions of the valley the entire sedimentary section is dominated by reworked silicic tuffs eroding from the Clan Alpine Range. Along the Stillwater Range the contributing rock types are more varied. Reworked silicic tuffs tend to dominate the deepest

(earliest) sediments in the geothermal production area. With decreasing depth the sediments are usually variations on a pebble conglomerate with clay matrix. Near the discharge of major Stillwater Range drainages (i.e. Cottonwood Canyon) conglomerates are most common and horizons of clay and silt are minor. Areas away from major drainages have basin filling sediment sections dominated by clay, silt, and sand size particles with less common conglomerate horizons.

### 3.2.3 Structural History

Three structural patterns are recognized in the vicinity of the Dixie Valley Geothermal Field. The first of these is thrust faulting associated with crustal shortening. The second and third are both normal faulting associated with crustal extension. Geothermal production in Dixie Valley is related to an extended complex network of fault and fracture permeability. The combined tectonic history is, therefore, quite important to interpreting the production potential of any given location within the geothermal field.

Thrust faulting of Jurassic oceanic crustal rocks over Triassic shelf-related marine sediments is observed in the Stillwater Range. This thrust faulting event is one of the last in a series of crustal shortening events that involved allochthonous thrusting of deep marine strata over older rocks (Antler Orogeny, Devonian-Mississippian; Sonoma Orogeny, Triassic; and Nevadan Orogeny, Jurassic-Cretaceous).

The Jurassic oceanic rock has undergone differential movement along horizontal planes within the overthrusting block resulting in horizontal cataclastic zones and inclusions of marine sediments into the thrusting Jurassic plate. Serpentinization of portions of the Jurassic mafic igneous rocks and of Triassic dolomitic sediments is common within melange-like features created by zones of turbulence along the leading edge of the thrust block.

The Dixie Valley area of Nevada appears to have been structurally quiet from the Cretaceous through the Oligocene. Subsequent to the silicic volcanism in the late Oligocene a series of north-striking normal faults developed. The best surface expressions of these faults can be observed along the western edge of the Clan Alpine Range and in the White Rock Canyon area in the Stillwater Range. Seismic line data show similar north-striking patterns to be present beneath the alluvium in Dixie Valley. The surface



expressions of this episode of normal faulting show evidence of rotation, suggesting that these were listric faults which flatten with depth. The relationship between the timing of the late Miocene basalt eruptions and the north-striking normal faulting is unclear. Both Jurassic and Oligocene rocks were affected by this fault movement. No outcrops of Miocene basalt show a similar rotational relationship.

The current high-angle NNE-striking normal faulting that defines the Stillwater Range and Dixie Valley physiographic features is relatively young, and is superimposed over the earlier two tectonic features. The uplift of the Stillwater Range occurred after the late Miocene basalt eruptions, as is evidenced by the flat lying basalt flows and palagonite tuffs which occupy some of the highest elevations within the range. The onset of this last episode of faulting, therefore, can be no older than very early Pliocene. Historic earthquakes along the basin-range boundaries attest to the continuing activity of this latest structural feature.

#### 3.2.4 Hydrothermal Mineralogy

Multiple thermal and metasomatic events have left a mineralogical signature in the host rocks in the Dixie Valley area. The temperatures of most of these metasomatic events have ranged from 120 to 500 deg. F., similar to the range of temperatures in the currently active geothermal system. As a result many of the secondary minerals are stable in the present geothermal environment and may be representative of more than one thermal event. The mineralogical effects of fossil thermal systems must be distinguished from those of the active system before any interpretations pertaining to this current system can be made.

The earliest thermal and metasomatic event recognized in the Dixie Valley area involves the Jurassic oceanic crustal rocks. The pre-alteration rocks of this group were basalt, diabase, gabbro, and locally more leucocratic fractionations of this suite. Extensive sodium metasomatization is manifested in nearly complete albitization and local scapolitization of plagioclase. Extensive secondary calcite occurs within the rock and in veins, an effect of the pervasive sodium metasomatization. Chloritization of mafic minerals is ubiquitous, and varies in degree from minor to near complete replacement of the mafics. Additional secondary minerals, including epidote, pyrite and chrysotile, are irregularly distributed throughout portions of the Jurassic igneous suite. The post-alteration rock

suite consists of spilite, keratophyre, trondhjemite, albitite, and plagiogranite.

The spilitic rock suite of the Jurassic section is typical of the igneous rock suites observed in many ophiolite complexes. The sodium metasomatization most likely had to occur while this section was still in a marine environment. The only reasonable sodium reservoir to support this type of extensive alteration would be sea water.

A second metasomatic event, confined to the Jurassic oceanic rocks, involves silica and iron oxides and is represented by quartz-filled veins in association with specular hematite replacement of spilitic rock.

The timing and possible relationship between the two events has not been determined. Both of these secondary features may have developed at or near the same time, while these rocks were still part of an ocean environment.

Additional thermal and metasomatic events in the Dixie Valley-Stillwater Range area include contact metamorphism associated with Cretaceous plutonic intrusives and Oligocene silicic volcanism. In the Dixie Valley region these thermal events have concentrated both base and precious metals to the extent that mining districts are rather common.

The most recent volcanism in the Dixie Valley area is the late Miocene basaltic eruptions and associated subvolcanic dikes. Contact metamorphic effects are usually limited to a few tens of centimeters away from the edge of the intrusives and consist mainly of chloritization. No hydrothermal activity has been observed to be associated with this intrusive event.

Hydrothermal mineralization associated with the active geothermal system varies with temperature and host rock type. The fluid has low oxygen activity, low total dissolved solids, and limited sulfur and carbonate activity. Precipitation mineralization in the deeper production from Jurassic igneous rock is usually limited to quartz. Host rock alteration by the hot fluid is limited to pyrite forming at the expense of Fe-Ti oxide. The Jurassic igneous rock is already at a chlorite-albite grade of greenschist metamorphism and is chemically stable in the presence of the hot fluid.

Hydrothermal mineral reactions within the Miocene basalt are substantially different from the reactions observed in formations underlying the basalt. Here, chlorite, pyrite,

albite, calcite, and locally epidote are present as hydrothermal alteration products of the formerly hematite altered basalt. Hydrothermal precipitation minerals in these basalts include quartz, chlorite, pyrite, calcite, epidote, laumontite, and rarely wairakite.

The marked difference between the hydrothermal mineral assemblages in the two mafic igneous units is the combined result of the stable mineral phases prior to the introduction of the geothermal fluids and the gas content of the geothermal system. The Miocene basalt is oxidized where unaffected by geothermal fluids, with reddish hematite as a major stable Fe mineral. The Jurassic spilitic series has been albitized and partially chloritized prior to the current geothermal activity. The significant change within the geothermal fluid as it passes through the Jurassic section is limited to conductive heat loss. This results in slight but steady silica oversaturation, manifested by the precipitation of druse quartz forming along fracture surfaces.

### 3.2.5 Mineralogic and Lithologic Characteristics of Geothermal Production Zones

Geothermal production in the Dixie Valley field is defined by fault and fracture permeability. Rather than being strata bound, permeability is defined by and varies with the physical characteristics of each rock type. The production potential of a rock is best defined by its mechanical and mineral-chemical stability. Open fractures are dependent on brittle rock that will fail rather than deform under tectonic strain. Producing fractures are, therefore, most likely to occur in brittle igneous rock and least likely to occur in soft, clay-rich sedimentary rock. Subsequent to fracturing, the longevity of permeability is dependent upon the mineral and chemical stability of the rock in the presence of geothermal fluid and gas.

The occurrence of faults or fractures within a brittle rock does not automatically guarantee production. Fault planes are not always "planer". Normal faults associated with extensional tectonics in Dixie Valley tend to undulate, which results in portions of the fault plane being under high compression and impermeable, regardless of the rock type involved. Conversely other portions of the fault plane will be under tension and contain open spaces possibly tens of centimeters wide. An example of the former would be the fault zone intersected by SWL 3 from 8730 to 8880 feet; and example of the latter would be the fault zone intersected by 76-7 between 7332 and 7334 feet.

STRICTLY

33

CONFIDENTIAL

The two most common host formations of geothermal production in Dixie Valley are the Miocene basalt and the Jurassic oceanic crust. The basalt contains cooling fractures and flow breccias that can complement fault-related fracturing and provide additional production permeability. The pervasive mineralogy within the basalt, secondary hematite, zeolite, and clay, is not stable in the presence of the geothermal fluids and gas. Interaction between the basalt and the geothermal system results in chloritization. With extreme chloritization fractures tend to seal and the rock becomes less competent. Fracture production within the basalt tends to be in zones of very fresh to moderately chloritized rock. The typical hydrothermal mineralogy includes alteration chlorite, pyrite, albite, and minor calcite; and precipitation quartz, chlorite, minor calcite, and locally epidote. Fracture production from basalt is not associated with rock strongly dominated by hematite, zeolite, and clay alteration. Loss of drilling fluid or the occurrence of methane are not, by themselves, reliably distinct indicators of geothermal production fractures in the basalt.

Geothermal production from fault zones in the Miocene basalt is usually associated with chlorite and pyrite alteration minerals and quartz, chlorite, ± epidote precipitation minerals. Major to total loss of drilling fluid is always, though not uniquely, associated with fault production in the basalt. Permeable fault zones are much less susceptible to the subtle nuances of physical rock characteristics of the basalt than are fracture zones.

The Jurassic oceanic crust rocks have undergone a substantially different history from the Miocene basalt as evidenced by the mineralogical and mechanical rock characteristics. The rocks range from spilite and keratophyre to trondhjemite and rarely to gabbro, albitite, and plagiogranite. Physically the rocks range from competent blocks to cataclastized horizontal shear zones. The rock is pervasively albitized and variably chloritized, a mineral assemblage that is generally in equilibrium with the geothermal fluids. The more mafic portions (spilite, keratophyre, trondhjemite) fracture under tectonic strain and the fractures tend to remain open. The rocks dominated by feldspar and calcite (albitite and plagiogranite) are less brittle and tend to be poorer hosts for fracture and fault permeability. Cataclastized zones resulting from Jurassic-age thrust faulting are much more ductile than the equivalent uncataclastized rock, and are less likely to host current production.

The physical parameters of rock likely to host production in Dixie Valley are easy to define. These features are not strata bound, however. In coal fields or sedimentary basins structural and stratigraphic projections can be made for kilometers with some degree of accuracy. Crustal thrusting, two episodes of normal faulting, and volcanic stratigraphy render analogies between layer-cake sedimentary basin geology and the Dixie Valley geothermal field meaningless. Projection of the general formations and normal faults within the Dixie Valley geothermal field can be approximated for short distances with the well controls and seismic data now in hand. Predicting exact locations of production zones within these formations is more problematic. Evaluation of the production potential in any well in any given formation is most effectively done at the well site as drilling is underway.

### 3.2.6 Determination of Production Zones by Electrical Logging and Drilling Records.

Production zones for each producible well have been defined using a combination of electric logging and physical drilling parameters. Methods employed for each well and the resulting definition of production zones is detailed in Appendix B. These production zones are shown graphically in Figure 3.2 and are summarized on Table 3.1.

### 3.2.7 Age of the Geothermal System

Age estimates have been made on two hydrothermal silica specimens from the geothermal system using the ionium/thorium method. The facilities at the Argonne National Laboratories in Argonne, Illinois were used. The first sample is of dense clear cryptocrystalline silica from a silicious sinter hot spring deposit in section 15, T24N, R36E located 2 miles southwest of the Section 18 wells along the range-front fault. The hot spring is no longer active and the area has been uplifted by ongoing normal faulting along the Stillwater Range front. Total uplift since the hot springs deposits formed may be as much as 200 feet. The estimated age of this deposit is determined to be  $9,000 \pm 2,000$  years.

A second sample was collected for dating from hydrothermally precipitated cryptocrystalline silica from near the Senator Fumaroles in section 32, T24N, R37E. This sample formed near the boiling plane below the topographic surface. Subsequent uplift by normal faulting along the Stillwater Range from the time of silica deposition until now positions

this rock 250 feet above the Dixie Valley floor. The age of this sample is much less definitive, with a maximum possible age of 300,000 years and a minimum possible age of 150,000 years.

### 3.3 Structure of the Dixie Valley Geothermal Reservoir

Structure within the Dixie Valley geothermal reservoir has been defined using well bore geology and electric logging techniques, coupled with seismic reflection profiling. Stratigraphy, faulting, and deformation are defined with high precision within the existing well field. The stratigraphy, faulting, and deformation can then be followed several miles to the north, south, and east using seismic reflection profiles run by SUNEDCO and Southland Royalty.

Structure within the productive portions of the reservoir is dominated by the Stillwater range-front fault and associated secondary sympathetic and antithetic faults. Three styles of faulting are observed in the productive part of the field. These styles are shown in cross section in Figures 3.3.1-3.3.3. The locations of these cross sections are shown in Figure 2.2. The transition between the three regions is probably gradational.

The Section 18 area (Fig. 3.3.1) is characterized by numerous sympathetic and antithetic faults of relatively small displacement. These intersecting secondary faults form a rubble zone of high permeability and relatively high fracture porosity. The high density of fracturing appears to be most strongly developed in the Miocene basalt (Tb). This style of fracturing extends northeastward through well 76-7. Wells 84-7 and 73-7 further to the northeast show decreasing fracture permeability in the basalt. Wells 82-5, 27-33, and 45-33 at the northeast terminus of the field encountered no permeable fractures in the basalt.

The northwest-southeast width of the highly faulted area appears to decrease from the Section 18 area to the vicinity of well 82-5. The region extending from well 84-7 to 82-5 is characterized by the existence of one or two secondary faults which parallel the main range-front fault surface. These faults separate the down-dropped graben block into two or three slivers with vertical offsets of several hundred feet between each sliver. This style of faulting is shown in Figure 3.3.2. Within this region, commercially productive fractures are encountered between the slivers. Seismic reflection profile No. 6 which passes through well 84-7 perpendicular to the range-front fault, shows two

relatively large slivers and their relationship to the major down-dropped graben block (Fig. 3.3.4)

The range-front fault system becomes more coherent north of 82-5 as the secondary faults appear to die out and all offset between the two blocks is confined to the main range fault (Fig. 3.3.3). Drilling results from 45-33 and 27-33 confirm this structural interpretation which was originally developed by Okaya and Thompson (1985) using a seismic reflection profile passing through 27-33 perpendicular to the strike of the range-front fault.

Development of the differing faulting styles may be related to the relative magnitude of dip - slip and strike - slip movement in the fault planes as discussed in Appendix D. The increasing component of strike-slip movement going south from 27-33 to the Section 18 area is predicted for the corresponding change in strike of the range-front fault. As the range-front fault strike swings farther to the west in the Section 18 area, increased strike-slip movement causes dilation of the down-dropped block. This dilation breaks the down-dropped block into numerous smaller slivers, thereby producing the abundant permeable fractures observed in the production zones. Apparent decrease in the magnitude of strike-slip movement north of 84-7 results in less tensional force so that fault movement tends to be confined to a single fault zone with a thickness of less than 200 feet when measured perpendicular to the plane of the fault.

The attitude of bedding within the fault slivers has been determined from seismic reflection profiles and dipmeter logging runs. Dips derived from the dipmeter survey in 73-7 are shown in Figure 3.3.2. Dips in the 5000 foot to 8300 foot depth interval range from 20 to 36 degrees to the south and southeast. These dips are confirmed by Sunmark Seismic Profile No. 6 as shown in Figure 3.3.4.

Thickening of the Tertiary section (Tts, Tb, and Ts) in the northwest to southeast direction is evident from seismic reflection profiles. Seismic reflection profile No. 6 (Fig. 3.3.4) shows a thickening from approximately 1500 feet adjacent to the range-front fault to a thickness of 3000 feet at the apex of the graben located approximately 2000 feet southeast of 65-18. Apparent thicknesses observed in the production wells are affected both by stratigraphic thickening and by thinning resulting from normal fault extension. The thinning effect of normal faulting is much greater than the lateral increase in thickness in the southwest direction, thereby causing an apparent net thinning of the Tertiary section in the Section 18 and

Section 7 wells. Section 33 wells show a full stratigraphic thickness in the Tertiary section of approximately 3000 feet which indicates an absence of secondary normal faulting.

### 3.4 References Cited

Speed, R.C., 1976, Geologic map of the Humboldt Lopolith: Geol. Soc. Amer. Map Series MC-14.

Willden, R. and Speed, R.C., 1974, Geology and mineral deposits of Churchill County, Nevada: Nevada Bur. Mines Bull. 83.

Okaya, D. and George Thompson, 1985, Geometry of Cenozoic extensional faulting: Dixie Valley, Nevada, Tectonics, V.4, no. 1, pp. 107-126.

SECRET



#### 4. GROUND WATER HYDROLOGY

##### 4.1 Regional Hydrologic Setting

The Dixie Valley basin is topographically the lowest of seven valleys that constitute a closed shallow ground water hydrologic unit. This unit includes Fairview Valley, which is a topographically closed basin, and Dixie Valley with the five smaller valleys that drain into Dixie Valley--Jersey, Pleasant, Eastgate, Cowkick, and Stingaree Valleys (Figure 2.1) (Cohen and Everett, 1963). Shallow ground water flow within Dixie Valley is toward the Humboldt Salt Marsh (Figures 4.1.1 and 4.1.2) which is the topographic low point of the seven valley system and is the ultimate destination or sink for both surface and ground water.

According to Cohen and Everett (1963), precipitation within the seven valley system is the source of virtually all of the surface and ground water in the system. The estimated average annual natural recharge to and discharge from the ground water reservoir in the entire seven valley system is on the order of 18,000 acre-feet. Precipitation within Dixie Valley accounts for about 40 percent of the average annual recharge. Recharge to the shallow ground water system from the Dixie Valley geothermal reservoir was not taken into account by Cohen and Everett.

For the ground water system, approximately 90 percent of the 18,000 acre-feet per year estimated perennial yield, is discharged by transpiration from phreatophytes and evaporation from bare soil within the Humboldt Salt Marsh.

Under Dixie Valley climatic conditions, evapotranspirative potential is approximately five feet of water per year, and is defined by the 3440 foot elevation contour line. This area is characterized by numerous seeps, springs, artesian wells, and large areas of exposed moist playa and standing water. The surface area contained within this contour is approximately 146 square miles so that evapotranspirative potential is approximately 467,000 acre-feet of water per year. The potential for discharge of fluid from the ground water system to the atmosphere is therefore about 26 times greater than the observed recharge to the basin. Because of the great imbalance between recharge to the system and potential for loss from the system, minor contributions of geothermal waters could be discharging into shallow aquifers without creating obvious hydrothermal surface manifestations such as prolific boiling springs.

# Potentiometric Relationship Between Geothermal & Ground Water Systems

Elevation (feet)

8500

7500

6500

5500

4500

3500

2500

Zone of Recharge

Zone of Lateral Flow

Zone of Increasing Ground Water Potential

Zone of Active Ground Water Discharge

● Height to which water will rise in a well cased to its total depth

Stillwater Range

Regional Saturation

Ground Surface

Air-Water Interface

Humboldt Salt Marsh (elev. 3380')

Flow Lines

Geothermal System 3100'

Equipotential Lines

4700

4400

3800

3600

3500

3450

3425

# Potentiometric Relationship Between Hydrologic Systems – Thermal & Non-Thermal Northern Nevada

Elevation  
(feet)

6000'

5000'

4000'

3000'

2000'

Cottonwood  
Canyon

Cottonwood  
Canyon

Soda Lake  
4100'

Stillwater  
3900'±

Humboldt Sink  
3890'

Carson Sink  
3870'

Lower Ranch H.S.  
3960'

Sou H.S.  
3700'

McCoy H.S.  
3720'

Dixie H.S.  
3428'

DF 45-14  
3400'±

DF 66-21  
3415'±

Humboldt Salt Marsh  
3380'

62-21  
3480'±

SWL-3  
3133'

Brinkerhoff Well  
3450'

Hyder H.S.  
3586'

Lamb Windmill  
3428'

Beowawe  
Hot Springs

Leach H.S.  
4700'

Kyle H.S.  
4500'

General North, South Orientation

#### 4.2 Deuterium and Oxygen Isotopes

The hydrologic system of the deep geothermal reservoir in Dixie Valley appears to have very limited interaction with the shallow ground water system. This limited interaction is indicated by isotope, chemical, and pressure data available from various aquifers within Dixie Valley.

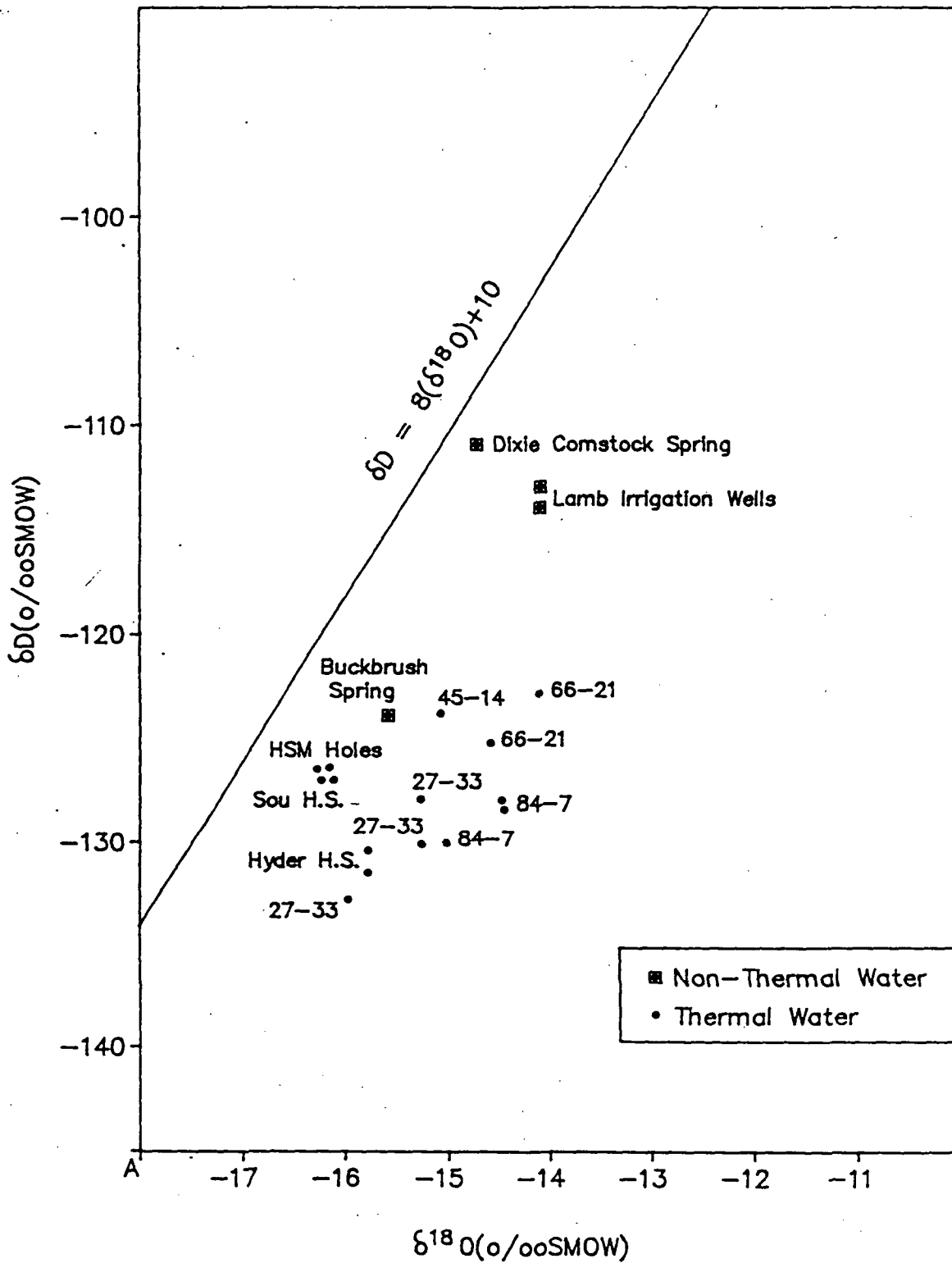
Deuterium and oxygen isotope data can be used to delineate, in a general manner, possible recharge zones and/or recharge mechanisms. Deuterium values for the deep geothermal system are very close to those of numerous surrounding hot springs (compare Figures 4.2.1 and 4.2.2). The deuterium values are centered around a value of  $-130$  ‰. Note that hot springs with similar deuterium value extend as far as the Beowawe geothermal system that is 90 miles northeast of the Dixie Valley reservoir.

The existence of similar deuterium values does not necessarily prove a common recharge zone for all of the geothermal systems exhibiting similar values. However, it does suggest that the recharge mechanisms in operation for the widely separated systems share common characteristics, resulting in similar deuterium values for the various geothermal waters.

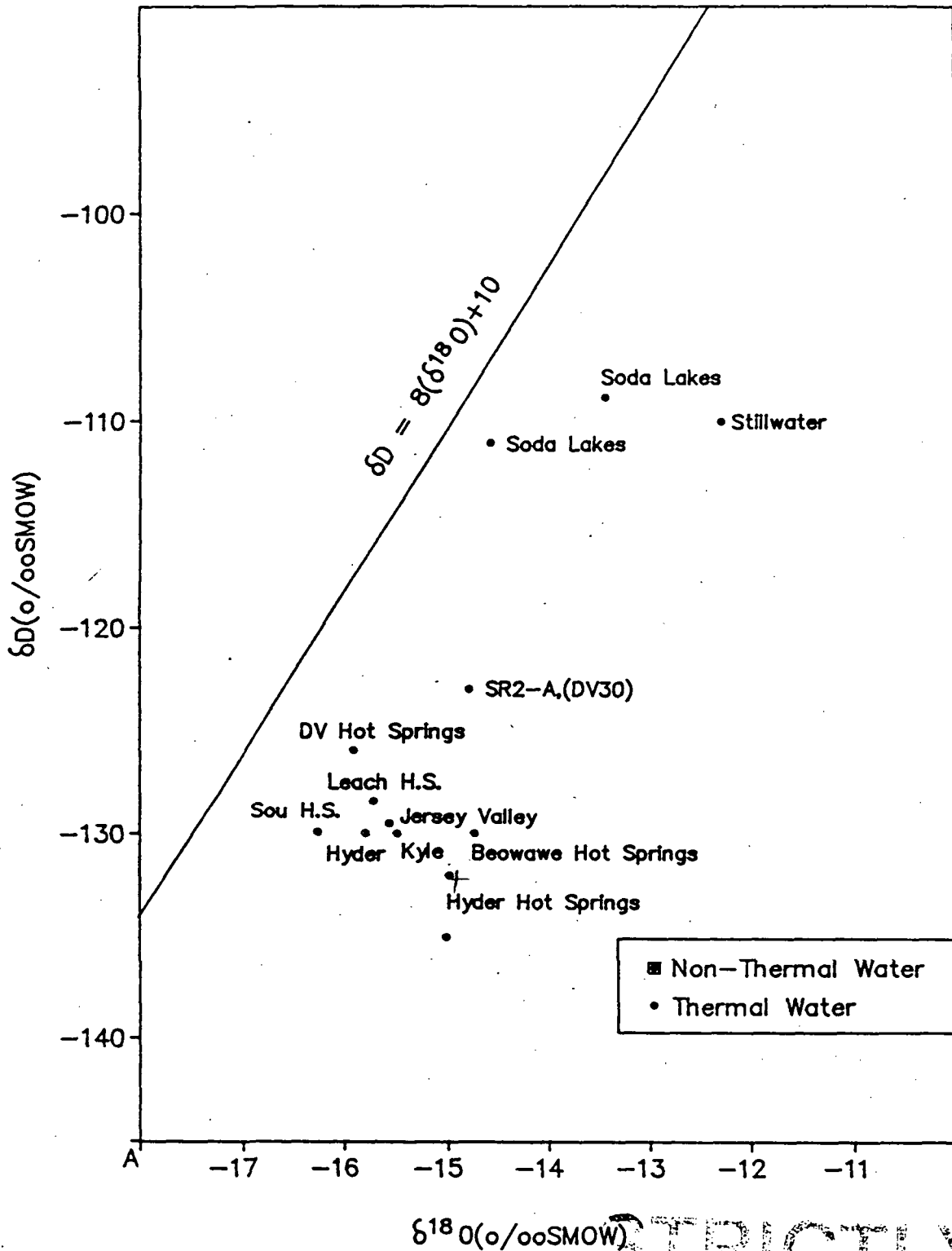
The geothermal fluids have consistently greater negative deuterium values (i.e., "lighter") than those for the nonthermal waters from the nearby eastern slope of the Stillwater Range or the Clan Alpine and Augusta Mountains (Figure 4.2.3). A similar isotopic relationship between thermal and nonthermal waters was observed by Welch *et al.* (1981) at the Leach Hot Springs in southern Grass Valley, 48 miles north of the Dixie Valley reservoir. Welch *et al.* (1981) suggest that this isotopic disparity either results from modern-day recharge from precipitation at an elevation higher than that in the immediate vicinity of the Leach Hot Springs or the present discharge was recharged during an earlier, colder climatic period.

Elevation zones where modern precipitation would have the same deuterium value as the Leach Hot Springs are so far away (100 miles) that under a flow rate of 30 feet/year, the infiltration event could have occurred up to 16,000 years ago and thus the recharge water still would be considered "paleowater" (Welch *et al.*, 1981). Young and Lewis (1980) suggest present-day discharge from the Bruneau-Grand View geothermal system in Idaho was recharged during late Pleistocene glacial advances when the climate averaged 6-10 deg.F colder than at present.

# Dixie Valley Oxygen and Deuterium Isotope Values Thermal, Non-Thermal & Geothermal Wells

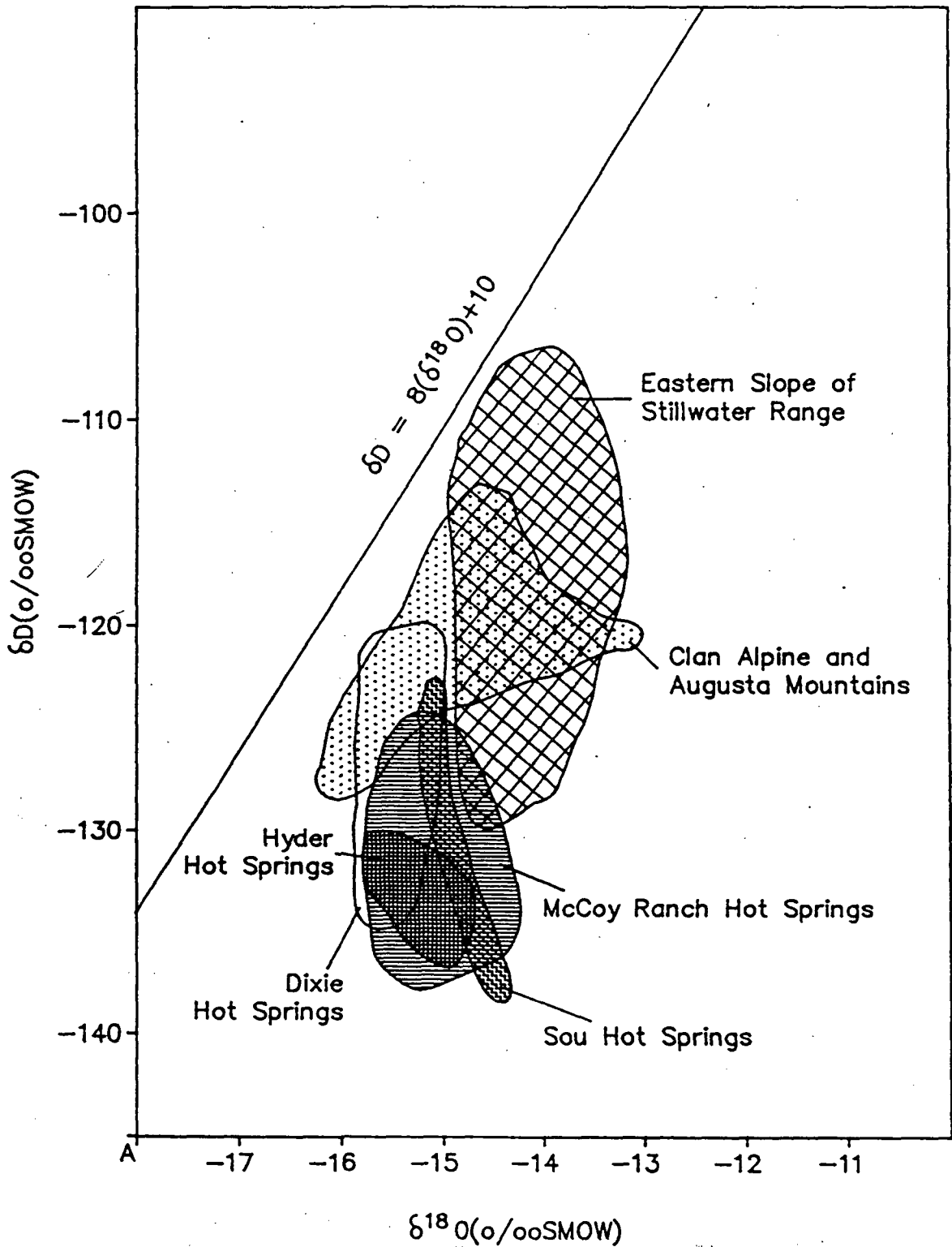


# Regional Oxygen and Deuterium Isotope Values



STRICTLY

# Local Oxygen and Deuterium Isotope Values



The deep Dixie Valley geothermal system presents the same situation. The closest mountains significantly higher than the 8,000-9,000 foot heights of the Stillwater and Clan Alpine Ranges are in the Toiyabe Range, some 60 miles to the east. The climatologic influence may therefore be the dominant factor in creating the regional isotope characteristics, as at Bruneau-Grand View. Lower average temperatures during the late Pleistocene, when Lake Lahontan reached its maximum extent and abundant surface water was available for recharge of deep aquifers, may have resulted in the isotope characteristics of the thermal waters now observed throughout the region.

#### 4.3 Carbon and Sulfur Isotopes

Geothermal well fluids, hot springs waters, and rock chip cuttings from geothermal production zones were analyzed for the  $^{13}\text{C}/^{12}\text{C}$  and  $^{34}\text{S}/^{32}\text{S}$  isotope ratios. A gas sample from well 27-33 was analyzed for  $^{14}\text{C}$ , hydrogen/deuterium, and  $^{15}\text{N}/^{14}\text{N}$  isotope analysis.

The stable isotopes of carbon and sulfur can be used in a general manner to delineate separate or common subsurface flow systems, much in the same manner as the hydrogen/deuterium and  $^{18}\text{O}/^{16}\text{O}$  isotope data.

As with the hydrogen/deuterium data, the carbon and sulfur isotope data suggest, in a very broad manner, a common flow path, in part, between the Hyder and Sou Hot Springs and the deep high temperature geothermal system in Dixie Valley. A regional flow system can be inferred from the data but the volumetric extent of such a system remains unquantified.

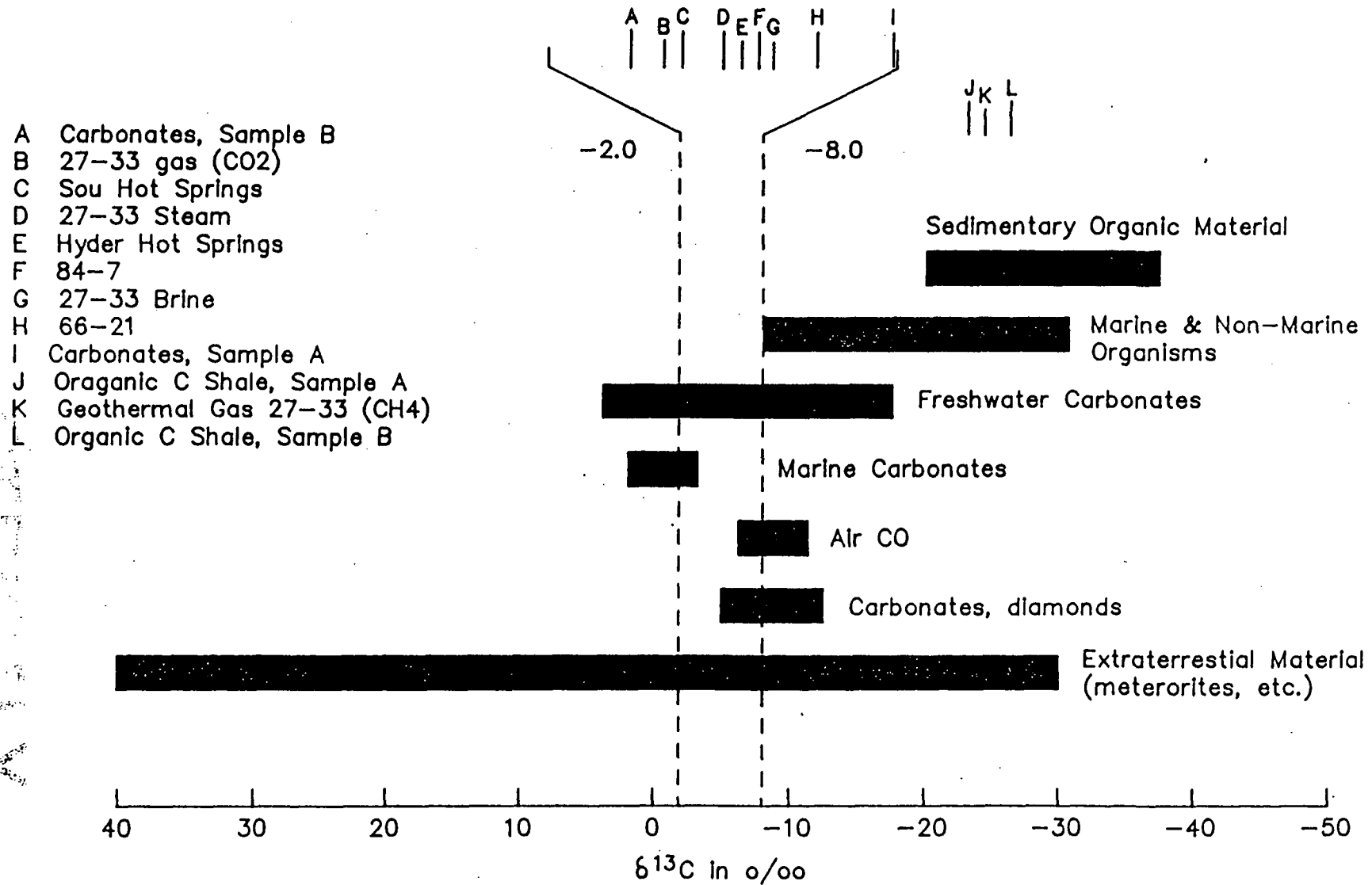
#### Carbon Isotope Data

The  $^{13}\text{C}/^{12}\text{C}$  ratios for the carbonate ions in the geothermal fluids from the deep geothermal wells and the hot springs show a tight clustering around a  $^{13}\text{C}$  value of  $-5.0$  ‰ (Fig. 4.3.1) The absolute difference between geothermal wells 27-33 and 84-7 and the Sou and Hyder Hot Springs is less than  $2.0$  ‰. With well 66-21 included, the absolute difference is still less than  $3.0$  ‰. Thus, like the similarity of the deuterium values, the similarity of the carbon isotope values suggests a common factor between the high- and low-temperature geothermal systems in northern Dixie Valley.

Two rock chip samples (A and B) were analyzed for their carbon and sulfur isotope ratios. The samples consisted of shale cuttings from the Favret Formation from wells 62-21



# $^{13}\text{C}/^{12}\text{C}$ Ratios for Geothermal Wells & Hot Springs Compared to Ratios in Geologically Important Materials



and 45-33 (Al Waibel, personal communication). Sample B with a  $^{13}\text{C}$  value of  $-3.4$  ‰ and Sample A with a  $^{13}\text{C}$  value of  $-7.9$  ‰ completely bracket the carbon isotope values for the sampled geothermal fluids (Fig. 4.3.1). A possible conclusion is that both the high and low-temperature geothermal systems have reached a carbon isotopic equilibrium with the carbonate minerals in the Favret Formation.

Carbon isotopes were determined from carbon dioxide ( $\text{CO}_2$ ) and methane ( $\text{CH}_4$ ) from well 27-33. For the  $\text{CO}_2$  the  $^{13}\text{C}$  value is  $-4.0$  ‰. This is within the values measured from the liquid phase and indicates a  $\text{CO}_2$  (gas)/ $\text{HCO}_3$  (liquid) equilibrium.

The  $\text{CO}_2$  gas from well 27-33 also was analyzed for a  $^{14}\text{C}$  age determination. The activity level of the  $^{14}\text{C}$  was below the detection limit of 1.2% of the standard activity. The age is therefore greater than 35,700  $^{14}\text{C}$  years before present (Geochem Laboratories Division of Krueger Enterprises Inc., rpt. of 6/9/86).

The  $^{13}\text{C}$  value for the  $\text{CO}_2$  gas radiometrically dated was  $-4.1$  ‰, almost identical to the  $^{13}\text{C}$  value of  $-4.0$  ‰ previously mentioned. These values are close enough to the  $^{13}\text{C}$  values from the liquid phase to be considered representative of the unflushed geothermal fluid.

Carbon in the methane gas has a  $^{13}\text{C}$  value of  $-23.8$  ‰. This is very close to and bracketed by the values for organic carbon in the Favret Formation shale cuttings. Samples A and B had  $^{13}\text{C}$  values of  $-25.4$  ‰ and  $-22.8$  ‰ respectively. This suggests the methane is a product of the thermal maturation of organic carbon in the Favret Formation.

The similar  $^{13}\text{C}$  values for both the deep high-temperature fluids and the hot springs fluids suggest a similar source environment for fluids from both systems. This is consistent with the deuterium values for the two systems as discussed above. The similarity suggests a common regional factor which may be the Favret Formation where the  $^{13}\text{C}$  values for two geothermal production zone cuttings narrowly bracket the  $^{13}\text{C}$  values for geothermal fluids from both the deep high-temperature system and the hot springs. Such a concurrence may result from the deep geothermal system and the hot spring fluids coming into  $^{13}\text{C}$  isotopic equilibrium with that of the Favret Formation during their subsurface circulation.

## Sulfur Isotope Data

The sulfur isotope data are presented in Figure 4.3.2. Once again there is a tight grouping of isotope values for both the deep geothermal system and the hot springs. Well 27-33 is the "heaviest" with a  $^{34}\text{S}$  value of +20.6 ‰. The other geothermal fluids are clustered around a  $^{34}\text{S}$  value of +15 ‰.

Sulfides from the Favret shale cuttings were analyzed for their  $^{34}\text{S}$ . These samples are significantly depleted in  $^{34}\text{S}$  relative to the fluid samples. The sulfides have  $^{34}\text{S}$  values ranging between +3.4 ‰ and -2.3 ‰.

The difference between fluid and mineral  $^{34}\text{S}$  isotopic values may be related to temperature-dependent fractionation processes. Hoefs (1980) reviewed the literature and noted several papers that suggested that at high temperatures isotopic exchange should lead to sulfides being depleted in  $^{34}\text{S}$  up to 75% relative to sulfates. The Dixie Valley data agree with such a temperature-dependent fractionation process. The  $^{34}\text{S}$  isotope values for the sulfide minerals in the geothermal production zones are from 12% to 23% lighter than the  $^{34}\text{S}$  values from the sulfate ions in the deep geothermal fluids from wells 27-33 and 84-7.

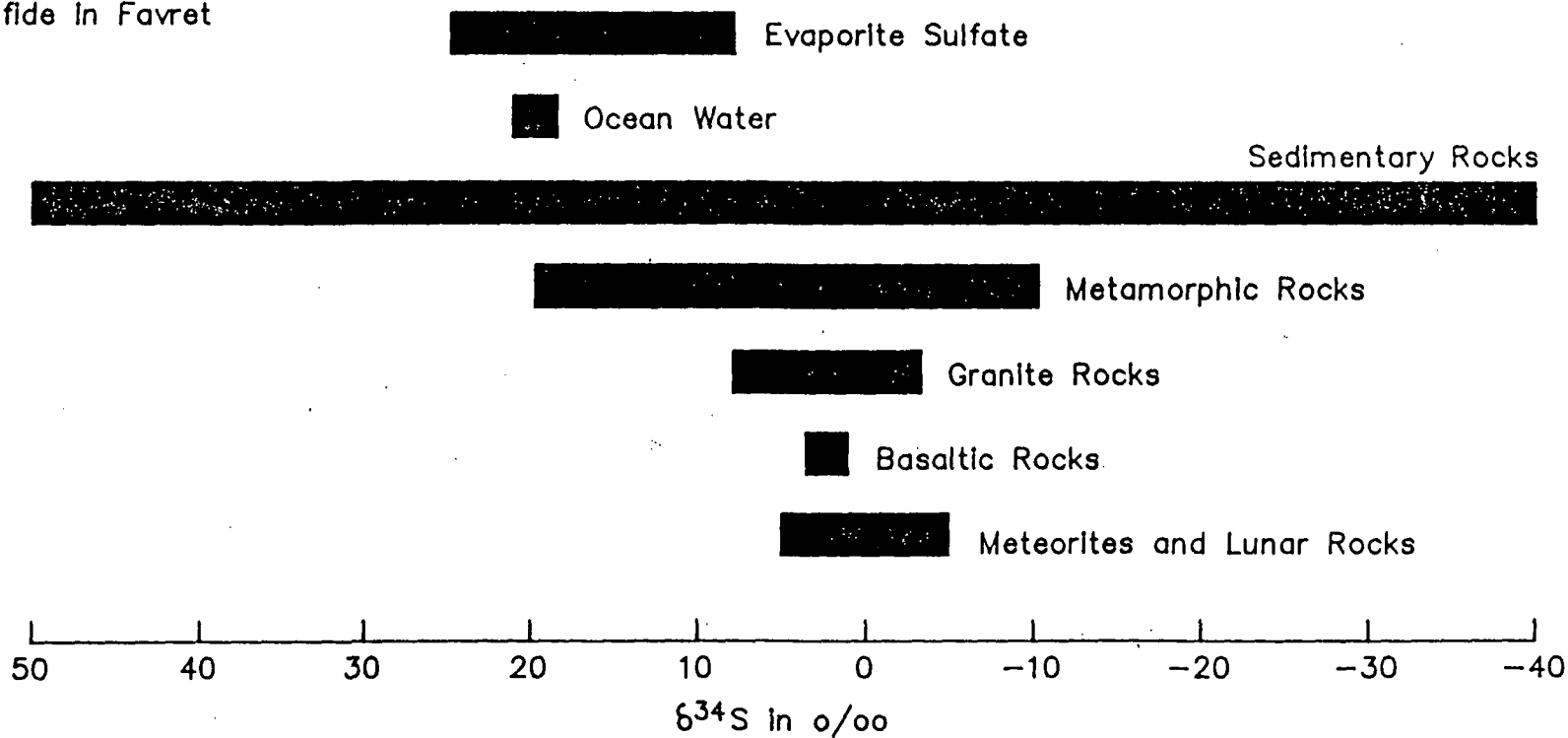
Note that the relative difference between  $^{34}\text{S}$  values for the sulfide minerals and those for the sulfate minerals in geothermal fluids decreases directly as the predicted maximum subsurface temperatures decrease. The maximum difference is found in 27-33 where the maximum predicted temperature is 459 F by both the quartz and the Na/K geothermometers (Table 5.2). Sou Hot Springs, with the smallest relative difference, 11%, has a maximum predicted geothermal temperature of only 237 deg.F. No sulfide minerals from the Sou Hot Springs deposits have been analyzed for their  $^{34}\text{S}$  values. If there were subsurface mixing between thermal and non-thermal waters this could possibly alter the isotope ratios.

Although the sulfur isotope data are not as amenable to interpretation as the carbon isotope data, a generalized interpretation is consistent with that given for the carbon isotope data. Where the higher temperature fluids are in contact with sulfide-bearing minerals, the sulfide minerals are depleted in  $^{34}\text{S}$  relative to the  $^{34}\text{S}$  isotope in the sulfate ions of the geothermal fluids. Lesser differences are noted between the sulfide minerals and the lower temperature hot spring fluids. Such relationships can exist if the hot spring fluids have circulated through the same

# $^{34}\text{S}/^{32}\text{S}$ Ratios for Geothermal Wells & Hot Springs Compared to Ratios in Geologically Important Materials

A      B C D      E      F G  
 ↑      | | |      |      | |

- A 27-33
- B 84-7 and 66-21
- C Hyder Hot Springs
- D Sou Hot Springs
- E Sulfide Favret
- F Sample A Cds
- G Sulfide In Favret



sulfide-bearing Favret Formation shale but at lower temperatures than the deep high-temperature geothermal fluids. *- great, source of reality*

Based on the isotopic data, it is possible to conclude that the potential recharge area for the deep geothermal system in Dixie Valley is regional in extent. In theory, any body of water in northern Nevada has the hydraulic potential to recharge the geothermal system. Ongoing tectonic activity is capable of maintaining deep, permeable flow paths for recharge.

Isotope data suggest a long-lasting system with present discharge having been recharged at least 35,000 years ago. Source rock for transport and storage of the recharge fluid may be early Mesozoic carbonates and shales which extend over thousands of square miles in west-central Nevada. Isotopic patterns of recharge correspond well with the regional hydrologic setting of the geothermal system as described below.

#### 4.4 Deep Temperature Profiles

Static temperature profiles for the production wells (Figures 4.4.1-4.4.11) are characteristic of conductive heat flow from the producing fractures at depths of 7000 to 10,000 feet up to the surface. Only the section 18 wells have convecting zones and these are the producing zones near the bottom of the wells.

Thermal gradients for all the productive wells with the exception of 45-33 are tightly grouped around the average gradient of 4.7 deg.F/100 feet (Fig 4.4.12). Well 45-33 has a significantly lower conductive gradient of 4.2 deg.F/100 feet in the vertical portion of the hole to a depth of 7530 feet. The vertical open-hole leg of this well encountered very low fracture permeability in the range-front fault fracture system in contrast to other production wells. The low thermal gradient is consistent with the drilling results and indicates that the wellhead location is over a part of the range-front fault which is effectively sealed and does not contain an active hydrothermal system. Production from 45-33 is encountered in the deviated open hole at a horizontal distance of 1600 feet southwestward from the surface location at a depth of approximately 9500 feet (Fig. 2.2).

The absence of significant changes in slope, reversals, and isothermal intervals in the production well temperature profiles indicates that no major outflow zones exist below a

# Temperature/Pressure Survey

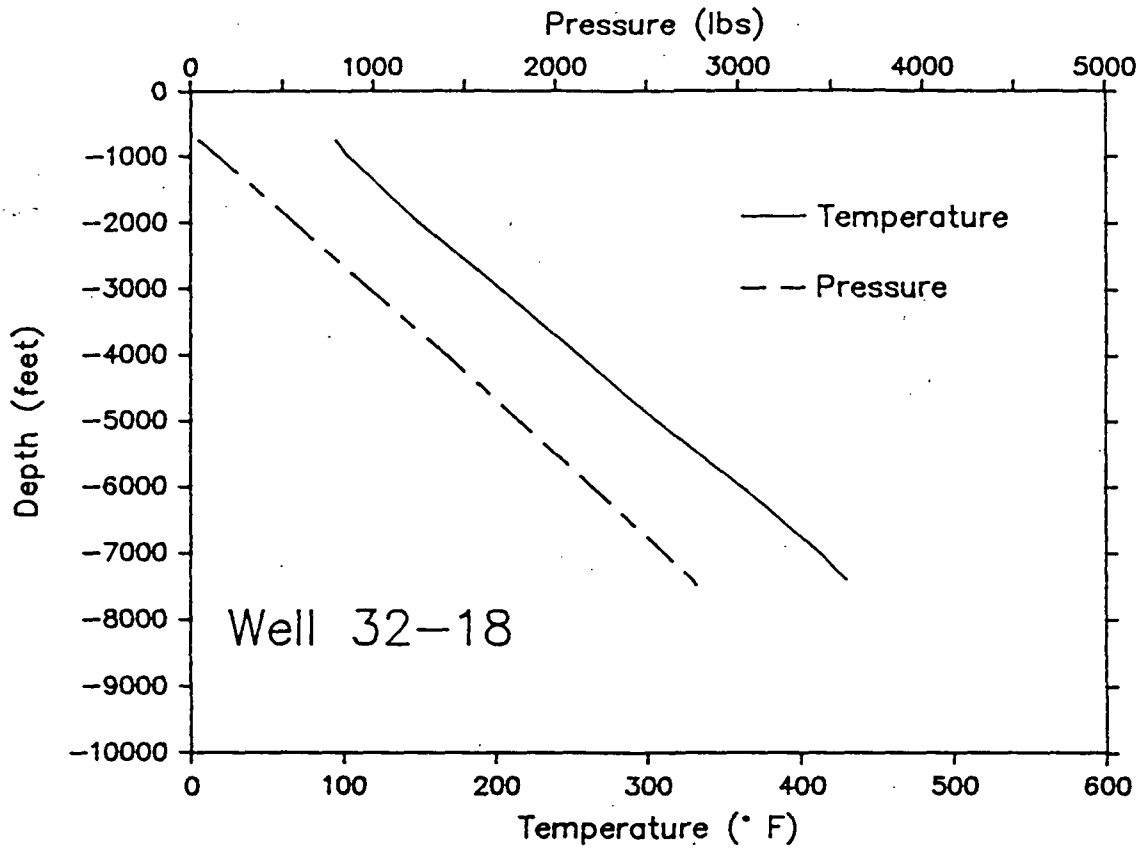


Figure 4.4.1

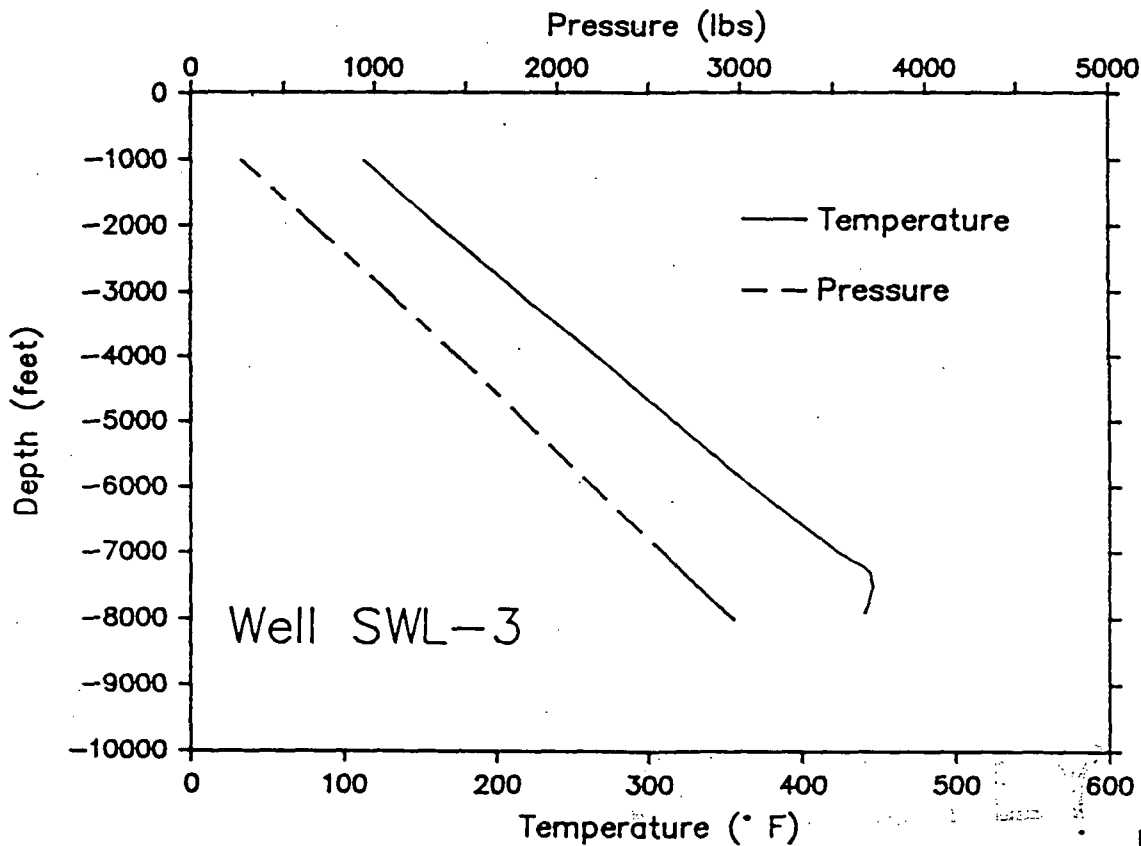


Figure 4.4.2

# Temperature/Pressure Survey

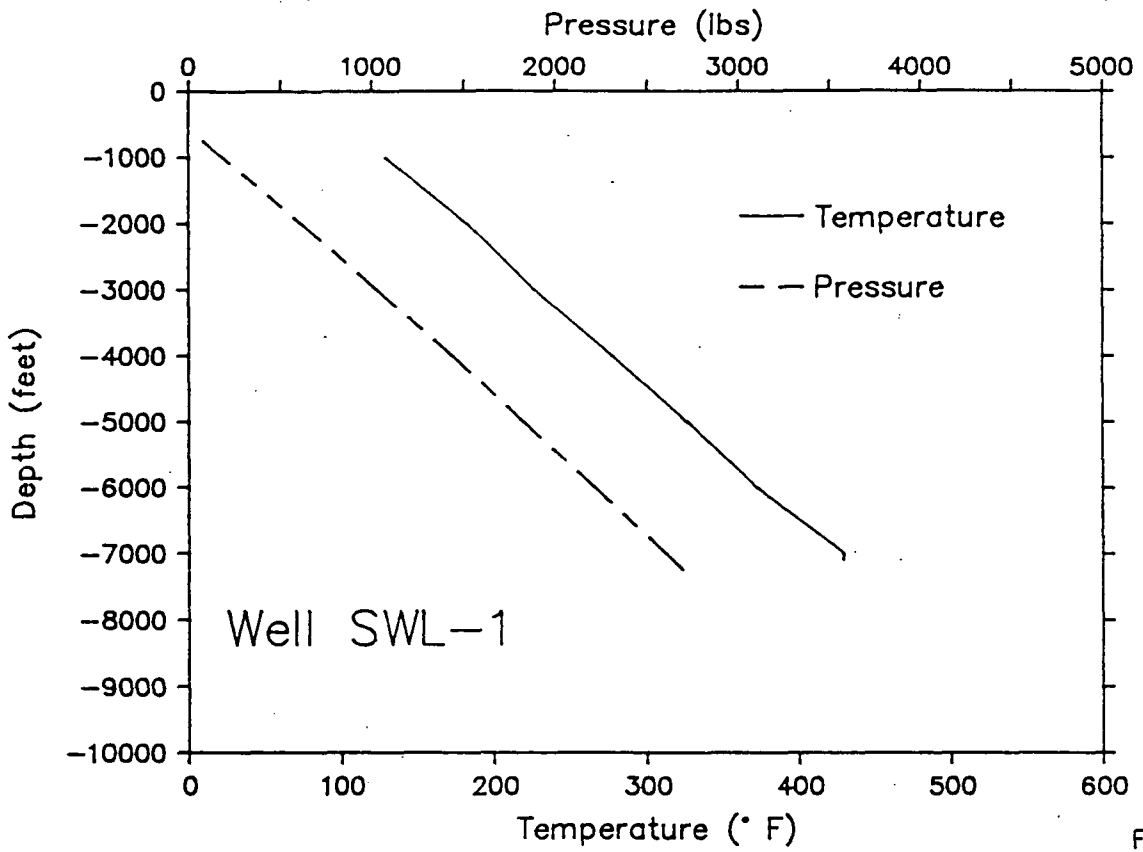


Figure 4.4.3

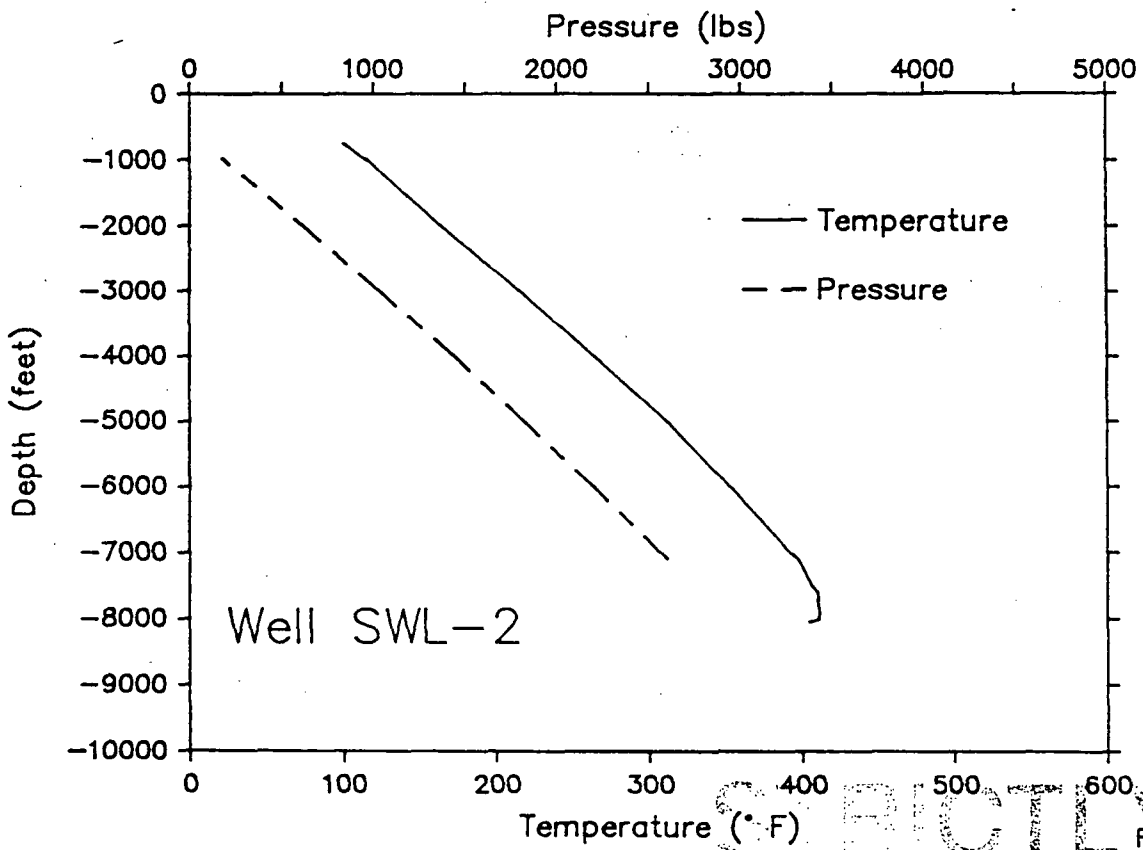


Figure 4.4.4

# Temperature/Pressure Survey

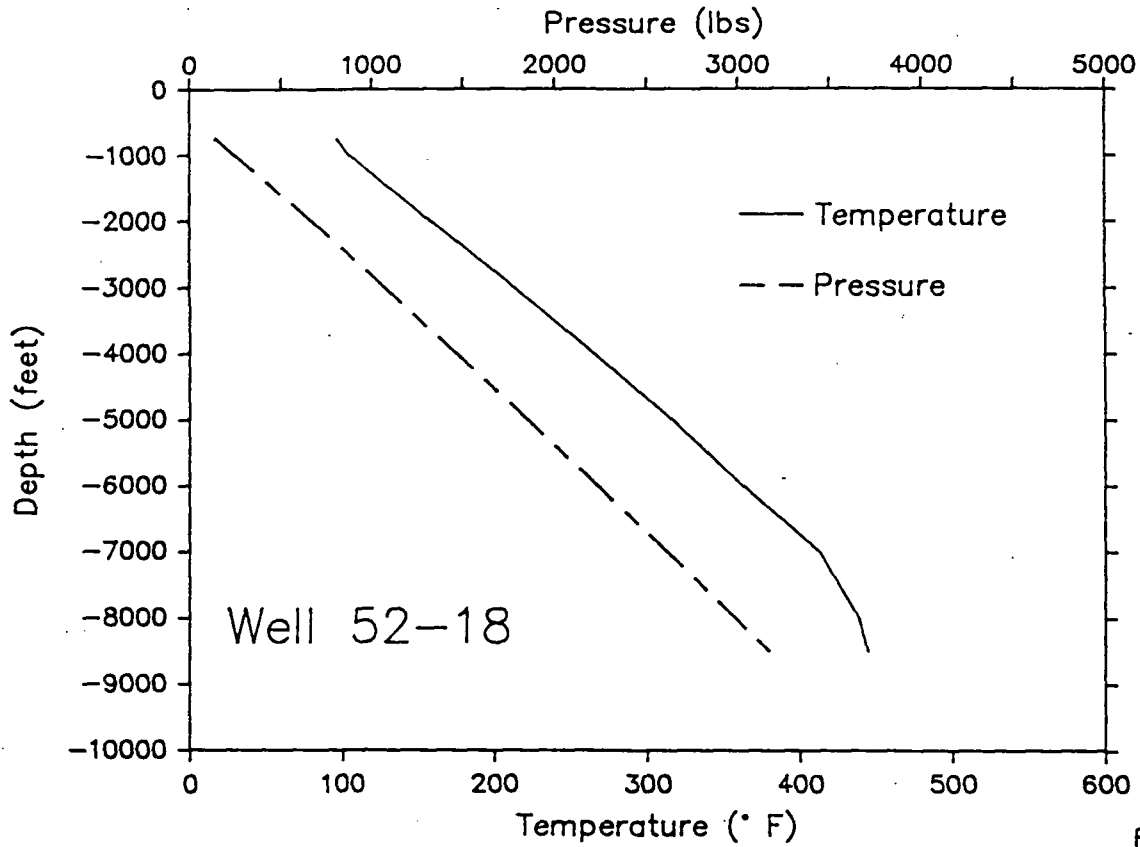


Figure 4.4.5

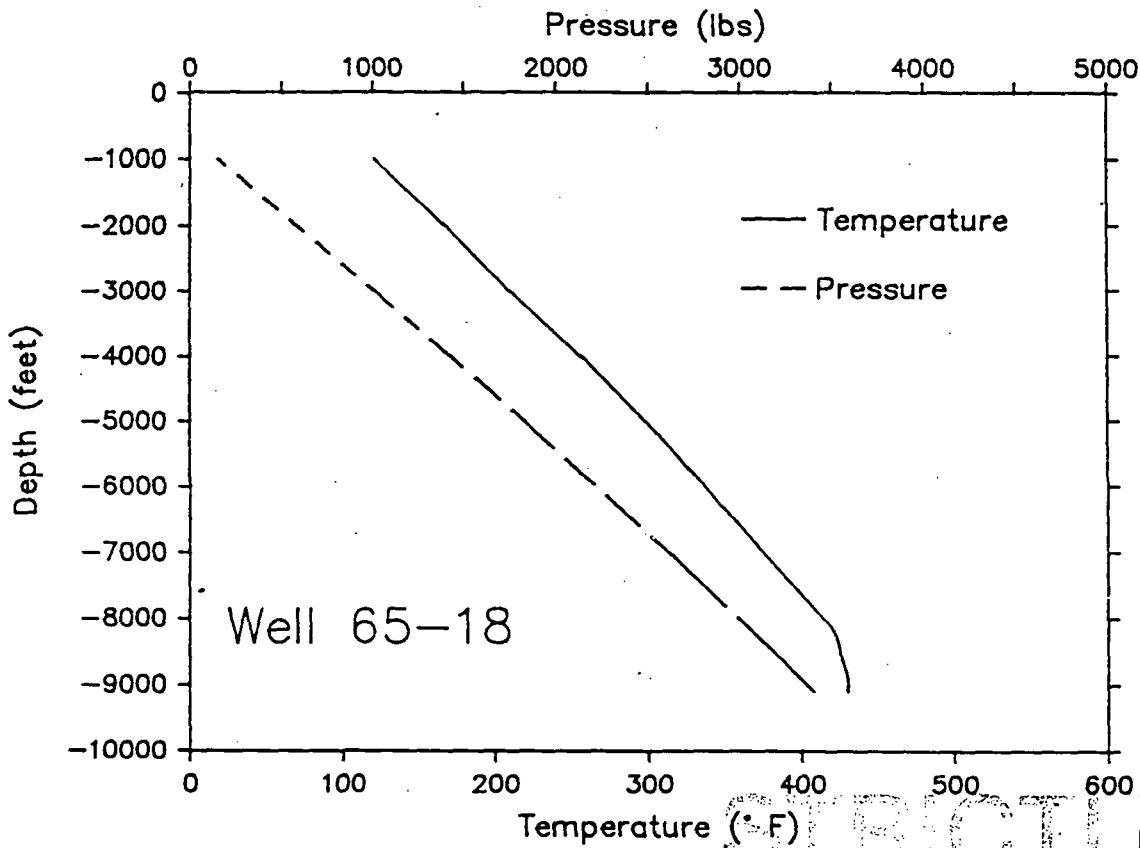


Figure 4.4.6

STRICTLY  
CONFIDENTIAL



# Temperature/Pressure Survey

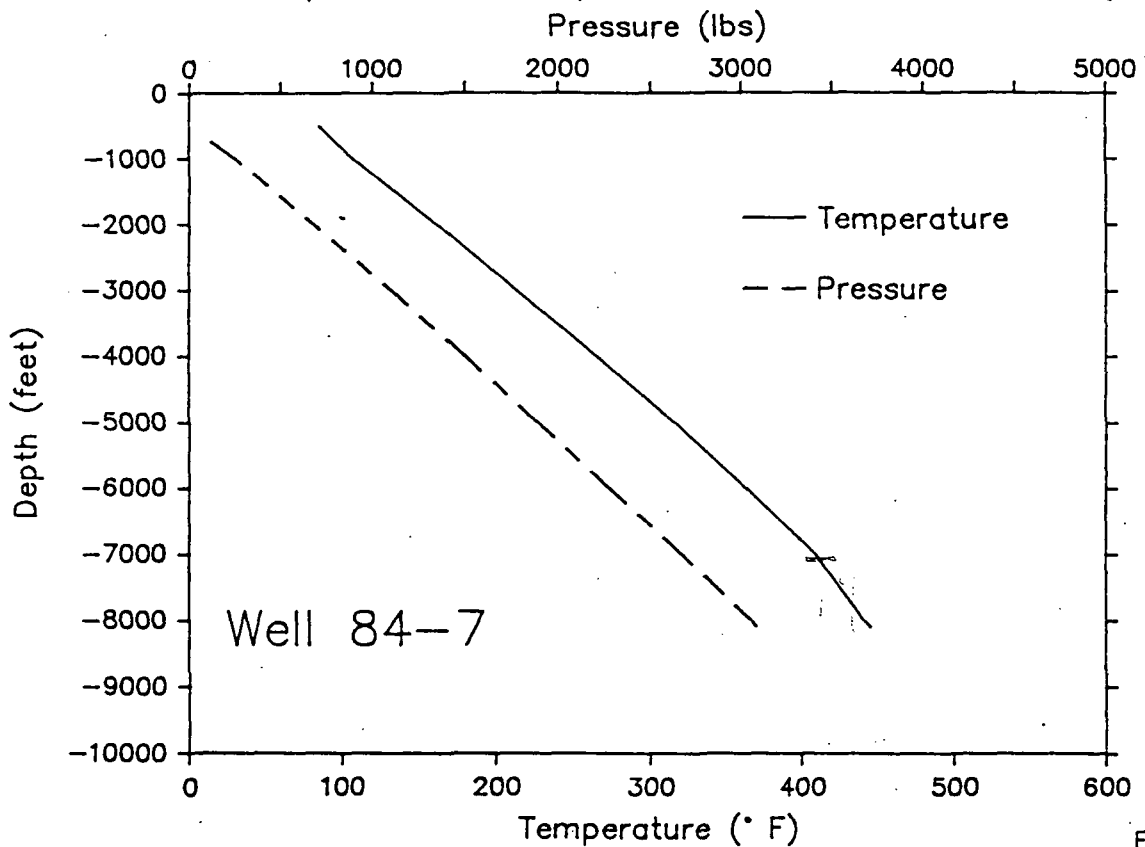


Figure 4.4.7

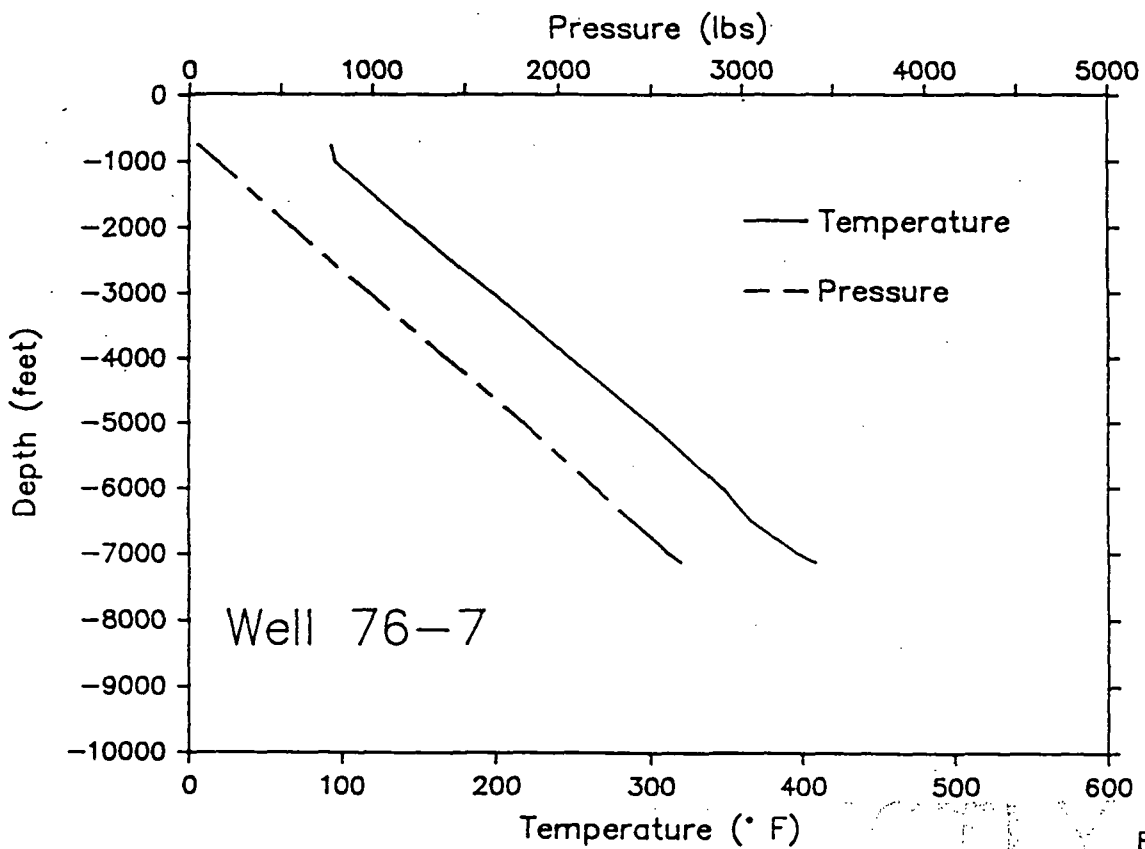


Figure 4.4.8

# Temperature/Pressure Survey

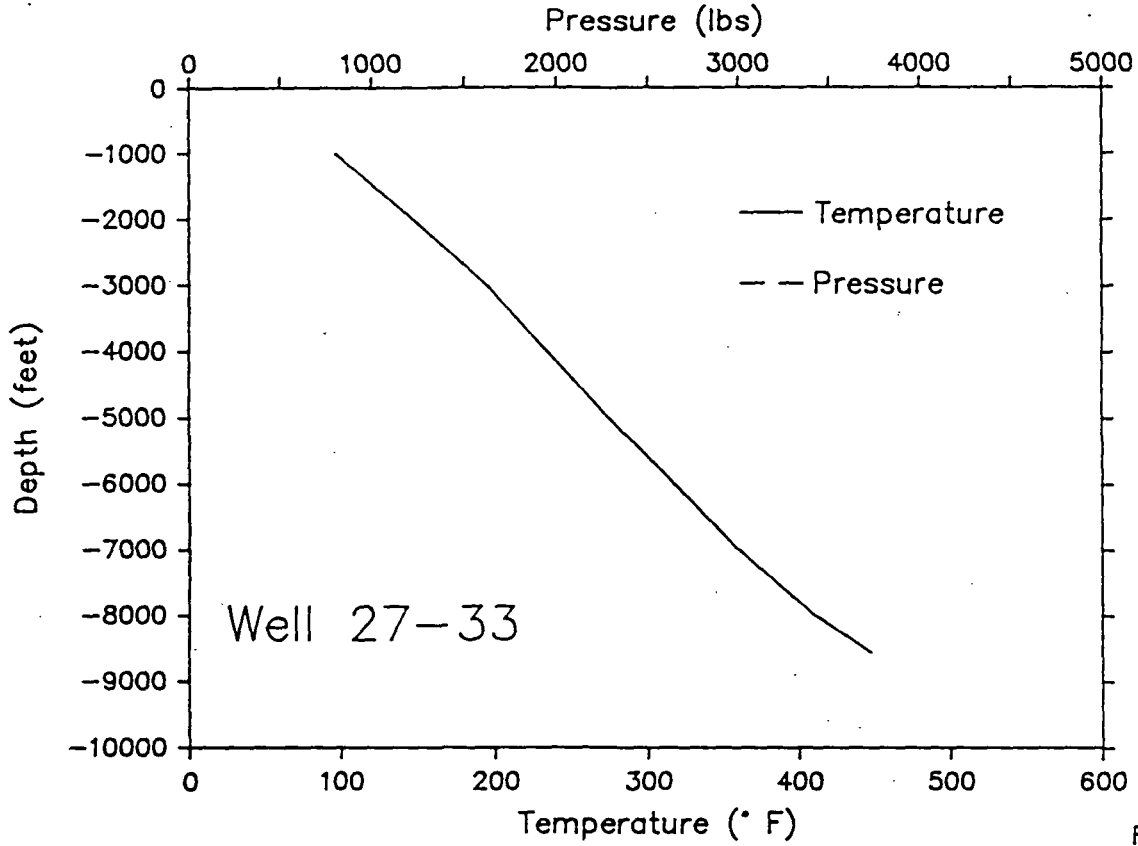


Figure 4.4.9

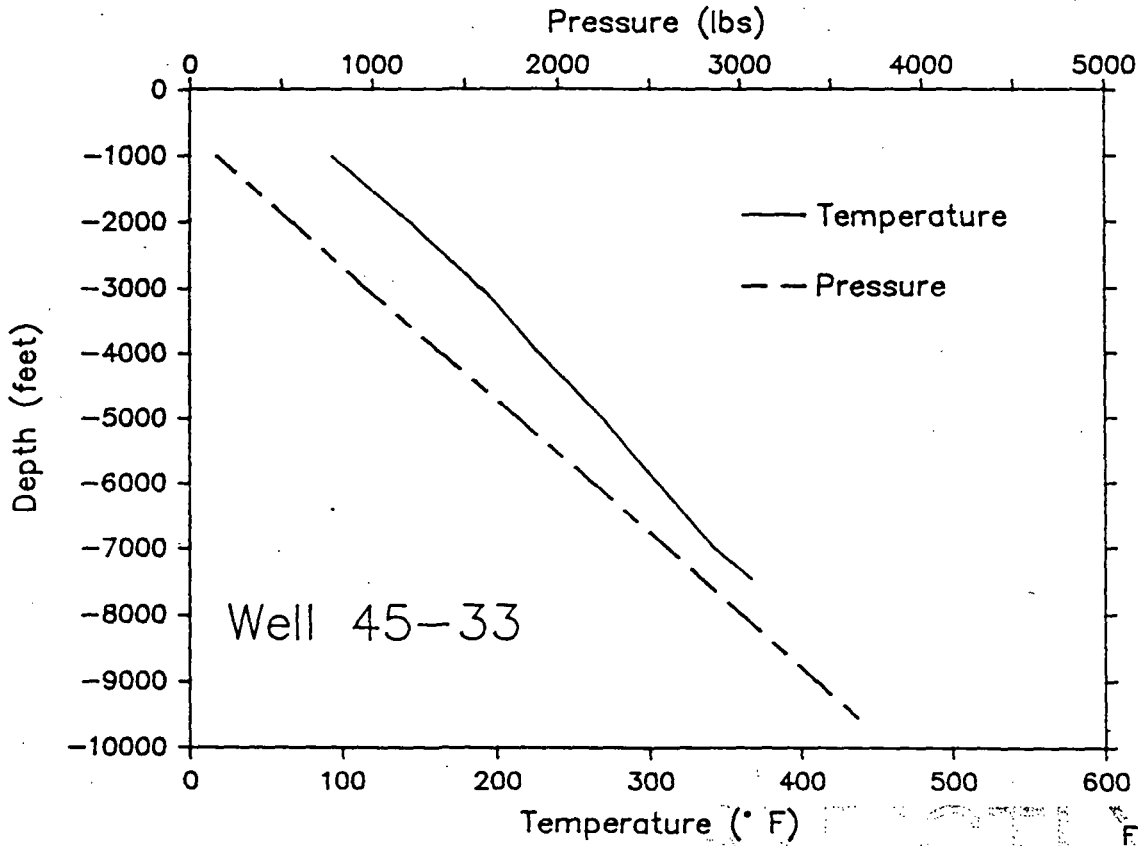
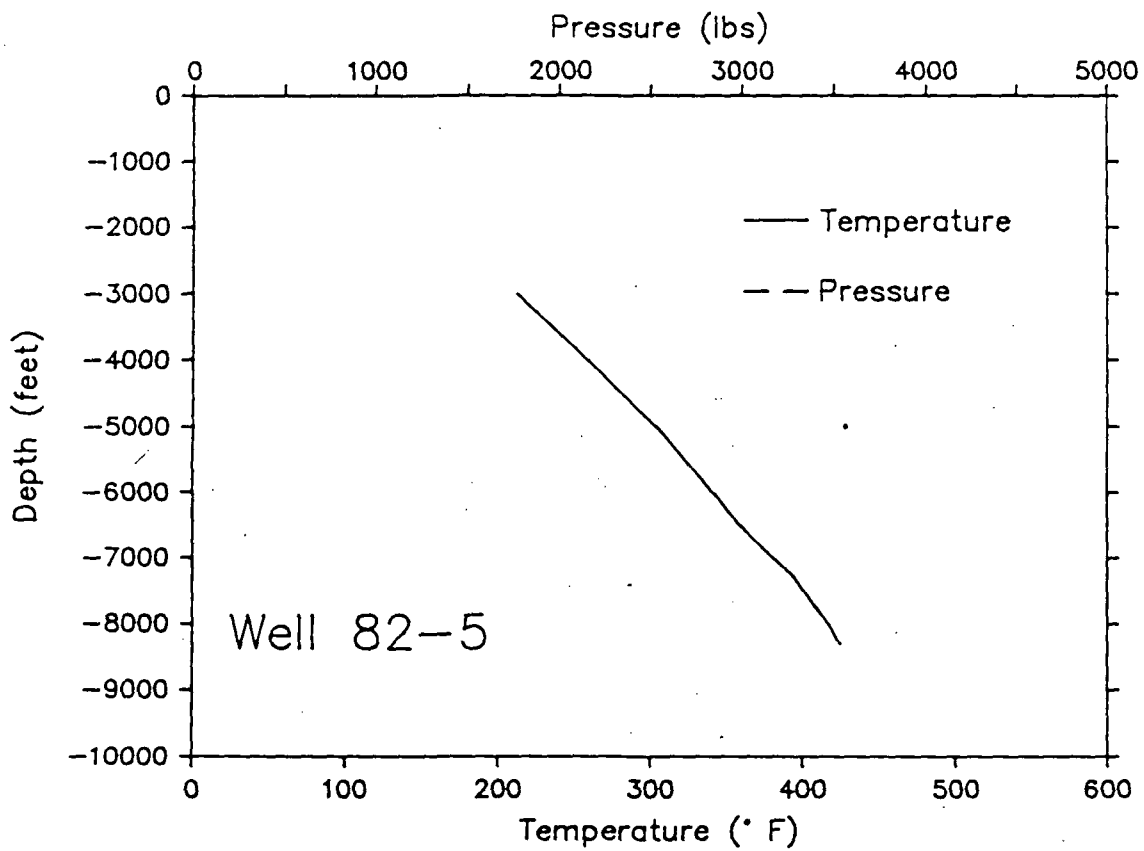
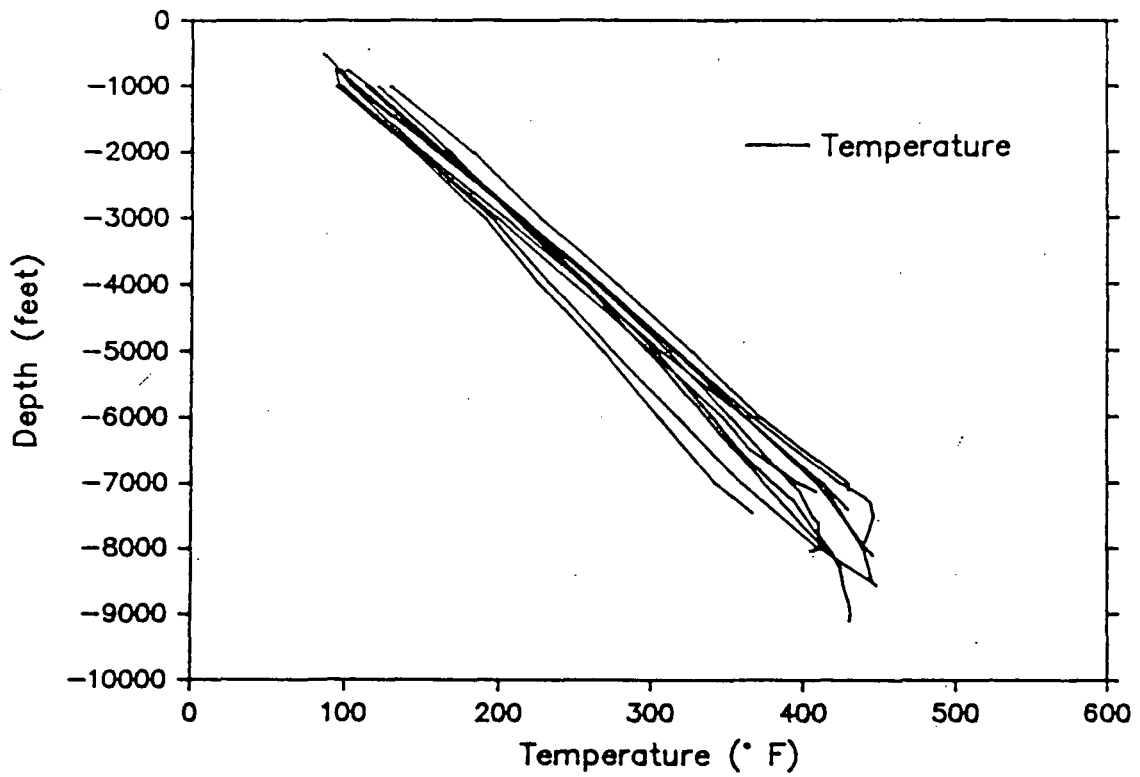


Figure 4.4.10

# Temperature/Pressure Survey



# Temperature Survey Section 18, 7, 5, and 33 Wells



depth of 1000 feet that would allow significant hot fluid transport away from the range-front fault. This observation is consistent with the lack of fluid entries during air drilling and the absence of fluid loss during mud drilling through several thousand feet of Quaternary-Tertiary sediments and volcanoclastics.

#### 4.5 Deep Hydrostatic Pressure Distribution

The regional distribution of hydrostatic pressure at a depth of 5000 feet below mean sea level (MSL) is shown in Figure 4.5. Static pressure profiles for production wells are shown in Figure 4.4.1-4.4.11. Static reservoir pressures within the high temperature production zones of the Dixie Valley reservoir range from 3130 to 3160 psi. Wells 62-21 and 66-21, which lie 3-5 miles away from the productive part of the field, have pressures at the -5000 foot MSL datum of 3631 and 3440 psi respectively. Geothermal production wells to the west of the Stillwater Range in and around the Carson Sink have pressures within the range of 62-21 and 66-21 (Figure 4.5). This indicates that the deep geothermal waters outside the highly permeable Dixie Valley production zones are in regional pressure equilibrium over an area of several thousand square miles.

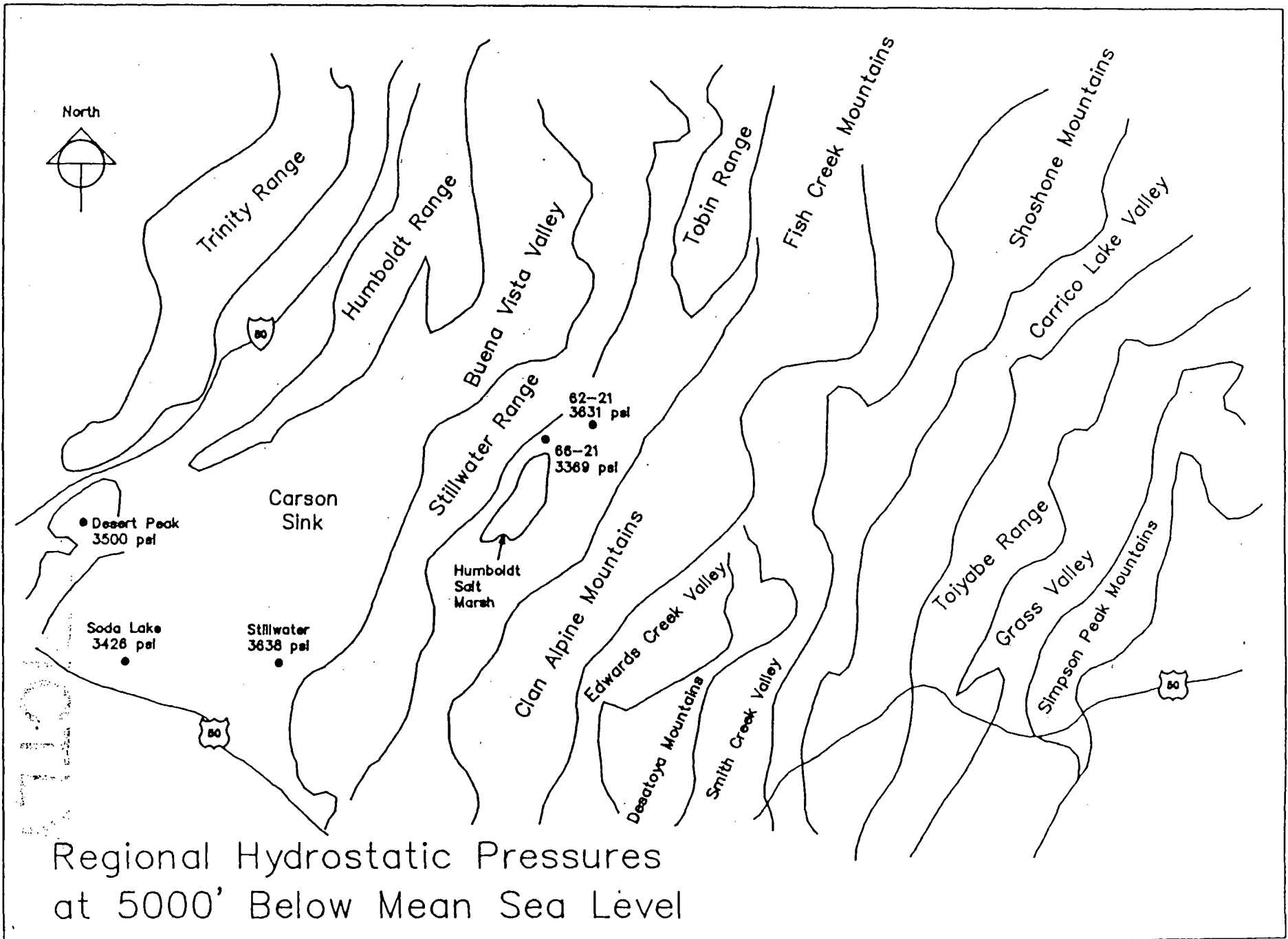
The static temperature gradients observed in 62-21 and deep wells drilled in the Carson Sink area range from 2.7 to 3.0 deg.F/100 feet. Water stored below a depth of 14,000 feet below MSL will obtain a temperature of 480 deg.F which is characteristic of the high-temperature fluid produced from the Dixie Valley reservoir. The regional geologic cross section (Fig 3.1) shows that much of the Triassic-Jurassic marine sedimentary section in west-central Nevada lies at a depth below the 480 deg.F isotherm.

Non-thermal groundwater as observed in irrigation wells in the vicinity of the geothermal reservoir has a projected hydrostatic pressure of 3621 psi at the -5000 foot datum which indicates that the shallow groundwater aquifers are in hydrostatic equilibrium with the deep aquifers penetrated in 62-21 and by wells in the Carson Sink.

The regional and local pressure data therefore demonstrate that the high-temperature production zones of the Dixie Valley reservoir have pressures 300 to 500 psi below the regional and shallow groundwater pressures extrapolated to production depths.

*Pressure - hydro head, 8000 ft*

*hi T, low P*



#### 4.6 Thermo-artesian Pressure Gradients

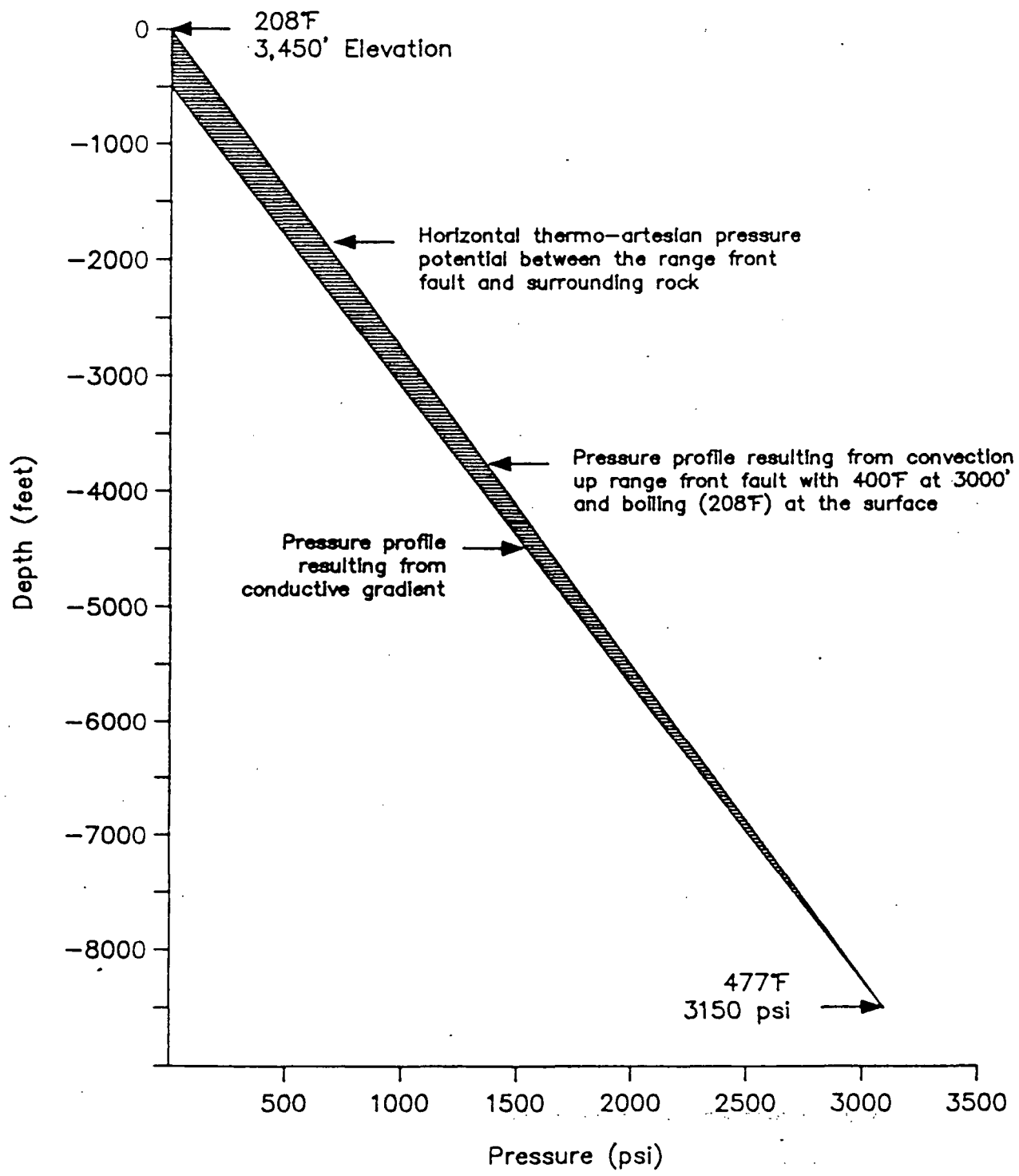
Penetration of geothermal fluid with an initial temperature of 480 deg.F to shallow depths along the range-front fault fracture system can create significant pressure gradients between fluid in the fracture system and fluid in the surrounding aquifers. This mechanism for developing a local horizontal pressure differential is shown graphically in Figure 4.6. Temperatures in excess of 400 deg. F. measured in well 45-5 at a depth of 5700 feet and near-surface boiling water that supplies steam to Senator Fumarole demonstrate that high-temperature fluid does penetrate to the near-surface along the range front fault.

Penetration of high temperature to shallow depths creates higher pressures within the range-front fracture system in comparison to the surrounding cooler aquifers despite the low reservoir pressure feeding the fractures from below. Because these pressures exceed the local groundwater hydrostatic pressures at all depths above the reservoir (Fig. 4.6), water penetrates from the fracture system into the surrounding aquifers. Evidence for this outflow is seen in the chemistry of shallow warm aquifers overlying the reservoir. Elevated levels of K, Si, B, Li, Sr, NH<sup>+</sup>, Cl, and F clearly show mixing of high-enthalpy fluid from the high temperature reservoir with shallow ground water (Johnson, personal communication).

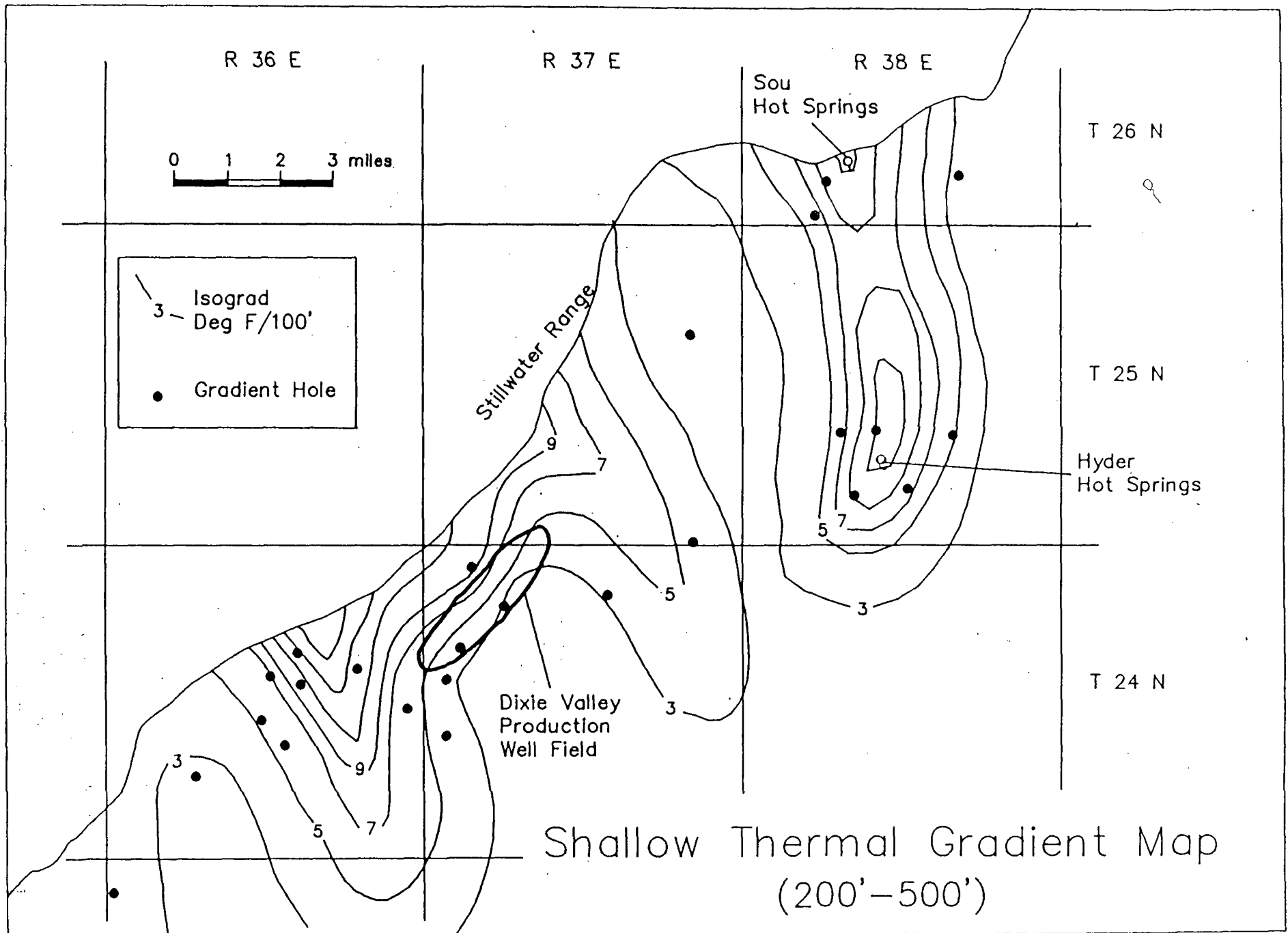
#### 4.7 Shallow Thermal Anomalies

Shallow thermal anomalies overlying and surrounding the Dixie Valley reservoir are evidence for hot water discharge from the deep geothermal system into the shallow alluvial aquifers. Heat flow anomalies that may represent leakage of fluid from the deep reservoir are defined by the 4 deg.F/100 isograd measured to a depth of 500 feet as shown in Fig. 4.7. The anomaly which surrounds the Dixie Valley geothermal reservoir exhibits two southeast trending lobes with a total surface area of approximately 39 square miles. A separate anomaly associated with Sou and Hyder Hot Springs trends southward from the Sou Hills and has an areal extent of approximately 28 square miles. The combined area of these shallow anomalies is similar to other commercial geothermal reservoirs in Nevada though it may be of lower overall intensity. Desert Peak exhibits a heat flow anomaly of approximately 75 square miles contained within the 4 deg.F/100 feet isograd. The Stillwater anomaly has an area of 54 square miles within the 4 deg.F/100 feet isograd.

# Mechanism for Development of Thermo-Artesian Pressure in the Dixie Valley Reservoir







Morgan (1982) has calculated that the geothermal recharge to the Stillwater system is approximately 55 kg/sec. Approximately 2/3 of the heat contribution from this recharge is lost due to shallow (<2000 feet) subsurface flow and only 1/3 is lost due to conduction. Chemistry of the shallow thermal discharge zones in Stillwater is identical to that of the deep reservoir recharging the system. A major temperature reversal in the 900 to 1500 foot depth range is observed in all the Stillwater production wells. This discharge plume, defined both chemically and thermally, confirms Morgan's assertion that most of the heat loss from the system is due to shallow subsurface flow of reservoir fluid as opposed to conductive heat loss. The shallow thermal water in Dixie Valley, by contrast, contains only a small component of reservoir fluid which is estimated by Johnson (1986, personal communication) to be on the order of 5%. These shallow thermal waters must therefore acquire most of the observed heat through conductive heat contribution from the reservoir. The small chemical component of reservoir fluid in the shallow thermal water and lack of reversals or isothermal temperature profiles verify that the contribution of reservoir fluid to the shallow ground water system must be very small. Because the Dixie Valley near-surface thermal anomaly is primarily conductive, the actual throughput of reservoir fluid may only be a small fraction of the 55 kg/sec flow calculated for the Stillwater anomaly though it is of similar areal extent.

The Sou-Hyder thermal anomaly appears to be separated from the anomaly centered around the Lamb Ranch by a north-south trending strip of low heat flow one to three miles wide. However, stratigraphic continuity between the deep reservoir and the Sou-Hyder anomaly may provide a conduit for supplying water to the hot springs and surrounding area. Permeable Tertiary volcanic rocks that contain water at temperatures above 400 deg.F within the reservoir form a continuous pathway for hot fluids to migrate up-dip to the eastern and northern margins of the valley. These Tertiary volcanic and volcanoclastic units are located at a depth of 6000 to 8000 feet within the reservoir. The units are tilted upward to the east and surface close to Sou and Hyder Hot Springs. Southwest dipping step faults with tens to hundreds of feet of displacement in the Tertiary volcanic rocks allow thermal fluid moving northeastward to penetrate to the surface, creating the hot springs. Isotope data discussed previously indicate that the high-temperature reservoir fluid and fluid discharging from Sou and Hyder Hot Springs share some common ancestry.

#### 4.8 Summary and Conclusions Regarding the Hydrologic System

1. Hydrostatic pressures in the -5000 to -9000 foot MSL depth range within a radius of 3 to 5 miles of the Dixie Valley productive area are in equilibrium with regional thermal and non-thermal aquifers over an area of several thousand square miles.

2. Commercially productive high-temperature zones within the Dixie Valley geothermal field have hydrostatic pressures of up to 500 psi below those observed in the surrounding regional aquifers in the -5000 to -9000 foot MSL depth range.

3. Isotope data indicate that the high-temperature reservoir fluid is in equilibrium with Triassic-Jurassic carbonate rocks which are distributed over several thousand square miles surrounding the Dixie Valley reservoir. Much of this stratigraphic section is found at depths below the 480 deg.F isotherm over a large region surrounding the reservoir. The age of the fluid produced from these rocks is greater than 35,000 years.

4. Shallow thermal anomalies overlying and surrounding the Dixie Valley reservoir may represent discharge of high-temperature fluid from the deep production zones to the near-surface alluvial aquifers, though the actual discharge rate is small compared to other major Basin and Range hydrothermal systems.

5. Evapotranspirative potential of the Humboldt Salt Marsh and surrounding playas is several times greater than the total supply of groundwater and geothermal fluid to the basin.

6. Linear temperature profiles in production wells show the absence of significant hot water movement in the depth interval from 1000 feet to the production zones in the 7000 to 10,000 foot depth range.

#### 4.9 References

Cohen, P. and D. E. Everett, 1963, A brief appraisal of the groundwater hydrology of the Dixie Valley-Fairview Valley area, Nevada: Dept. of Conservation and Natural Resources, Ground-Water Resources Reconnaissance Series, Report 23.

Hoefs, J., 1980, Stable isotope geochemistry; Springer-Verlag, New York, New York, 208 p.

Morgan, D. S., 1982, Hydrogeology of the Stillwater geothermal area, Churchill County, Nevada:, USGS Open File Report 82-345.

Welch, A. H., Sorey, M. L., and Olmsted, F. H., 1981, The hydrothermal system in southern Grass Valley, Pershing County, Nevada: U. S. Geological Survey Open-File Report 81-915, 193 p.

Young, H. W., and Lewis, R. E., 1980, Hydrology and geochemistry of thermal ground water in southwestern Idaho and north-central Nevada: U. S. Geological Survey Open-File Report 80-2043, 40 p.

## 5. GEOCHEMISTRY

The deep wells at Dixie Valley produce fluids with a downhole enthalpy range of 405 to 462 btu/lb. These fluids are all fairly similar chemically but there are apparently real chemical differences between most of the wells. These differences can be used to formulate a geochemical model which can shed light on the origin of the different enthalpies. Enthalpy differences can be caused by conductive gain or loss of heat or by gain or loss of heat through mixing fluids with different enthalpies. An important subset of the latter method would be by the addition or loss of steam. The geochemical data from Dixie Valley indicate the enthalpy variations are the result of mixing of up to 5 separate fluids, each with a distinct enthalpy.

### 5.1 Analytical Quality

The available data from Dixie Valley are highly variable in quality. For many of the early analyses performed by SUNEDCO the sampling conditions were either not recorded or not passed on to Oxbow. The analytical quality of some analyses is in question as there are large variations between different labs. Some analyses are incomplete so that no charge balances can be performed to verify the analytical quality. Unfortunately several of the wells have not been recently tested so there has been no opportunity to obtain data of a higher quality. Consequently, use of this earlier data is limited to calculation of ratios of conservative elements which are not affected by steam separation.

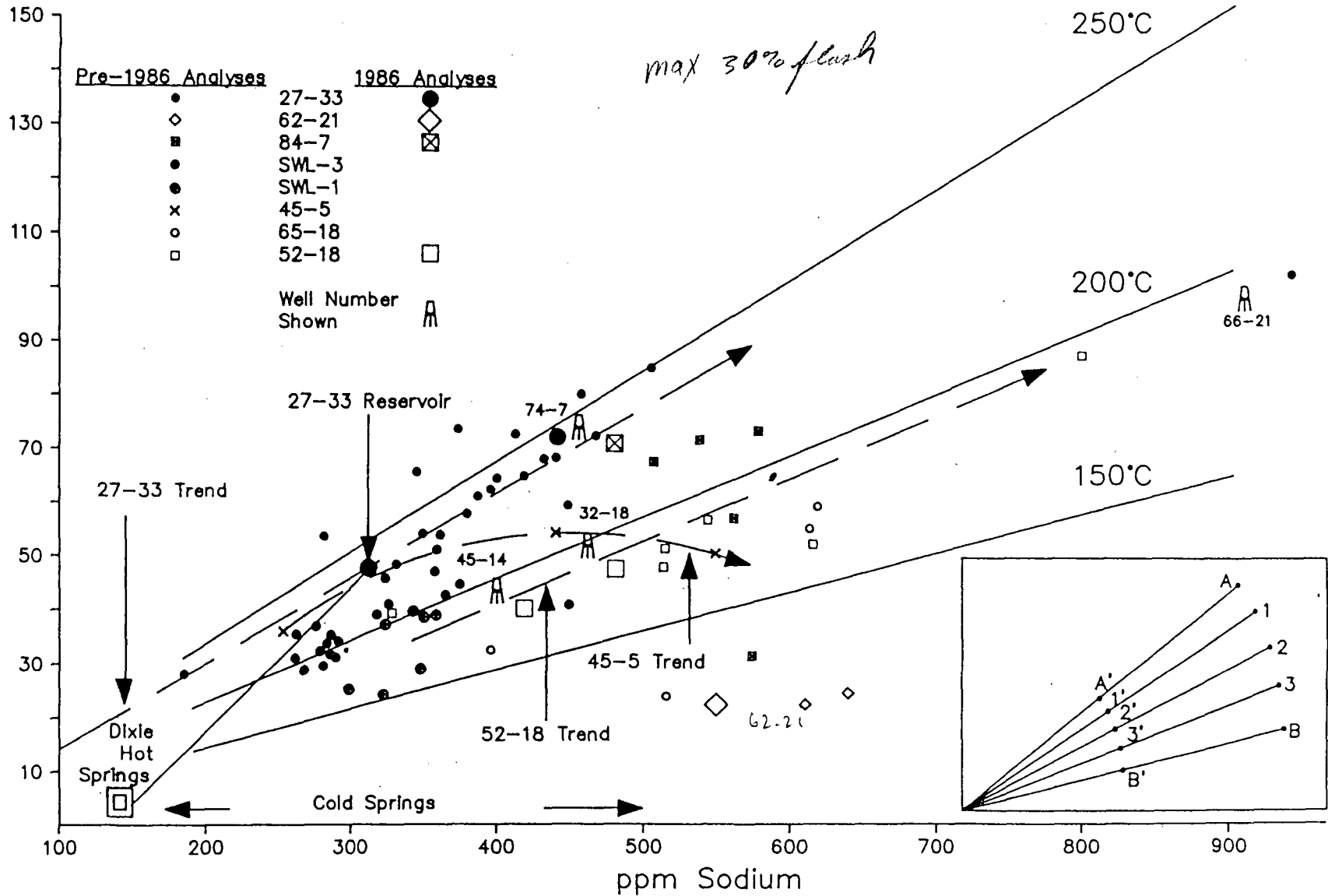
### 5.2 Definition of Populations

The approach to this geochemical modeling has been to define populations of water types and then to compare the different populations to find common characteristics which might show relationships between the populations. These populations are then examined in terms of geothermometry and enthalpy relationships to further clarify the relationships. Finally the populations are grouped as to the degree of shared ancestry, and spatial relationships are defined.

The populations are defined on a sodium - potassium (Na - K) cross plot (Figure 5.2). This plot shows the trends most

# Sodium - Potassium Cross Plot

ppm Potassium



clearly and has the advantage of providing a visual impression of reservoir temperatures as a geothermometer overlay is included. The data on the Na - K plot have not been corrected for steam loss, hence a given well composition will plot as a linear feature trending away from the origin, *i.e.*, trends A-A' or B-B' on Figure 5.2. Constant proportion mixtures or single source end members will also plot as linear trends through the origin, *i.e.* trends 1-1', 2-2', or 3-3' on Figure 5.2. However, variable proportion mixtures of end members with different enthalpies will plot as curved trends that will not project through the origin, *i.e.* trend B', 1', 2', 3', A' which arises from mixing along A-B and flashing to a constant pressure (Figure 5.2). If the pressure were variable this last trend would be smeared out along one or more of the trend lines radial to the origin.

The pre-1986 data suggest that well 27-33 produces a constant composition fluid along the trend labeled "27-33". The geochemical data from well 45-33 are virtually identical to those from well 27-33, as expected from the close bottomhole spacing, so only the 27-33 data are discussed. The Berkeley Group calculated a reservoir composition that is both shown on the trend and summarized in Table 5.1. The higher concentrations along the trend are due to greater steam loss; the lower concentrations are suspected to be due to sampling errors, *i.e.* steam enrichment, since no shift in the Na - K ratio is apparent. The 1986 data from well 27-33 also plot on this trend, thus confirming the original interpretation. The 1986 data for wells 74-7 and 84-7 also plot on or close to this trend.

A separate trend was defined by the pre-1986 data and is labeled as the "52-18" trend. It is about 50 deg. C lower in temperature than the 27-33 trend. If the spread of the 52-18 trend was created solely by steam loss it would require at least a 40% steam loss, which is far too great to be accounted for by the low measured enthalpy of this fluid (Table 5.2). In addition the great depths and pressures where these fluids are found rule out any steam separation processes. The 52-18 trend suggests that a higher salinity end member mixes with a lower salinity end member to create this compositional variation.

Waters from wells SWL-1 and SWL-3 plot at the low salinity end of the 52-18 trend and may be a low salinity end member. The SWL-1 and SWL-3 waters tend to overlap both the 52-18 and 27-33 trends. However, a tight cluster of SWL-3 analyses near 275 ppm sodium may hold the key to the proper interpretation of these waters. They are clearly lower in

Table 5.1  
Total Calculated Reservoir Water Composition

SPECIES	WEIR WATER (mg/kg)	SEPARATOR STEAM (mg/kg)	RESERVOIR WATER (mg/kg)
SiO <sub>2</sub>	710		512
H <sub>3</sub> BO <sub>3</sub> (from B)	(8.45)		34.8 (6.09)
Na <sup>+</sup>	438		316
K <sup>+</sup>	69.7		50.2
Li <sup>+</sup>	2.98		2.13
Ca <sup>++</sup>	0.99		0.71
Mg <sup>++</sup>	0.01		0.01
Sr <sup>++</sup>	0.17		0.12
Cl <sup>-</sup>	352		254
F <sup>-</sup>	15.2		11.0
HS <sup>-</sup>			48.9
(from S=)	(0.07)		(0.05)
(from SO <sub>4</sub> =)	(139)		(100)
(from H <sub>2</sub> S)		(87.9)	(15.4)
HCO <sub>3</sub> <sup>-</sup>			3,080
(from CO <sub>2</sub> )		(12,900)	(2,260)
(from HCO <sub>3</sub> <sup>-</sup> )	(278)		(200)
(from CO <sub>3</sub> =)	(16.8)		(12.1)
NH <sub>4</sub> <sup>+</sup>			2.00
(from NH <sub>3</sub> )		(10.8)	(1.89)
N <sub>2</sub>			22.3

127  
STRICTLY  
22.3



Table 5.1

SPECIES	WEIR WATER (mg/kg)	SEPARATOR STEAM (mg/kg)	RESERVOIR WATER (mg/kg)
CH4		16.7	2.93
Ar		3.17	0.556
He		0.444	0.0779
H2		0.0605	0.0106

Note: The composition of reservoir water is given in terms of the major species, and contributing species are shown in parentheses below.

STRICTLY

TABLE 5.2  
COMPARISON OF CHEMICAL VERSUS MEASURED ENTHALPY

WELL	MEASURED STATIC TEMP	MEASURED FLOWING TEMP	MEASURED DOWNHOLE ENTHALPY	MEASURED WELLHEAD ENTHALPY	PREDICTED Na-K ENTHALPY	PREDICTED SILICA ENTHALPY
45-33	N/A	477	461	446		
27-33	448	477	461	443	459	459
45-5	404	401	376	322		
84-7	445	477	461	443	444	467
74-7	452	478	462	450	459	464
52-18	443	446	426	417	332	384
32-18	443	427	405	395	367	440
SWL-3	453	N/A (Probably 428)	406	395	382	384
SWL-1	429	428	406	402	379	414
65-18	430	438	417	410	336	483
62-21		356	328			
66-21					357	404

::

STRICTLY

salinity than the 27-33 reservoir fluid. Thus, unless they are the result of steam enrichment during sampling, they cannot be derived from 27-33 type waters by conductive heat loss. If this is the case the SWL-3 waters are the low salinity end member on the 52-18 trend. The SWL-1 waters form two possible sub-populations based on potassium content. The lower potassium waters will be discussed with the 62-21 well.

While the 27-33 fluids cannot be the parent for the SWL-3 fluids, the converse is not true. Heating and a slight increase in salinity could produce a 27-33 type fluid. A second possibility to explain the SWL-3 type waters would be to invoke a very dilute water such as a Dixie Hot Spring type to dilute the 27-33 type water. The involvement of SWL-3 waters in the 52-18 trend is shown by the high salinity (975 ppm sodium) sample and several other SWL-3 analyses along the trend.

The high salinity end member for the 52-18 mixing trend is water from well 66-21. This unflushed fluid, collected when the well was on bleed, is believed to be representative of the far southern portion of the Dixie Valley system. It is sodium chloride-rich and represents the most mature water type for this basin, in that carbonates and sulfate have been replaced by chloride, probably through precipitation reactions, indicating longer residence. It has a predicted Na-K temperature of 194 deg. C and has also been produced from the 52-18 and SWL-3 wells, as indicated by the presence of fluids produced from these wells plotting at the high salinity end of this trend.

Well 62-21 produces a low-enthalpy fluid from near the center of the basin. It is thought to be typical of the water which fills much of the basin at depths greater than a few thousand feet. For the identified water types in the study, the salinity of 62-21 makes it a potential parent water only for the 66-21 well, as its salinity exceeds that of the higher enthalpy fluids and as such could not parent such waters. As a potential mixing end member this well has much more significance. Wells 65-18, 45-5, SWL-1, and 84-7 have produced fluids which appear to have a 62-21 component. Mixtures of SWL-1 and 62-21 may account for the lower potassium cluster of SWL-1 subtype on Figure 5.2. The pre-1986 analyses of 84-7 also show a curved mixing trend with 62-21 end member (2 enthalpy mixing type curve).

Fluid from well 84-7 has in the 1986 tests shown a consistently close affinity to 27-33 fluids. The earlier data show that this well is connected to the deep basin

62-21 system and to the 66-21 type waters which are the end member for the 52-18 trend. The latter relationship is even more strongly supported when the Piper plot is examined (Figure 5.3.3).

Well 45-5 has three available analyses which suggest that the well began to produce a SWL-3 type fluid, but quickly became more strongly influenced by the 62-21 waters. The abrupt shift indicates mixing very near the wellbore. The shift is known to be abrupt because the well was only flowed for a total of 18 days. It should be made clear that no distinction can be made between multiple production zones that have been encountered by individual wells and the concept that fluids produced from a given well may be the result of several fluids mixing within the natural environment. The close spacing of producing intervals in most of the wells tends to argue against multiple production zones with different chemistries being a common feature.

Recent analyses of wells 45-14 and 32-18 indicate that both belong to the 52-18 compositional mixing trend with a 66-21 compositional component.

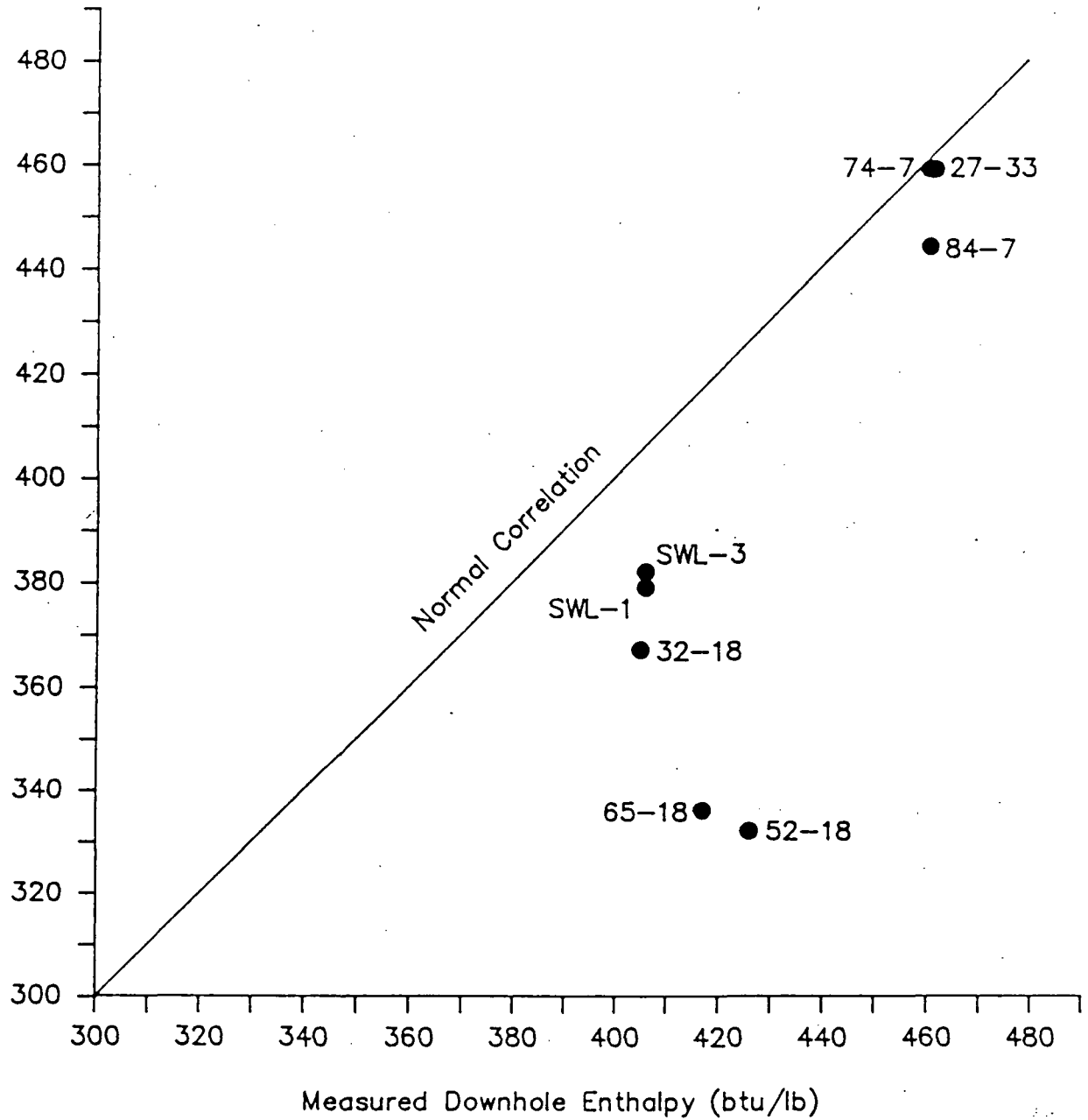
Recent analyses of well 74-7 show this fluid to belong with 27-33 fluid type. There is no evidence for mixing with other fluids.

### 5.3 Measured and Geochemically Predicted Enthalpies

The previous discussion in a qualitative sense has implied that the chemical evidence offers little support for the premise that the widely varying enthalpies in the Dixie Valley wells result from conductive cooling of fluids. This lack of support for conductive cooling can be quantified by comparison of the geothermometer estimates of reservoir enthalpy with the measured enthalpy for each well (Table 5.2). If conductive cooling were the main factor affecting enthalpy, the Na - K estimate of enthalpy would be expected to be greater than the measured enthalpy as a consequence of the relatively slow re-equilibration of the Na-K geothermometer in response to falling temperatures. Instead, the Na - K estimates of all of the lower enthalpy wells are much lower than the measured downhole flowing enthalpies (Figure 5.3.1). This situation is a result of logarithmic increase in relative amounts of sodium in lower enthalpy fluids. When these fluids are mixed with higher enthalpy fluids, the heat contents are balanced linearly but a disproportionate amount of sodium will be present and an abnormally low Na-K temperature will be an expected result. Note that the high enthalpy wells are in close agreement

# Measured Downhole Enthalpy vs Predicted Na/K Enthalpy

Predicted Na/K Enthalpy (btu/lb)



between measured downhole flowing enthalpy and the Na-K predicted enthalpy, whereas the lower enthalpy wells have large discrepancies (Figure 5.3.1).

The plot of silica predicted enthalpy versus downhole flowing measured enthalpy is less diagnostic, but also suggests mixing. Since silica increases as a log function with increasing enthalpy, mixed waters are expected to have a slightly higher silica enthalpies than the measured enthalpy. This is because the enthalpies of mixtures are nearly linear projections of the mixing ratio, whereas silica concentrations are skewed toward the higher enthalpy end member. Silica estimates of enthalpy of a mixture are in error on the high side. This is the case for wells 65-18 and 32-18, but others have a low silica enthalpy (Figure 5.3.2). These low discrepancies may be due to loss of silica between sampling and analysis. In conductively cooled systems, the silica equilibration kinetics are rapid enough that a close correlation between silica and measured enthalpies is expected. Since a close correlation is not seen in this data, cooling by mixing is believed to be the mechanism for the enthalpy loss. Again, the high enthalpy wells have close agreement between measured enthalpy and the silica-predicted enthalpy, while the lower enthalpy wells are subject to large differences.

The enthalpy considerations agree well with mixing of geothermal fluids with varying enthalpies at Dixie Valley.

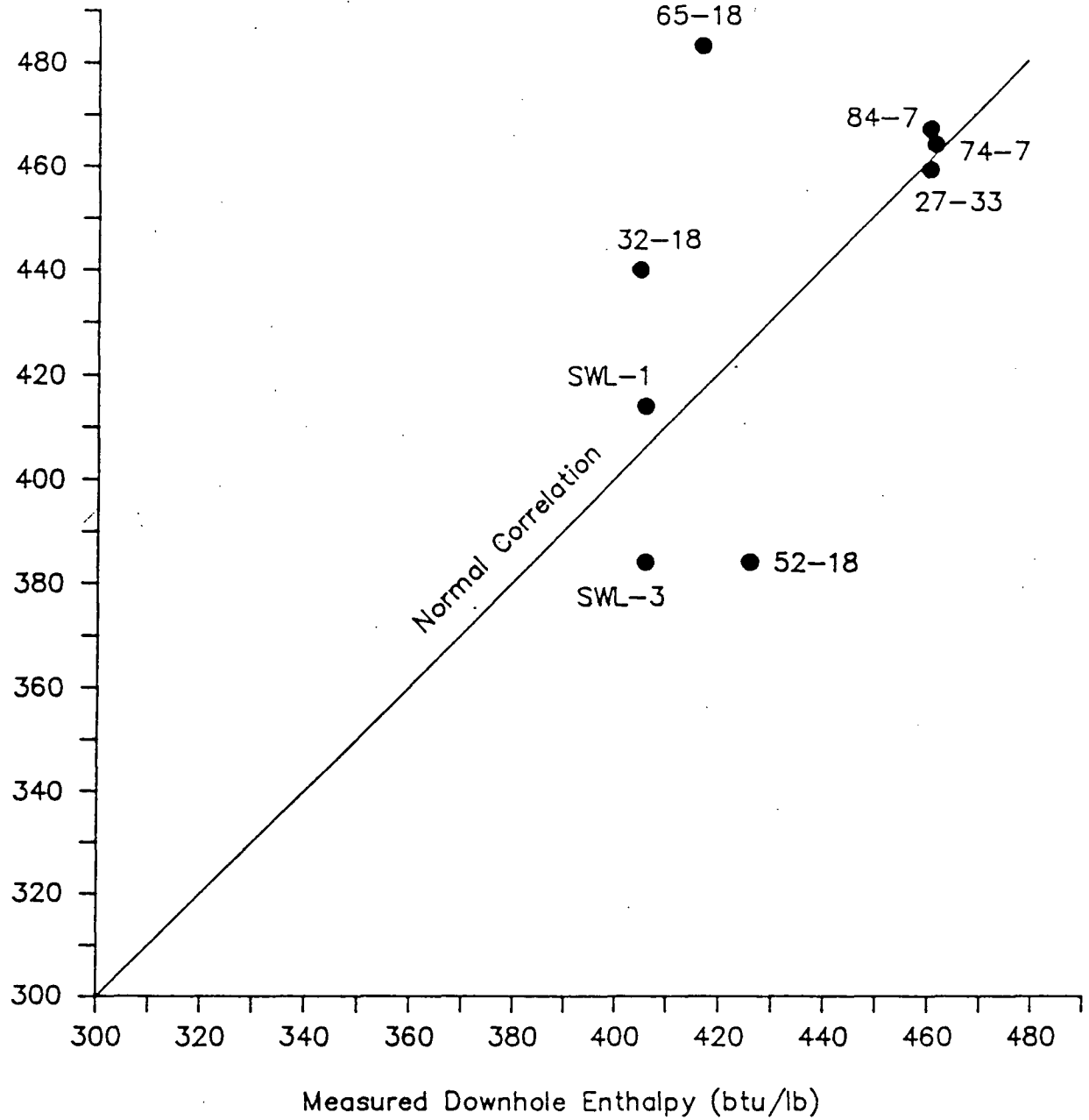
#### 5.4. Multivariate Analysis

All of the deep thermal waters in Dixie Valley are exceptionally dilute given the high temperatures at which they have equilibrated. Water from well 66-21 is the most saline by far and it barely exceeds 3000 ppm. The other well waters are generally between 1200 and 2000 ppm in total dissolved solids (Figure 5.3.3). The major chemical variation is a change in sulfate relative to chloride and bicarbonate as shown on a Piper plot with sulfate isolated (Figure 5.3.3).

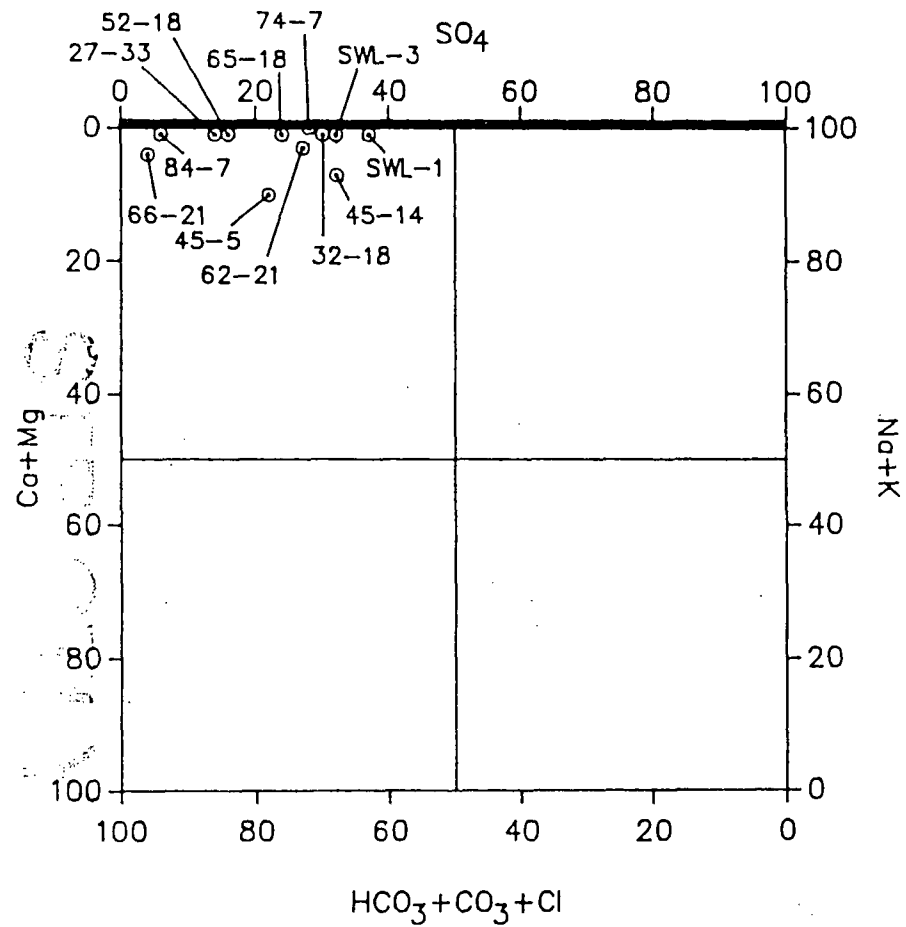
The Piper plot is incapable of showing salinity variations or relationships. To add this capability it is necessary to construct a separate diagram known as a three-dimension composition space. Basically this is a slice across a Piper plot that tapers up to an apex which is defined as zero salinity. Any convenient taper can be chosen for the sides of the three-dimension composition space. Salinity increases away from the apex. Another way to imagine this is to view the Piper plot as a horizontal slice through a

# Measured Downhole Enthalpy vs Predicted Silica Enthalpy

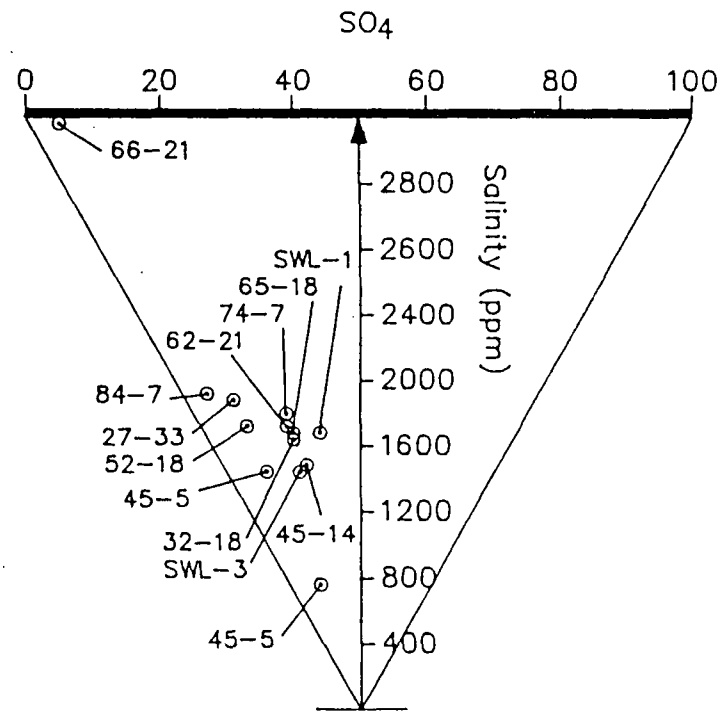
Predicted Silica Enthalpy (btu/lb)



# Piper Plot (Sulfate Isolated)



# Three Dimension Composition Space





pyramid with the apex of the pyramid representing zero salinity. The lower one cuts the slice horizontally across the pyramid the greater the salinity becomes. Figure 5.3.3 contains a three-dimension composition space drawn along the anion margin (top) of the Piper plot.

For purposes of this discussion the following three points are deemed most important from the trends shown on Figure 5.3.3.

1. There is a general increase in chloride from 62-21 to 66-21 shown on the Piper plot and all higher enthalpy wells lie within this trend.
2. Well 84-7 shows the strongest affinity to the 66-21 type of fluid on the Piper plot.
3. On the basis of salinity and cation ratios (highest calcium contents), wells 45-5 and 45-14 are most strongly skewed toward dilute surface water compositions.

These relationships lend support for the conceptual geochemical model which will be considered next.

### 5.5 Conceptual Geochemical Model of the Flow System

The conceptual model includes a mechanism for the mixing of geothermal fluids into the dilute surface waters; however, since wells 45-5 and 45-14, which show this relationship, are not being considered for production, this topic was not pursued. The purpose of the conceptual model is to define the probable chemical relationships by mixing fluids encountered in various production wells in Dixie Valley. The geologic-hydrologic context of these relationships is of course a critical factor in the commercial development of this resource. The following fluid types have been identified for purposes of the conceptual model.

1. The 27-33 high-enthalpy fluid. This system shows little compositional variation and is the high enthalpy parent of the SWL-3 water. The temperature of this fluid is near 250 deg.C.
2. The SWL-3 moderate-enthalpy fluid. These waters form by mixing of 27-33 fluids with dilute cooler waters. Temperatures range from about 215 to 240 deg.C.
3. The 66-21 lower-enthalpy system. These waters are

more mature than either of the above types in that the sulfate content is much lower. This is based on the assumption that as waters mature, insoluble sulfates precipitate and sulfate is lost from the system. This maturity, however, has been attained in a lower temperature environment of about 194 C. These waters are significantly more saline than any other fluid type.

4. The 62-21 deep basin waters. These fluids are similar to types 1 and 2 above in salinity but have matured in a lower enthalpy environment. Although mostly chloride in character they have a maximum temperature of only 167 C. They appear to have only this moderate temperature imprint and have never attained higher temperatures.
5. Surface waters. The requirement for more dilute waters is clear in the case of the hot spring systems present and possibly to explain the SWL-3 fluids. Also, these may influence the composition of 45-5 and 45-14 fluids.

The spatial-physical relationships of these fluids can be explained as a result of the mixing of 27-33 type fluid with various populations of cooler fluid stored with the basin. This mixing takes place within or in close proximity to the plane of the range-front fault. This plane of convection is broken into sub-cells at permeability nodes which extend out into the basin. These nodes are probably zones of high fracture density which serve as conduits for high enthalpy fluids from the range-front fault to penetrate into and mix with cooler fluids stored in the deep basin to the east and south.

The main source of high enthalpy fluid is centered near the Section 7 and 33 wells and serves as the thermal driving force for the system. The high-enthalpy fluid creates pressure differentials within the reservoir as a consequence of the density contrasts due to thermal expansion (See Section 4.5 and 4.6). Absence of temperature decline during flow testing of the high-enthalpy wells confirms that hot water preferentially flows upward along the range-front fault and penetrates into cooler aquifers to produce the observed mixing. Convection due to discharge of low-density thermal fluids to the shallower alluvium with loss by evapotranspiration serving as the ultimate sink for the net throughput of the system. Basin fluids are drawn into the convection cells at permeability nodes along the range-front fault and this results in the observed mixing of different

chemical populations.

Three distinct zones of fluid storage are defined by fluid chemistry. These zones are the 66-21 type fluid, the SWL-3 type fluid and the 27-33 type fluid. The southern-most cell, the 66-21 cell, is an end member compositionally and has a component of flow in the direction of the Section 18 wells to the northeast and a flow component to the south-southwest towards 45-14. The resultant mixtures of SWL-3 type fluids and the 66-21 type fluids provide what has been previously referred to as the 52-18 compositional trend. This trend would include the following wells, listed in order of an increasing component of 66-21 fluids: SWL-3, SWL-1, 45-14, 32-18, and 52-18. This mixing process is driven by the large regional pressure gradient which exists between 66-21 and the producing part of the field. Fluid from wells 52-18 and 65-18 shows significant mixing with fluid from the deep basin represented by 62-21. This mixing is also consistent with the observed pressure gradient between 62-21 and the production zones in 52-18 and 65-18.

The chemistry of the high-enthalpy fluid observed in wells 84-7 and 74-7 is nearly identical to that of 27-33. Only a very slight component of 66-21 is seen in the fluid, indicating that these wells are tapping directly into the same fluid source supplying 27-33 with only very slight mixing. Well 84-7 shows less sulfate than 27-3, but in terms of salinity it could have only a small component of 66-21 for the average produced mixture. It is thus closely related to 27-33.

## 5.6 Scaling

### 5.6.1 Silica Scale

Bench testing of produced geothermal fluid for silica scaling was performed by TGI during the flow testing of 45-33 in 1984. This testing is summarized in Appendix E, "Chemistry of Silica in Dixie Valley Brine" by Oleh Weres, 1984.

These experiments have demonstrated that if the separated brine is kept near the boiling point, silica polymerization is slow. This is in large part a function of the high pH of the Dixie Valley geothermal fluid, which is 8.43 at 96 deg.C. Even if the dissolved silica does polymerize to colloidal silica, the colloidal silica does not flocculate, and does not appear to adhere to solid surfaces. Therefore,

the silica in the brine is stable in two important respects.

If brine handling and reinjection procedures are designed to preserve this stability throughout the system, there will be no problem with silica scaling or injection well damage.

If the brine is maintained near the boiling point (205 deg. F), polymerization is very slow. Polymerization is also slow at 176 deg. F. If temperature is reduced to about 140 deg. F, the silica begins to polymerize within minutes. Reducing brine pH to 7.7 caused fairly rapid polymerization at 176 deg. F. These results suggest the lowest "safe" temperature for injecting the brine is about 176 deg. F. If, however, the pH of the brine is reduced, the minimum safe temperature will be higher, perhaps near the boiling point.

These results are sufficient to prescribe a safe and conservative brine handling and injection procedure: (a) Minimize heat loss at the surface by not exposing the brine to air and keeping pipelines insulated and/or short. (b) Do not decrease the brine pH, for example, by contacting it with condenser vent gas. (c) Inject the brine into a stratum where the temperature is 176 deg. F or higher. There is little doubt that the separated brine can safely be injected into the geothermal reservoir without requiring preinjection treatment.

The conclusion summarized above applies in full only to a brine that has been flashed to atmospheric pressure in one step. Extracting heat from the brine otherwise will produce brine in a different chemical state, possibly with different silica scaling potential; in particular, the "minimum safe temperature" may be different. If the steam is separated in two stages, the second at atmospheric pressure, the pH of the brine will be slightly higher, and the minimum safe temperature may be lower. As the Dixie Valley power plant is a dual flash plant this should further minimize any silica scaling problems. No silica precipitation was observed on surface brine handling equipment including the atmospheric flash tank and weir box used for several thousand hours of flow testing. This verifies conclusions made from the bench tests that silica does not tend to precipitate at temperatures above approximately 200 deg.F.

The idea of injecting the brine into shallower formations that have much lower temperature and different brine from the geothermal reservoir raises other, more difficult questions. If the receiving formation contains swellable clays, the injected brine may dispense and mobilize the

clays, causing formation damage. If the brine in the receiving formation is more saline and more acid, mixing it with the injection brine may accelerate polymerization and flocculation of the silica. However, Oxbow intends to inject the spent brine back into the reservoir for pressure maintenance so these problems should not occur.

Preliminary results from the silica scaling test skid on well 74-7 during the six well flow test have confirmed that silica scaling need not be a problem at Dixie Valley. After a month of flowing through the skid, designed to simulate a reinjection system, only traces of scale had formed on carbon steel components in the skid. The stainless steel mesh had absolutely no silica deposition.

#### 5.6.2 Carbonate Scaling

Carbonate scale deposits in the bores of production wells during flowing. A volumetric measure of scaling was made in wells 27-33 and 84-7 using caliper logging before and after long term flow tests. The results of this study are described in Appendix E. The scaling rates observed in the 9-5/8" casing string for both wells would require cleanout at three to six month intervals. The time between cleanout could be lengthened by varying wellhead pressures so that the flash point would move up or down the well. This movement of the flash point would distribute the scale buildup over a greater area per unit volume of scale deposition, thereby reducing the rate of effective well bore diameter constriction.

The 13 3/8" wells will not need nearly as many scale cleanouts as the 9 5/8" wells. Experience at other geothermal reservoirs in the Basin and Range province suggests that the 13 3/8" wellbores will flow between 3 and 4 times as long as the 9 5/8" bores before a cleanout is necessary. It is anticipated that wells 74-7 and 76-7 will need about one cleanout per year and the 10 3/4" casing in well 73-7 will need to be cleaned out about twice a year under maximum flow conditions.

The mechanical properties of the carbonate scale appear to be amenable to reaming. The scale tends to be friable, breaking into small fragments which are easily cleared from the well bore during reaming under flowing conditions.

## 6. CONCEPTUAL RESERVOIR MODEL

The geotechnical data described in Chapters 3, 4, and 5 are sufficient to develop a well-constrained conceptual model of the Dixie Valley geothermal reservoir. This conceptual model is a necessary step in converting the geotechnical data base into a representative numerical model. The accuracy with which the conceptual model represents the natural system is expressed in the relative ease with which the numerical model can be made to match observed reservoir behavior. Accuracy of the conceptual model also determines the accuracy of long term predictions made by the numerical model for periods of time and for reservoir volumes which are well beyond those observed during actual flow testing.

The conceptual model of the Dixie Valley reservoir incorporates the following geologic, geochemical, and hydrologic features as discussed previously:

1. Distribution of formation permeability must be consistent with observed structure and stratigraphy. High permeability is apparently confined to the range-front fault fracture system and Tertiary basalt aquifer. The Quaternary-Tertiary-Jurassic section comprising the rocks of the graben block above a depth of 9700 feet must have low vertical permeability to account for the observed conductive thermal gradients. Lack of water entries during air drilling through unfractured Tertiary and Jurassic sections verifies the existence of low intergranular permeability within the down-dropped block.

2. The production intervals must be supplied from an aquifer located at depths greater than 10,000 feet beneath the valley floor in order to supply 480 deg.F water to the deep production wells. No evidence of recent volcanism is found in the region that could supply heat to the system. Consequently, deep circulation of water to depths below the 480 deg.F isotherm is the only remaining mechanism that could create the observed high-enthalpy fluid. Isotope data indicate that this water is distributed regionally at depth over a minimum of several thousand square miles and is older than 35,000 years, indicating very slow rates of flow through the system. Gas and isotope characteristics of the high-enthalpy fluid indicate a source in the Triassic marine sediments which correspond to the depth of circulation required to produce the observed 480 deg.F temperatures (Section 4.3).

3. The geochemistry of reservoir fluids with varying enthalpies indicate that the temperature distribution within the productive portions of the reservoir must be accounted for by mixing of fluids as opposed to conductive heat loss. The highest-enthalpy fluids (from wells 27-33, 45-33, and 84-7) appear to be unmixed with cooler fluids. These wells therefore define the zone of upwelling of high-enthalpy fluid from the postulated regional aquifer described in 4.3. Fluids from outlying wells 66-21 and 62-21 appear to represent the cooler chemical end members that are available for mixing with higher-enthalpy fluid from depth to produce the wide range of temperatures observed in the reservoir (Section 5.5).

4. The distribution of permeability surrounding the reservoir and the natural rate of fluid flow in and out of the reservoir must be consistent with the observed regional and local pressure distribution. A pressure drop of 350 to 500 psi at -5000 foot MSL is observed between the regional deep aquifer system and the producing portion of the reservoir. Deep wells 62-21 and 66-21 appear to be in equilibrium with pressures observed in the deep geothermal reservoirs in the Carson Sink on the west side of the Stillwater Range. The low observed pressures within the producing portion of the reservoir appear to be constrained horizontally by these two wells which lie 3 and 6 miles respectively from the producing zones.

5. Horizontal pressure gradients created by thermo-artesian pressure within the producing fracture systems cause penetration of high-enthalpy fluids from production zones observed in Section 7 and Section 33 wells into lower-enthalpy production zones observed in the Section 18 wells. This produces the observed chemical and enthalpy mixing (Sections 4.6 and 5.5).

6. Thermo-artesian pressure caused by leakage of high-temperature fluid to the near-surface along the range-front fault must be sufficient to allow for penetration of reservoir fluid into the shallow ground water system to produce the observed surface heat flow anomaly. The quantity of near-surface and surface discharge must be consistent with the relatively weak heat flow anomaly and very small amounts of silica sinter observed at the surface. (Section 4.7).

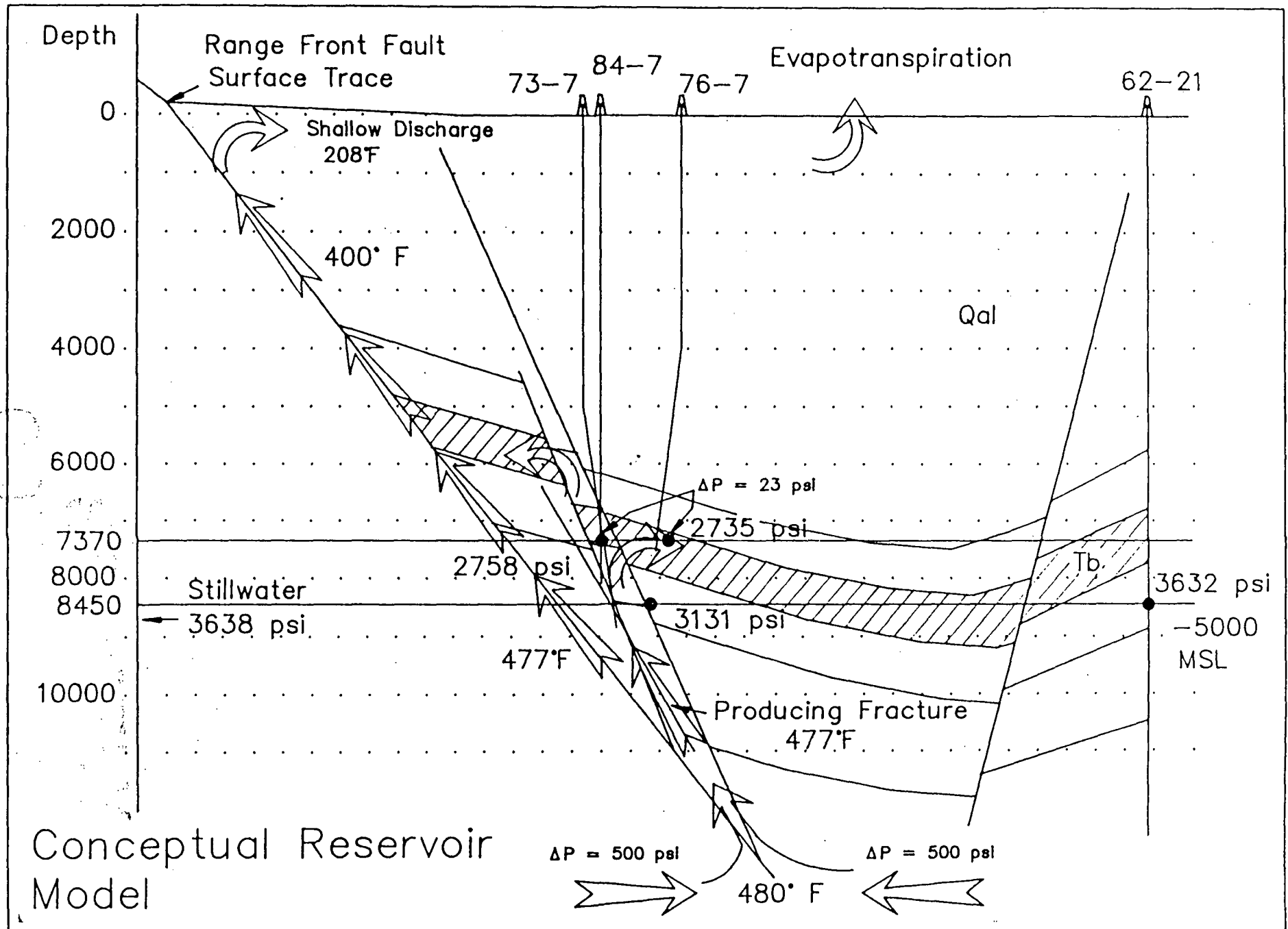
7. Natural discharge from the geothermal reservoir is readily accounted for by evapotranspiration from the Humboldt Salt Marsh and surrounding playa. The evapotranspirative potential of the Salt Marsh exceeds

probable natural geothermal discharge by three orders of magnitude. As a result of the essentially unlimited discharge potential, natural flow of water through the system is constrained only by thermo-artesian pressure gradients and the fracture and intergranular permeability of the reservoir and overlying rock.

The observed phenomena described above are shown schematically on the cross section shown in Figure 6.1. The conceptual model of the Dixie Valley geothermal system derived from these observations can be described as follows:

1. Pore water stored in the Triassic pelitic and carbonate sediments deeper than 10,000 feet below ground level attain a temperature in excess of 480 deg.F due to the relatively high regional thermal gradients in west-central Nevada. The high-temperature fluid is in hydrostatic equilibrium throughout the high heat flow region.
2. A rapidly dilating fracture system associated with the Stillwater range-front fault in the Section 18 area allows high-temperature fluid from the deep regional aquifer to penetrate into shallower fracture zones. Continuous fracturing of rock adjacent to the range-front fault creates significant fracture permeability and porosity storage of high temperature fluid in close proximity to the range-front fault system.
3. High vertical permeability in the fracture system allows a thermo-artesian pressure differential to develop in the 5,000-8,000 foot depth range thereby driving high-temperature fluid from depth into the cooler aquifers in the Tertiary basalt. The moderate-temperature reservoir of mixed fluid encountered in the Tertiary basalt is created by this mechanism.
4. Penetration of hot fluid along the range-front fault to the near-surface creates thermo-artesian pressure which overcomes cold water hydrostatic pressures thereby creating hydrothermal discharge plumes at the margins of the field. Water discharged from the plumes is lost to evapotranspiration in the Humboldt Salt Marsh.
5. Net loss of fluid from the system due to vertical flow and loss at the surface creates the large pressure drop between the high-temperature regional aquifer and the highly fractured zones which make up the productive part of the reservoir.





## 7. WELL AND RESERVOIR TESTING

## 7.1 Well Completions and Histories

The Dixie Valley geothermal well field considered in this assessment consists of 9 production wells and 5 non-commercial wells as shown in Figure 2.2. Two outlying noncommercial wells, 66-21 and 62-21, were also used in this study for background pressure and temperature data. The physical characteristics of each well are summarized in Table 7.1 and the geologic and flow characteristics of each well are summarized in Table 7.2. The following is a brief discussion of the drilling history, completion and flow characteristics, and current and projected uses of each well in the field.

## SWL-1

Well SWL-1, the discovery well in Dixie valey, was completed by SUNEDCO on November 29, 1978 to a total depth of 7255 feet (Figure 7.1.1). SWL-1 produces from the Miocene basalt between depths of 7191<sup>214'</sup> and 7255<sup>221'</sup> feet. Numerous flow tests of this well have been conducted by SUNEDCO. The most recent flow test of SWL-1 was a 7 hour test on March 27, 1986. The well flowed 252,000 lbs/hr with a wellhead pressure of 56 psig. Casing partings or collapse have occurred in SWL-1 in the 13 5/8", 9 5/8," and 7" casing strings. SWL-1 is not suitable for production. It will be used for observation purposes and conceivably could also be used as an injection well.

## SWL-2

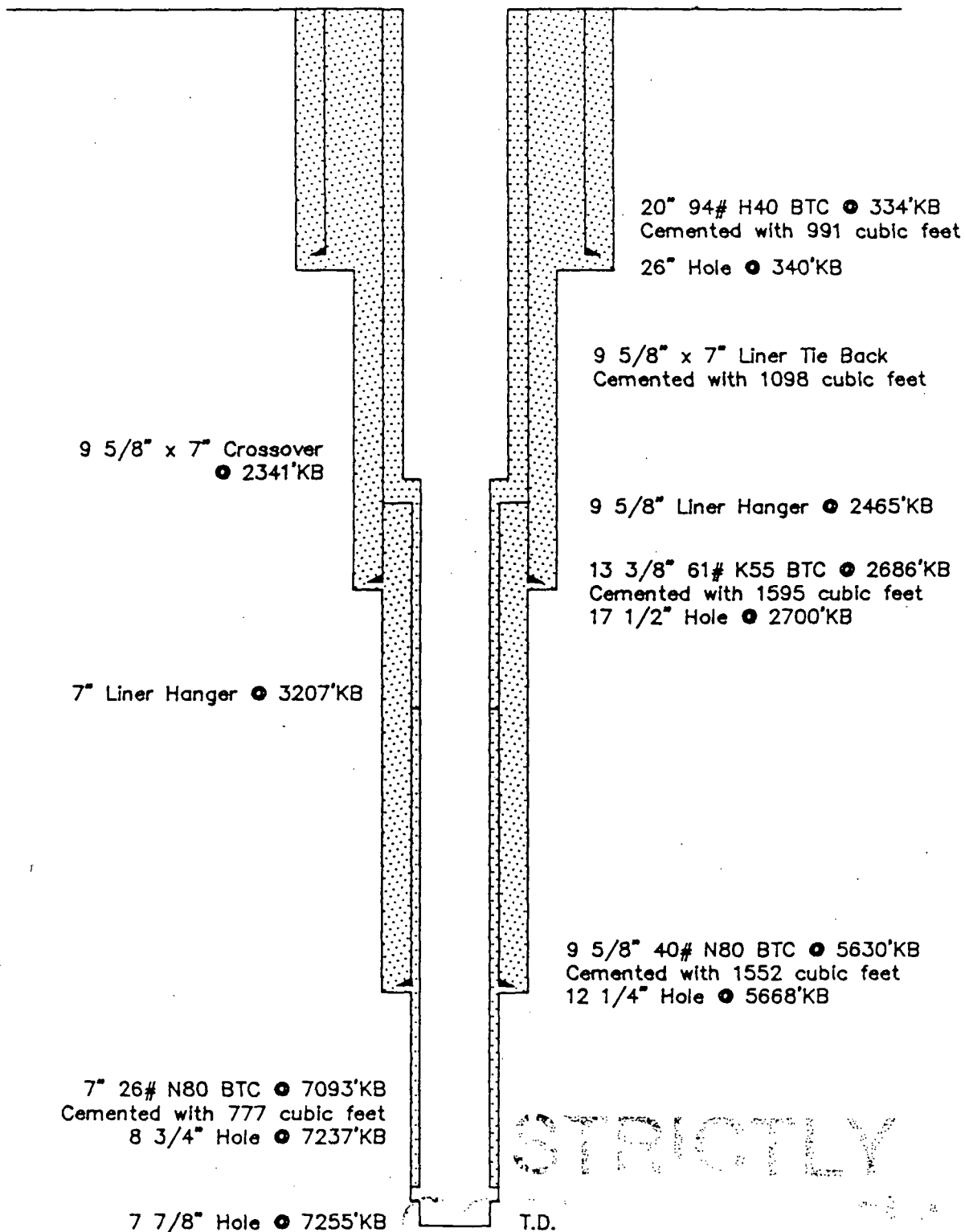
Well SWL-2 was completed by SUNEDCO on August 25, 1979 to a total depth of 8588 feet (Figure 7.1.2). The well produced from the 6570 to 8290 foot interval located within the Miocene basalt. The existing leg of SWL-2 is the second leg of the well and was drilled because the original leg was a dry hole completed in Cretaceous granodiorite. After completion the existing leg would not flow. In November 1979 a slotted 5" liner was run from 7994-8455 feet. SWL-2 was flow tested during January and February 1980 but would not sustain flow unassisted. The maximum flow acheived was 50,000 lbs/hr with a wellhead pressure of 38 psig. SWL-2 is currently being used for pressure observation purposes and this appears its only use.

# Well Completion Diagram Well SWL-1

Location: NW-NW-NW Section 18-24N-37E  
Churchill County, Nevada

Datum: 3496' KB, 16' Above Ground Level

Drilled: 11/29/78

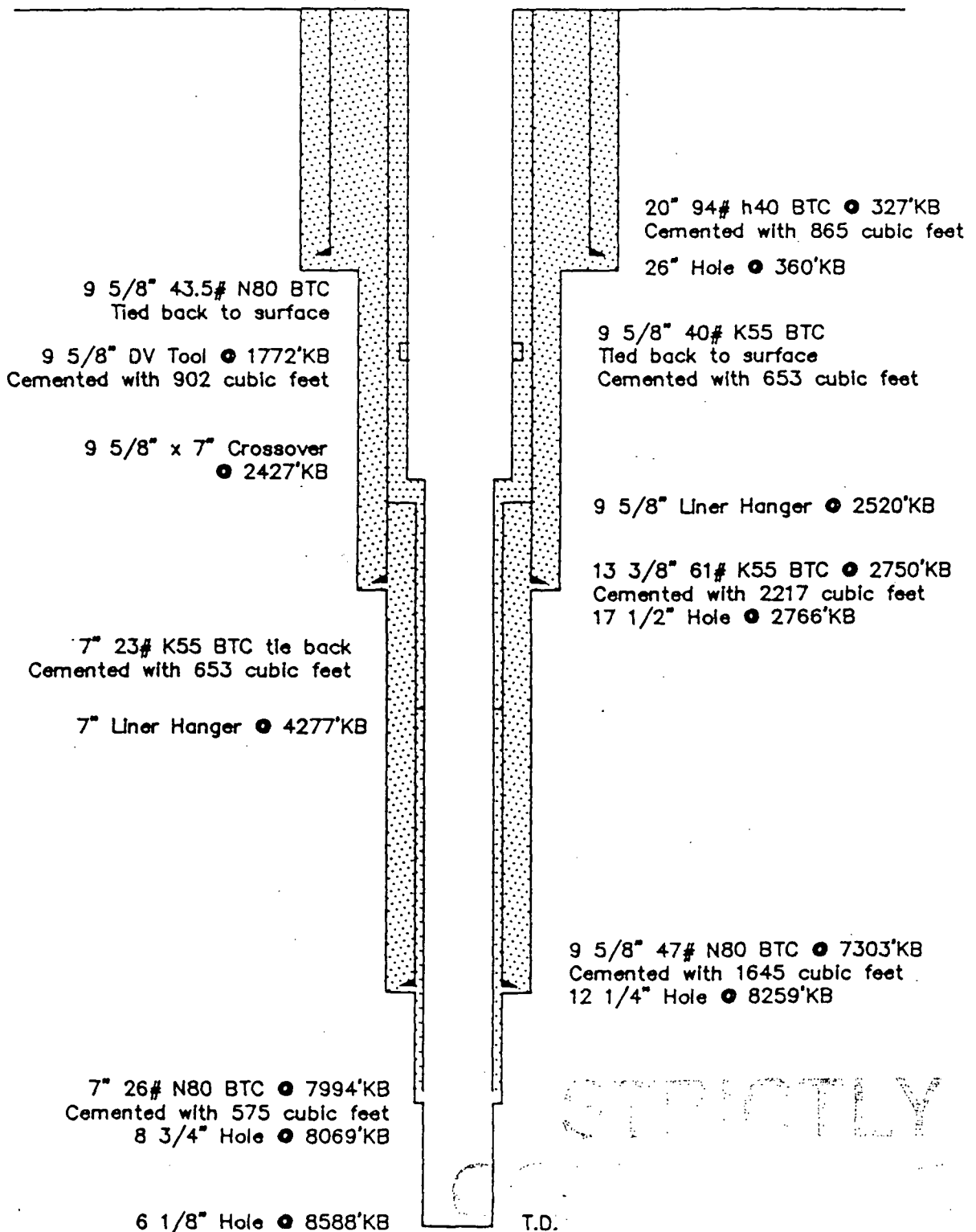


# Well Completion Diagram Well SWL-2

Location: SE-NE-NE Section 13-24N-36E  
Churchill County, Nevada

Datum: 3490.5' KB, 22' Above Ground Level

Drilled: 08/24/79

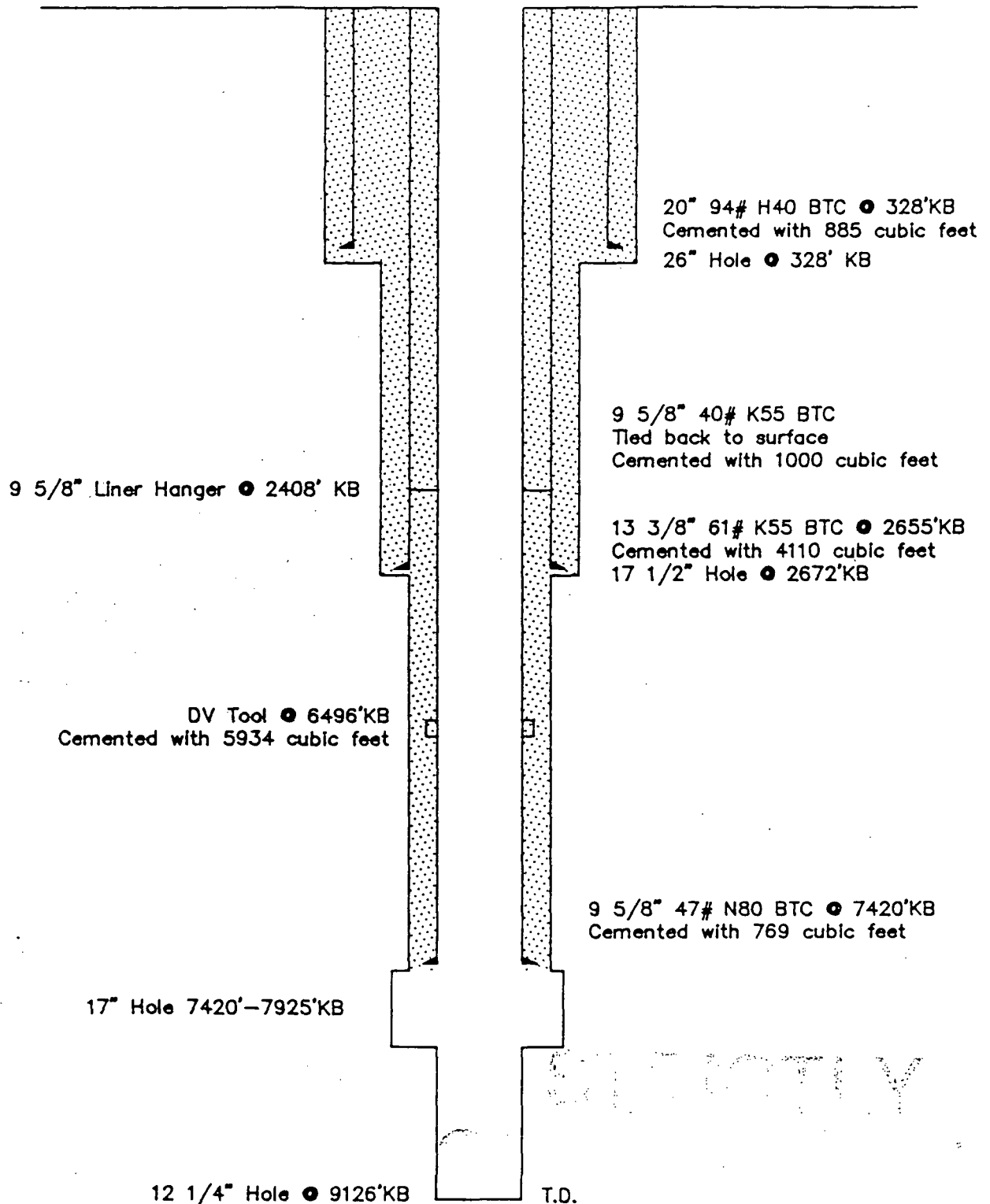


# Well Completion Diagram Well SWL-3

Location: SW-NE-NW Section 18-24N-37E  
Churchill County, Nevada

Datum: 3493' KB, 25' Above Ground Level

Drilled: 11/25/79

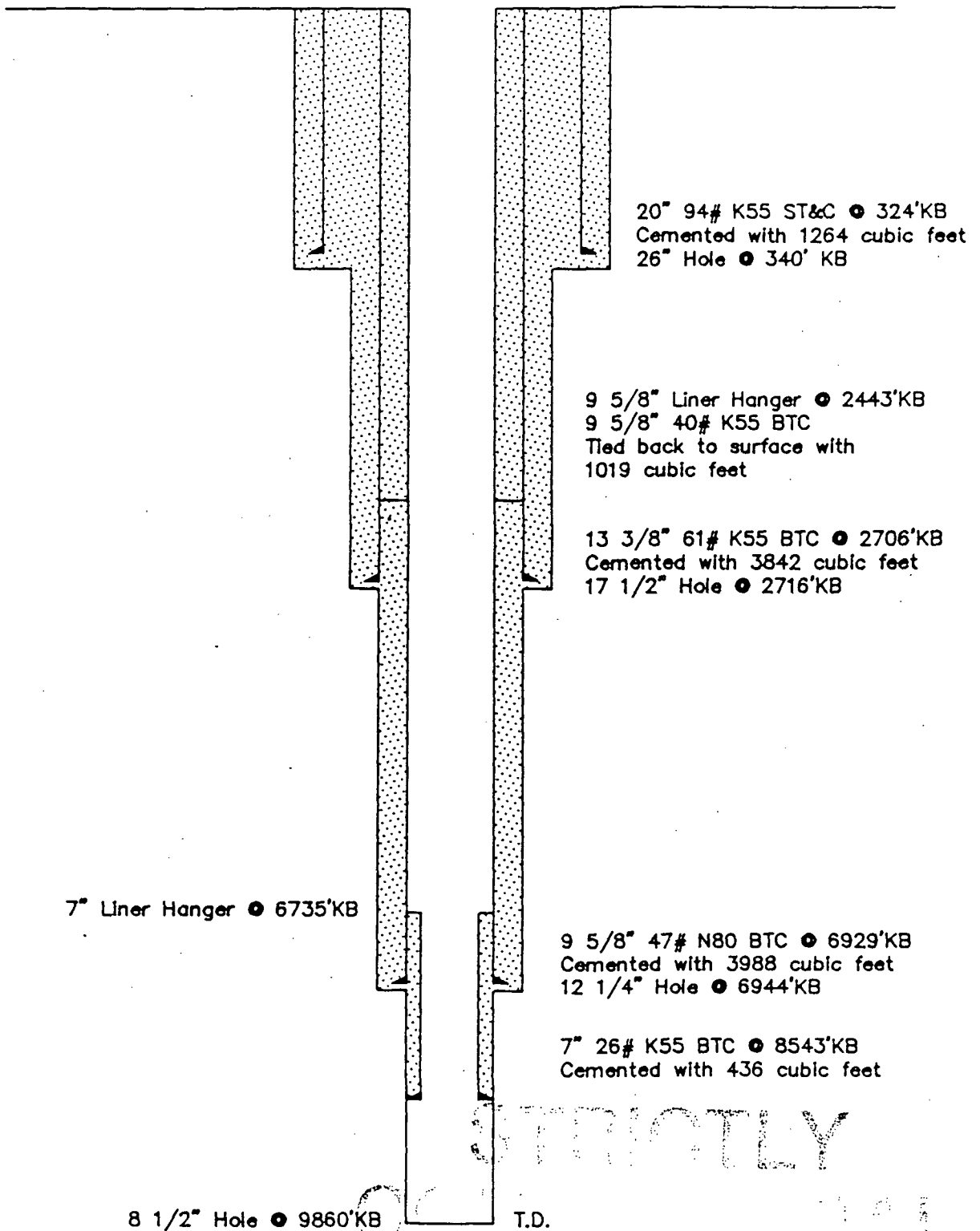


# Well Completion Diagram Well 52-18

Location: NE-NE-NW Section 18-24N-37E  
Churchill County, Nevada

Datum: 3486.5' KB, 25.5 Above Ground Level

Drilled: 02/08/80



## SWL-3

Well SWL-3 was completed by SUNEDCO on November 26, 1979 to a total depth of 9126 feet (Figure 7.1.3). SWL-3 produces through perforations in the 9 5/8" casing from the Miocene basalt in the 7070 to 7450 foot interval. SWL-3 has been flow tested several times, the most recent being in 1983. It will produce 300,000 lbs/hr with a wellhead pressure of 90 psig. Currently this well is being used for pressure observation purposes. It could also be used for injection purposes. In its current state it is incapable of commercial production.

## 52-18

Well 52-18 was completed by SUNEDCO on May 8, 1980 to a total depth of 9860 feet (Figure 7.1.4). The well produces from the 9055 to 9289 foot interval located within the Jurassic spilite sequence. The well has only been a marginal producer and this is believed to be due to the producing fractures being damaged by mud during drilling. The well has been flowed several times, the most recently being for 9 days in February and March 1986. During this sequence of flow tests the maximum flowrate was 263,000 lbs/hr at a wellhead pressure of 90 psig. Currently this well is being used for pressure observation purposes. It may be possible to use this as an injection well in the future.

## 62-21

Well 62-21 was completed by SUNEDCO on October 31, 1980 to a total depth of 12,500 feet (Figure 7.1.5). Well 62-21 produces from argillaceous sedimentary rocks in the 9040-12,500 foot interval. The small flow rate is artesian at a maximum temperature of 246 degrees F. The maximum static temperature in the well is probably near 380 deg. F. The shut-in wellhead pressure is approximately 73 psig. To date there is no evidence that well 62-21 has intersected the reservoir. This well is currently being used for pressure observation purposes.

## 84-7

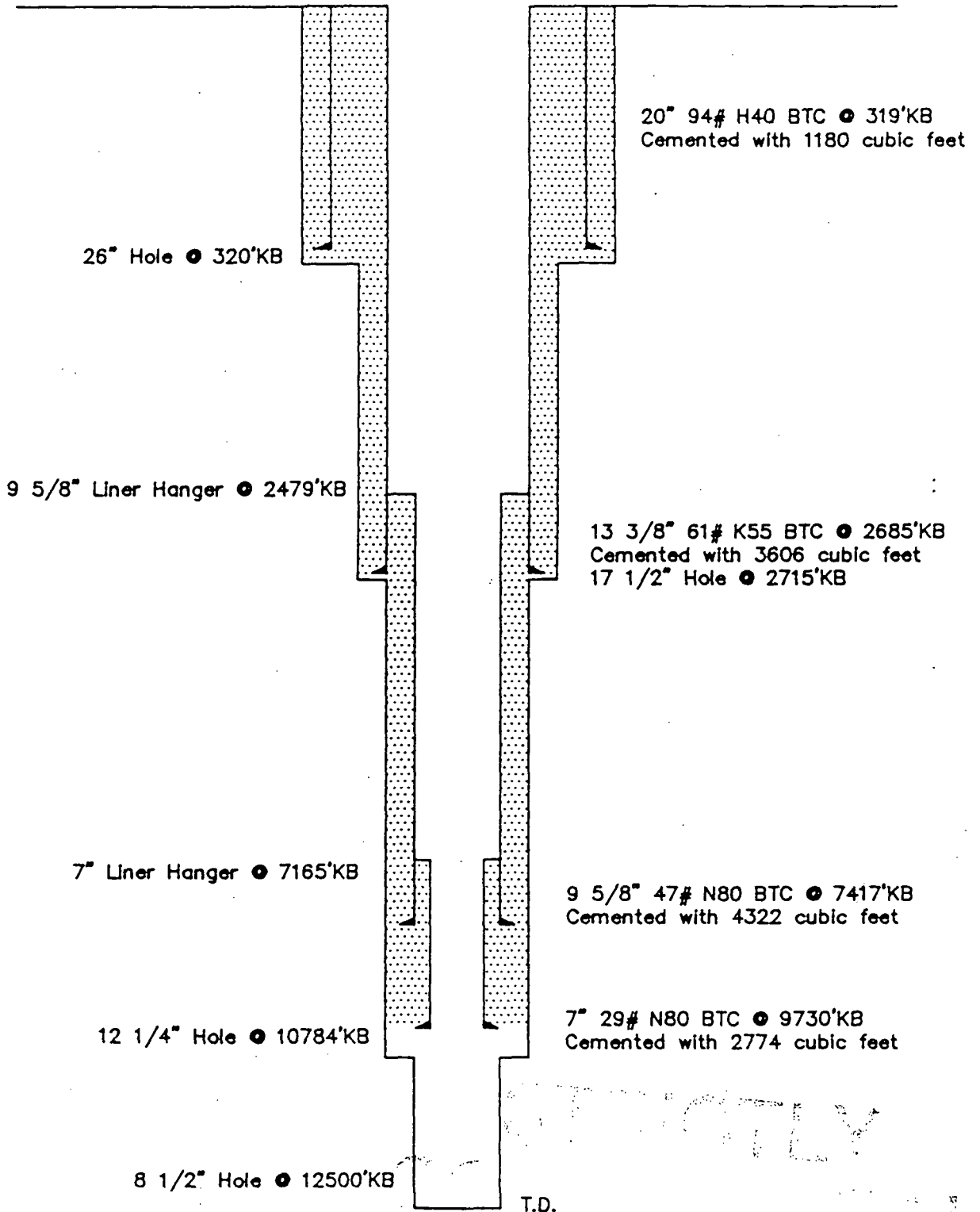
Well 84-7 was completed by SUNEDCO on January 17, 1981 to a total depth of 8142 feet (Figure 7.1.6). The well produces from the Jurassic spilitic sequence between depths of 8055 and 8142 feet. The production zone is associated with the range front fault. The well was most recently flow tested for 75 days during early 1986 as part of Oxbow's reservoir

# Well Completion Diagram Well 62-21

Location: NE-NE-NW Section 21-24N-37E  
Churchill County, Nevada

Datum: 3471' KB, 25.5 Above Ground Level

Drilled: 10/31/86



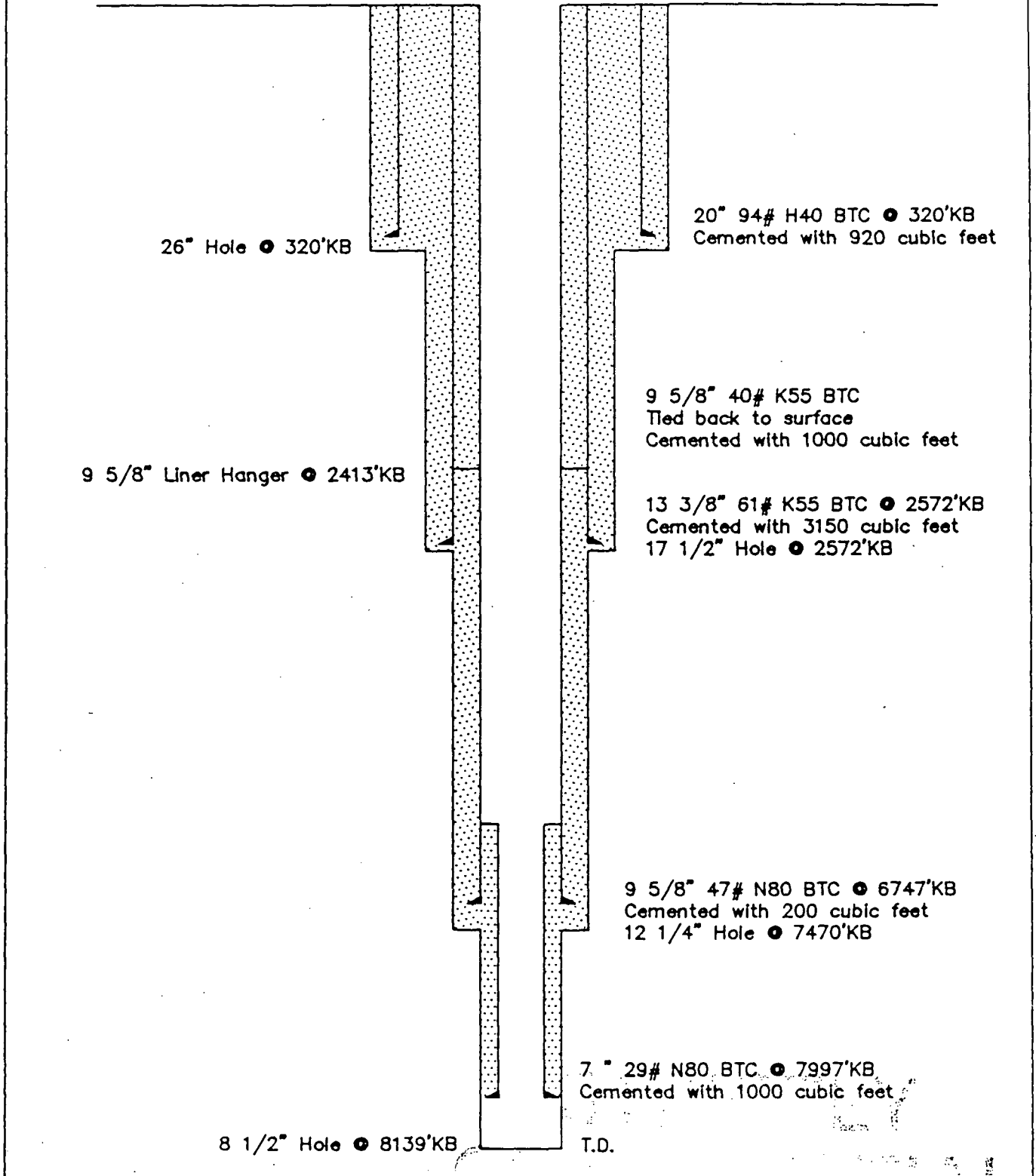


# Well Completion Diagram Well 84-7

Location: NE-SW-NE Section 7-24N-37E  
Churchill County, Nevada

Datum: 3498.5' KB, 25.5' Above Ground Level

Drilled: 01/17/81

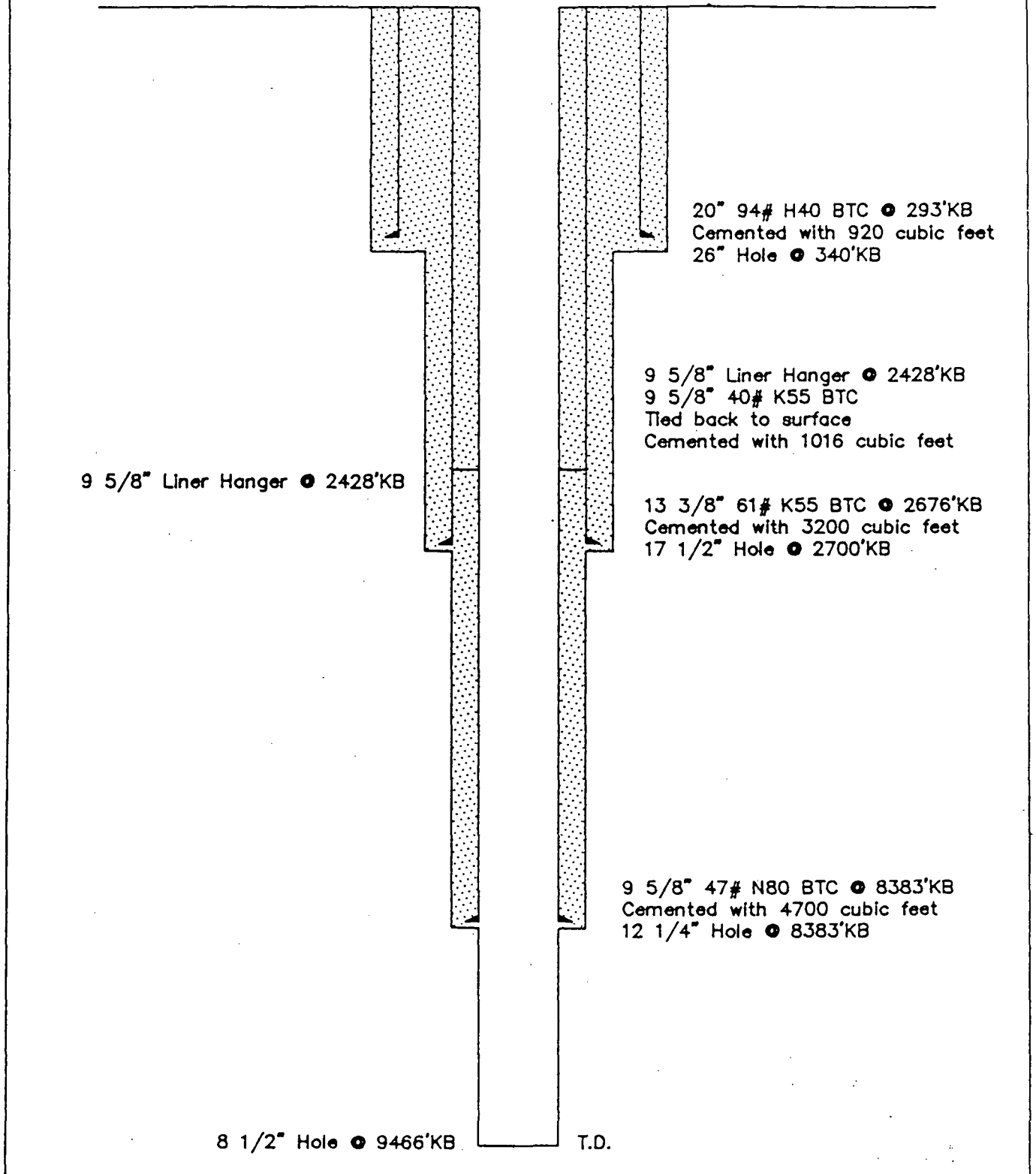


# Well Completion Diagram Well 65-18

Location: NW-NW-SE Section 18-24N-37E  
Churchill County, Nevada

Datum: 3469' KB, 32' Above Ground Level

Drilled: 01/21/81

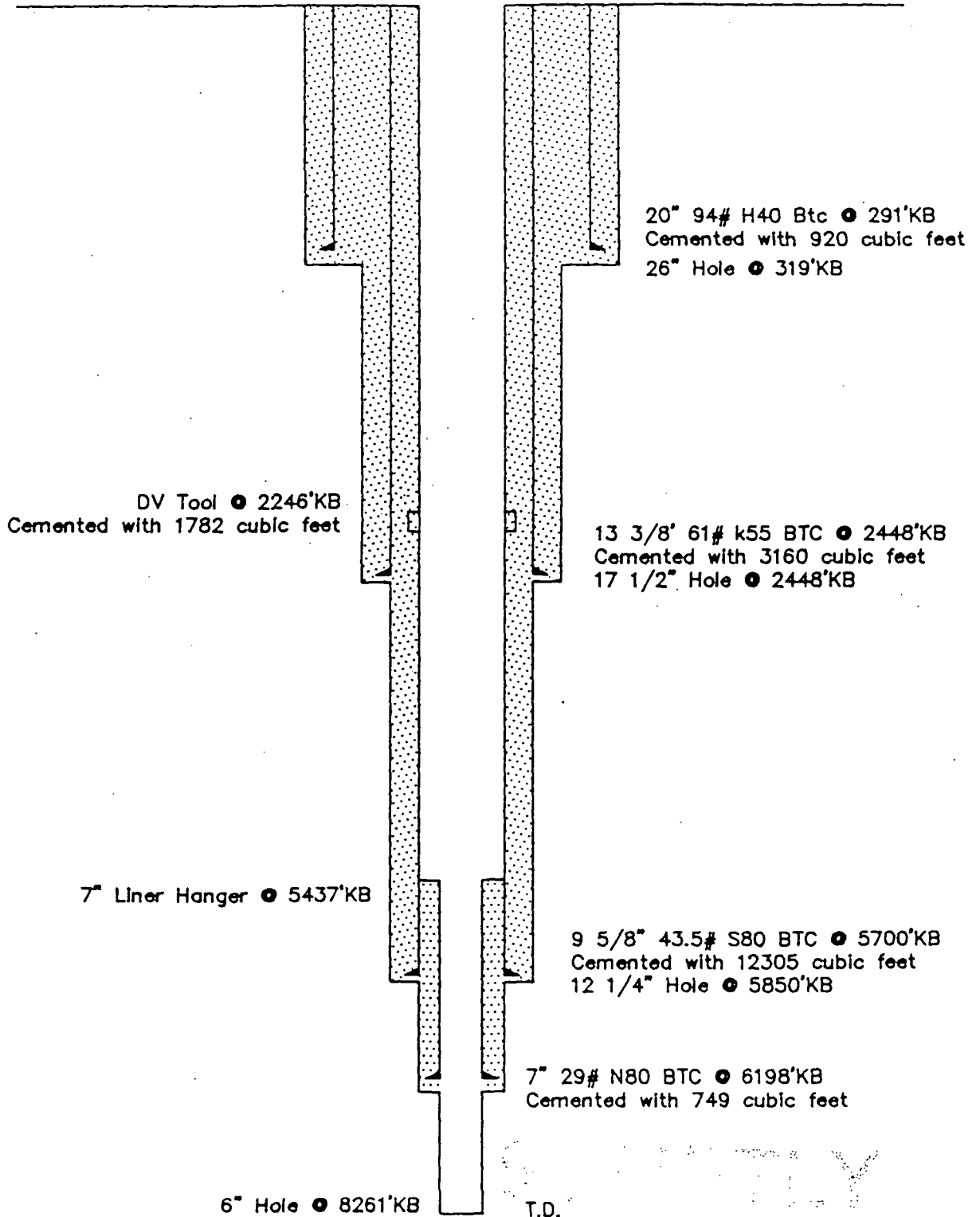


# Well Completion Diagram Well 45-5

Location: SE-SW-NW Section 5-24N-37E  
Churchill County, Nevada

Datum: 3478' KB, 27' Above Ground Level

Drilled: 06/24/81



assessment. During this flow test well 84-7 produced 650,000 lbs/hr of fluid at a wellhead pressure of 128 psig. Currently this well is being used as a pressure observation hole for the 6 well flow test. Future plans for this well include a cleanout and deepening to intersect additional fractures and increase its flow rate.

## 65-18

Well 65-18 was completed by SUNEDCO on March 30, 1981 to a total depth of 9305 feet. The well was subsequently deepened to 9466 feet during the March 1986 workover by Oxbow (Figure 7.1.7). Well 65-18 produces from the Jurassic spilitic sequence between depths of 9265 and 9417 feet. The well was flow tested twice during early 1981 and late 1982. During the latter part of 1981 and early 1982 the well was used as an injector. After the 1986 workover the well produced at flow rates up to 800,000 lbs/hr at a wellhead pressure of 100 psig. This is one of the wells flowed during the 6 well flow test. In the future well 65-18 will be evaluated as a possible injector.

## 45-5

Well 45-5 was completed by SUNEDCO on June 24, 1981 to a total depth of 8261 feet (Figure 7.1.8). The well produced from the Miocene basalt in the 6020 to 6200 foot interval. The production zone is associated with the range-front fault at a relatively shallow depth. Although the well produced up to 609,000 lbs/hr, the enthalpy (322 btu/lb) and wellhead pressure (65 psig) are abnormally low. The well has only been flow tested for three days in May, 1981, and fifteen days in July, 1981. Currently well 45-5 is being used for pressure observation purposes. In the near future well 45-5 will be evaluated as a possible injection well.

## 27-33

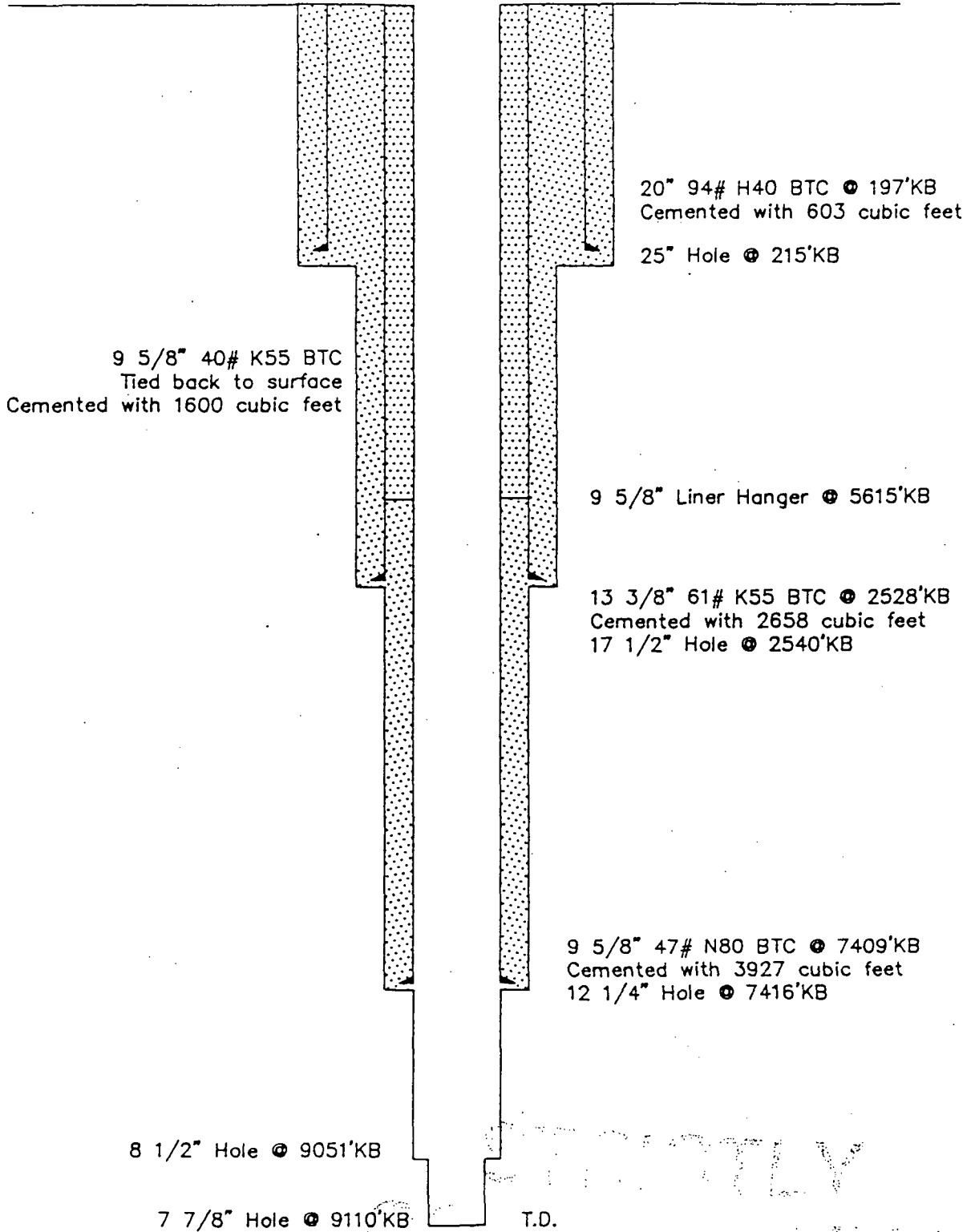
Well 27-33 was completed by TGI on August 30, 1983 to a total depth of 9051 feet. The well was subsequently deepened to 9110 feet during the March 1986 workover by Oxbow (Figure 7.1.9). Well 27-33 produces from the Jurassic marine sedimentary rocks in the 8862 to 9110 foot interval. The well was extensively flow tested prior to the 1986 workover. After the workover its flow rate increased from 370,000 lbs/hr to 720,000 lbs/hr. Currently this well is being used for pressure observation purposes in the 6 well test. This will be one of the wells supplying the power plant.

# Well Completion Diagram Well 27-33

Location: NE-SW-SW Section 33-25N-37E  
Churchill County, Nevada

Datum: 3469' KB, 23' Above Ground Level

Drilled: 08/31/83

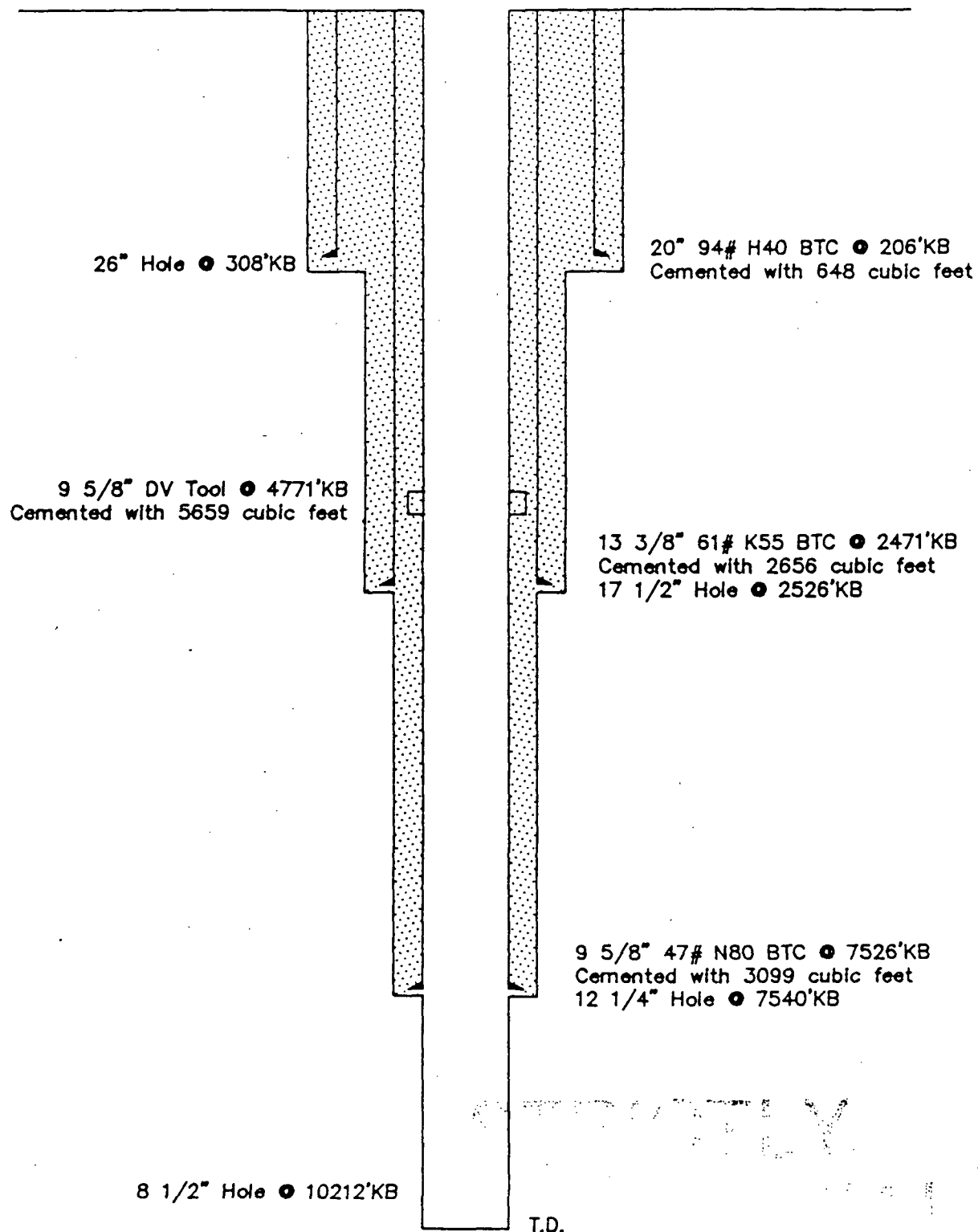


# Well Completion Diagram Well 45-33

Location: NE-NE-SW Section 33-25N-37E  
Churchill County, Nevada.

Datum: 3471' KB, 23' Above Ground Level

Drilled: 12/31/83

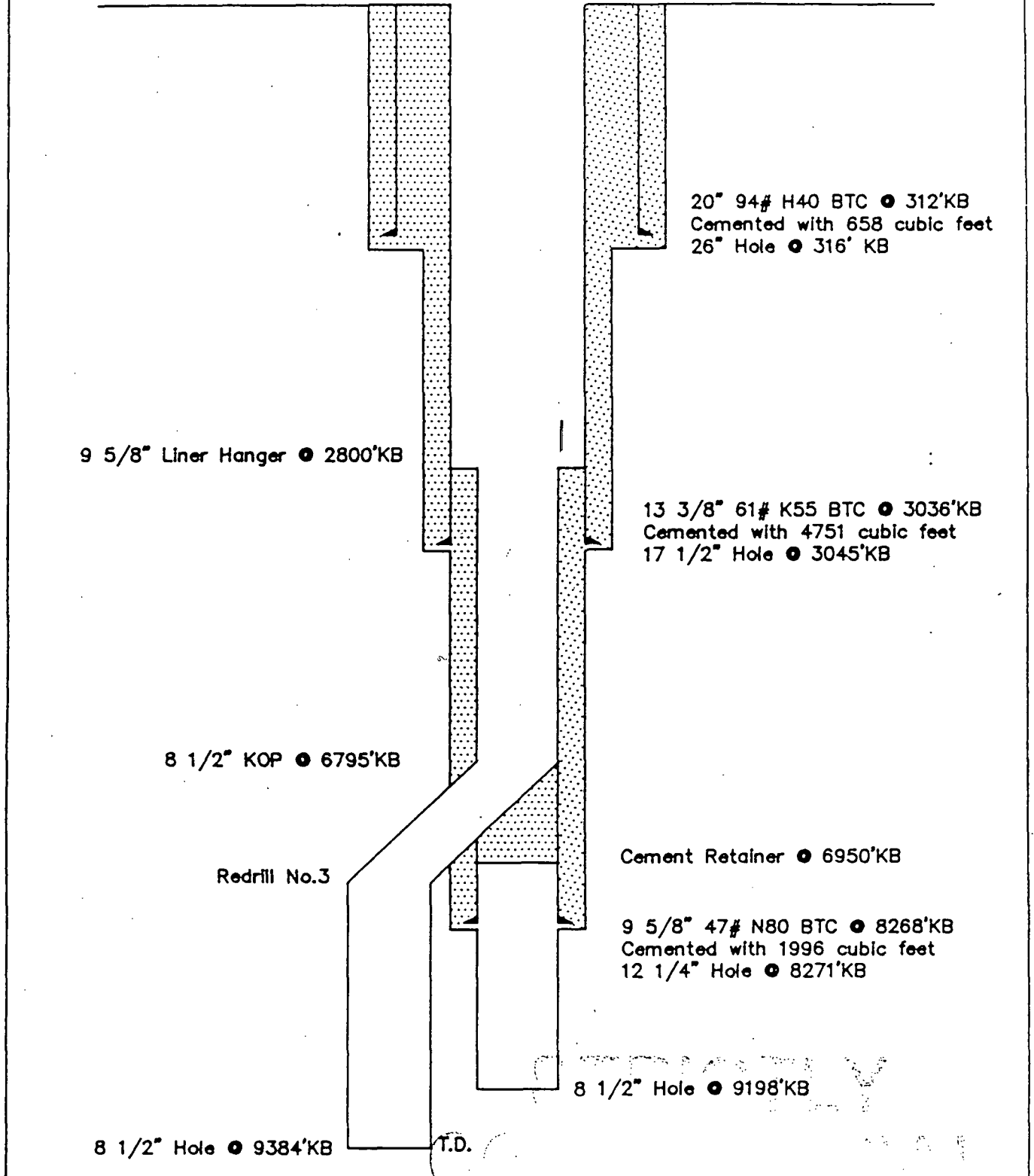


# Well Completion Diagram Well 82-5

Location: SE-NE-NE Section 5-24N-37E  
Churchill County, Nevada

Datum: 3467' KB, 23' Above Ground Level

Drilled: 02/18/86



45-33

Well 45-33 was completed by TGI on December 31, 1983 to a total depth of 10,212 feet. The well was subsequently deepened to 10,266 feet during the June 1986 workover by Oxbow (Figure 7.1.10). The workover was conducted to mill out two casing collapse zones located within the 9 5/8" casing. The well produces from the Jurassic marine sedimentary rocks in the 10,058 to 10,240 foot interval. The well was extensively flow tested prior to the Oxbow workover. Since the workover the flow rate for well 45-33 has increased from 610,000 lbs/hr to about 1,000,000 lbs/hr. Oxbow is currently flowing this well as part of the 6 well flow test. Well 45-33 is one of the wells that will be supplying the power plant.

82-5

Well 82-5 was completed by Oxbow on February 18, 1986, to a total depth of 9384 feet (Figure 7.1.11). The existing leg of 82-5 is the fourth leg of the well and is a dry hole completed in Cretaceous granodiorite. Only leg two of 82-5 was capable of production and this was at a wellhead pressure of 25 psig. Currently this well is idle. Future plans call for cleaning out the well so it can be evaluated as a long term pressure observation well.

74-7

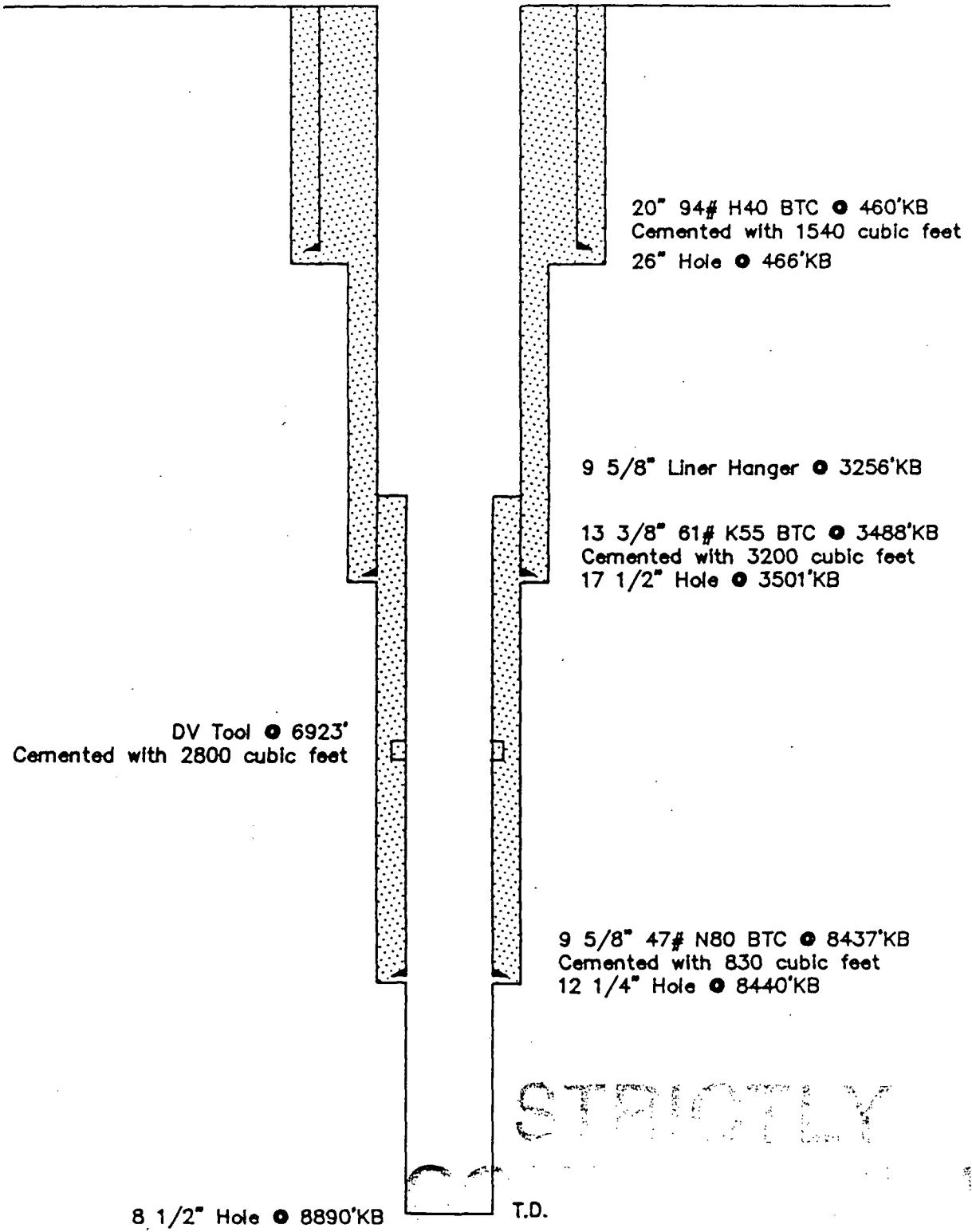
Well 74-7 was completed by Oxbow on March 29, 1986, to a total depth of 8890 feet (Figure 7.1.12). The well produces from the Jurassic spilitic sequence in the 8722 to 8890 foot interval. The production zone is associated with the range-front fault. Well 74-7 was the first well completed at Dixie Valley with 13 3/8" production casing set to a depth below the flash zone. Since completion this well has been extensively tested. Its maximum initial flow rate was 1,350,000 lbs/hr at a wellhead pressure of 162 psig. This well is currently producing as part of the 6 well flow test and will be one of the wells supplying the power plant.

32-18

Well 32-18 was completed by Oxbow on March 31, 1986, to a total depth of 7461 feet (Figure 7.1.13). The well produces from the Miocene basalt in the 7360 to 7374 foot interval. The well was flow tested for a short period before the drill rig was released and later in 1986 during the six well flow



Well Completion Diagram Well 74-7  
 Location: SE-SW-NE Section 7-24N-37E  
 Churchill County, Nevada  
 Datum: 3494.5' KB, 21' Above Ground Level  
 Drilled: 03/29/86



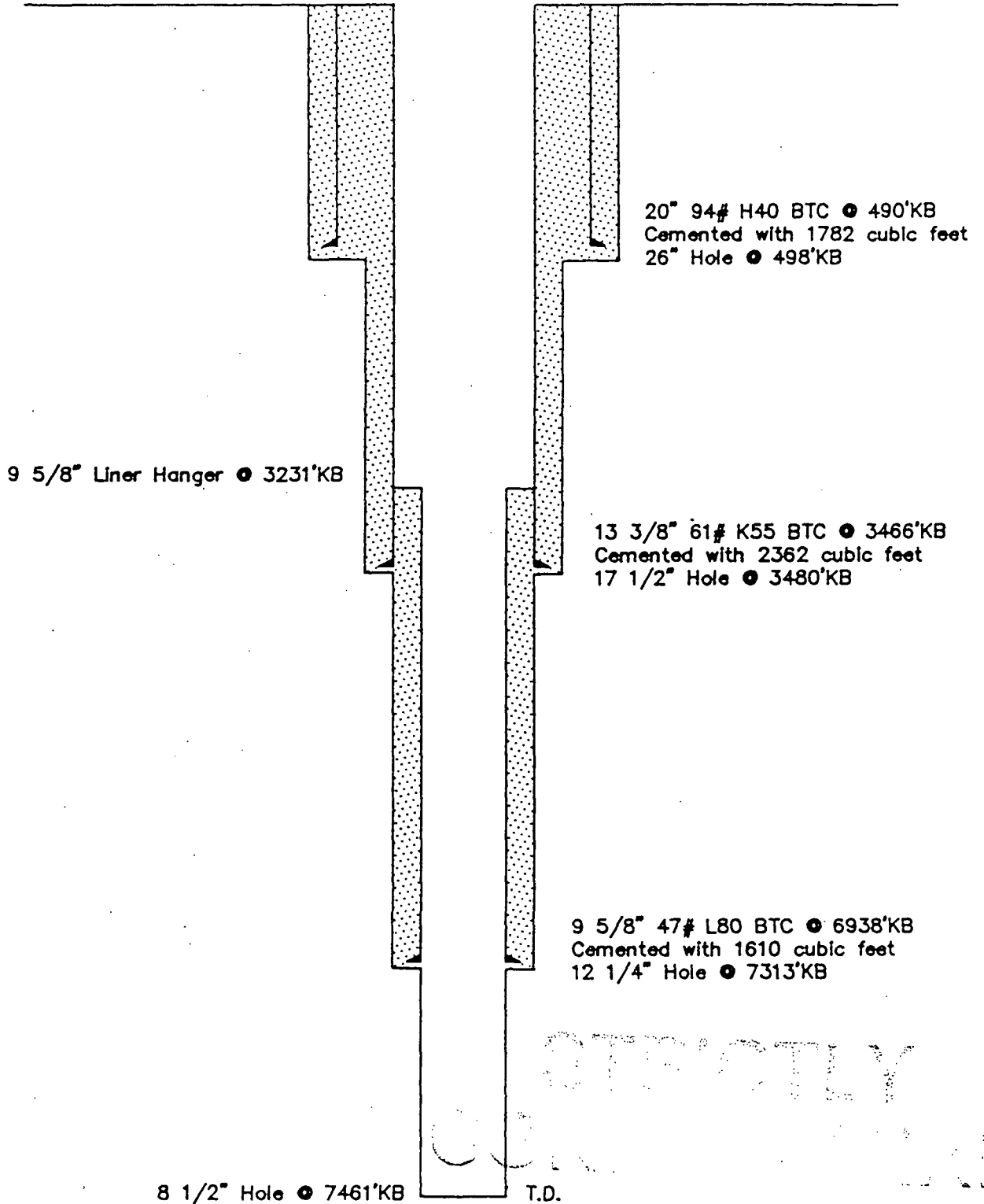
STRICTLY

# Well Completion Diagram Well 32-18

Location: SW-NE-NE Section 18-24N-37E  
Churchill County, Nevada

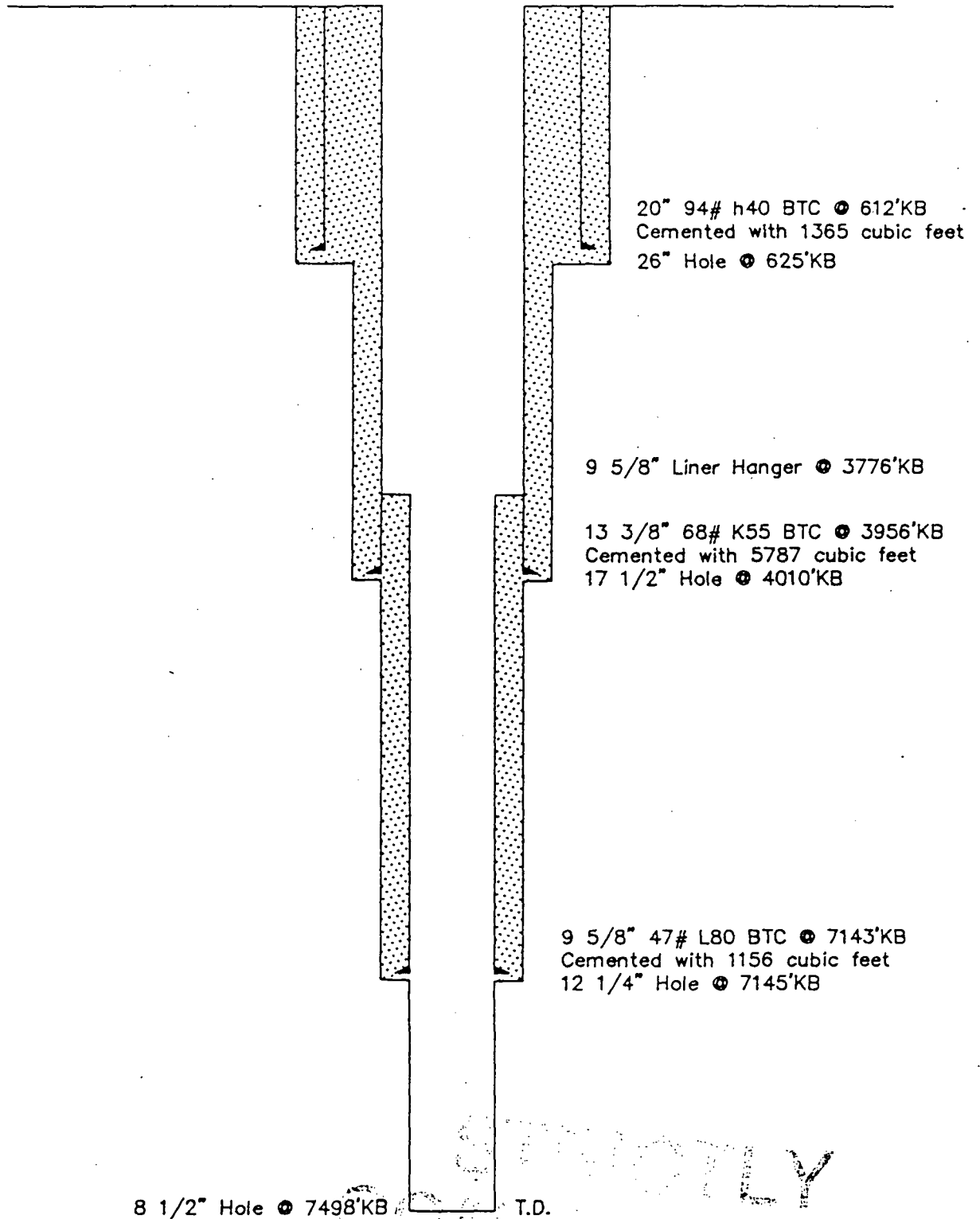
Datum: 3467' KB, 30' Above Ground Level

Drilled: 02/20/86



# Well Completion Diagram Well 76-7

Location: SW-NE-SE Section 7-24N-37E  
Churchill County, Nevada  
Datum: 3491' KB, 28.5' Above Ground Level  
Drilled: 05/24/86

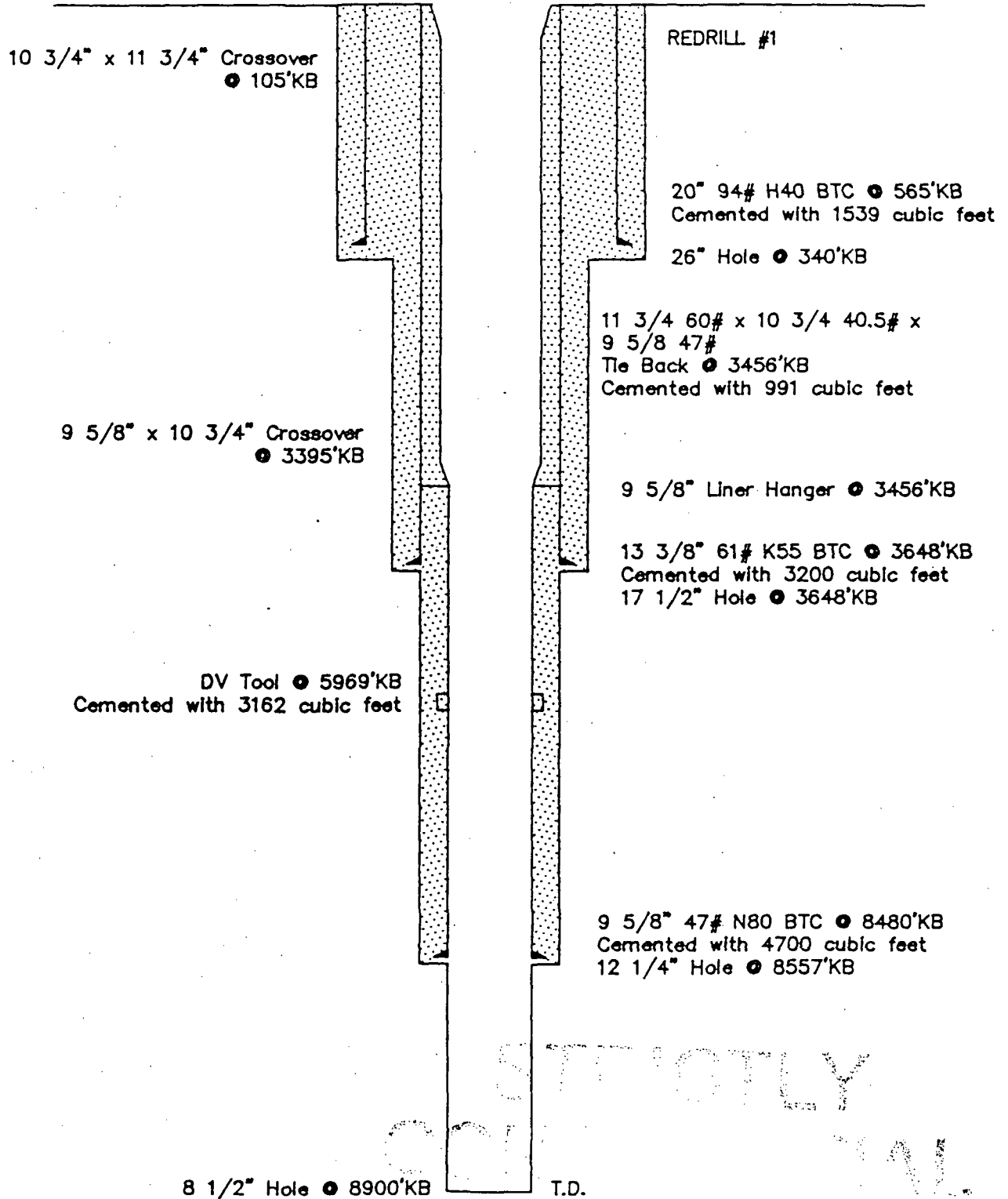


# Well Completion Diagram Well 73-7

Location: NW-NW-SE Section 7-24N-37E  
Churchill County, Nevada

Datum: 3508' KB, 32' Above Ground Level

Drilled: 08/07/86



test. Initially this well produced 922,000lbs/hr at a wellhead pressure of 100 psig. This well is being evaluated as a possible injector.

76-7

Well 76-7 was completed by Oxbow on May 24, 1986, to a total depth of 7498 feet (Figure 7.1.14). The well produces from the Miocene basalt in the 7315 to 7461 foot interval. The initial production of well 76-7 was 1,700,000 lbs/hr at a wellhead pressure of 148 psig. This is by far the hottest of the wells to produce from the Miocene basalt and it is one of the wells currently flowing in the 6 well test. This will be one of the wells supplying the power plant.

73-7

Well 73-7 was completed by Oxbow on August 7, 1986 to a total depth of 8900 feet (Figure 7.1.15). The well produces from the Jurassic spilitic sequence in the 8528 to 8913 foot interval. The production zone is associated with the range front fault. A leak in the 13 3/8" casing required the well to be completed with 10 3/4" and 11 3/4" casing tie back set to a depth below the flash zone. This is one of the wells producing for the 6 well test. Well 73-7 initially flowed 1,080,000 lbs/hr at a wellhead pressure of 118 psig. This well will supply the power plant.

## 7.2 Previous Testing

### 7.2.1 SUNEDCO Geothermal Testing

SUNEDCO conducted a number of flow and interference tests in conjunction with its drilling during the period 1979 to 1982. The testing and results have been summarized by GeothermEX in a report titled "Estimation of Geothermal Energy Reserves Underlying Sun Geothermal Company Leases in Dixie Valley, Nevada. November 1984."

The testing showed that all the SUNEDCO wells except 62-21 are in good hydraulic communication and the transmissivity of the reservoir in the area of the wells is between 15,000 and 70,000 md ft. Table 7.3 summarizes the reservoir test data obtained by Sun.

GeothermEX concluded that the reservoir consisted of a permeable region associated with and generally confined to the range front fault. Thermal boundaries were placed on the reservoir on the basis of temperature contouring as shown in Figure 7.2.1.

## 7.2.2 Trans-Pacific Geothermal Testing

Trans-Pacific Geothermal Inc. (TGI) conducted interference tests between its two wells 27-33 and 45-33 in 1983-4. The tests are documented in a Berkeley Group Inc. report titled "Resource Characteristics, Dixie Valley, Nevada. August 1984." Figure 7.2.2 reproduced from the report shows the interference data obtained in 45-33 while 27-33 was flowing and Figure 7.2.3 shows the interference data when the roles of the two wells were reversed.

The test data were analytically interpreted by idealizing the reservoir as a homogeneous and infinite system containing a large uniform flux fracture. A diagram illustrating the conceptual model is shown in Figure 7.2.4. The two wells intersect the fracture and the fracture draws fluid from the reservoir along its length, delivering it to the wells.

The transmissivity of the reservoir given by type curve matching was about 70,000 md-ft and the storage-fracture length group (Ochxj exp 2) was 25,000 ft/psi. Matches to the TGI test data using the fracture model are shown in Figures 7.2.5 and 7.2.6.

The model can be interpreted physically by considering the range-front fault to be representative of the uniform flux fracture in the analytical model. The fault acts as the very permeable conduit drawing fluid from surrounding lower permeability zones and delivering it to the wells.

The TGI and SUNEDCO activities were entirely separate, neither party having access to the other's data. However, once the two properties were consolidated by Oxbow, it was possible to integrate data from the two regions. Figure 7.2.7 and 7.2.8 show pressure measurements made in 45-5 and 52-18 by SUNEDCO during the period when TGI was conducting flow tests of 45-33 in 1983.

Well 45-5 is about 6000 feet and well 52-18 about 17,000 feet from well 45-33. Both wells showed a pressure response to flow at 45-33 with 52-18 exhibiting more direct communication even though it is three times further away. Also, the response in 52-18 was nearly half that observed in 27-33. This is not consistent with a homogeneous reservoir response when it is considered that 27-33 is only 500 feet from 45-33 compared with 17,000 feet to 52-18.

STRICTLY

117

COPY

Pressures in Well 45-33  
While Flowing Well 27-33

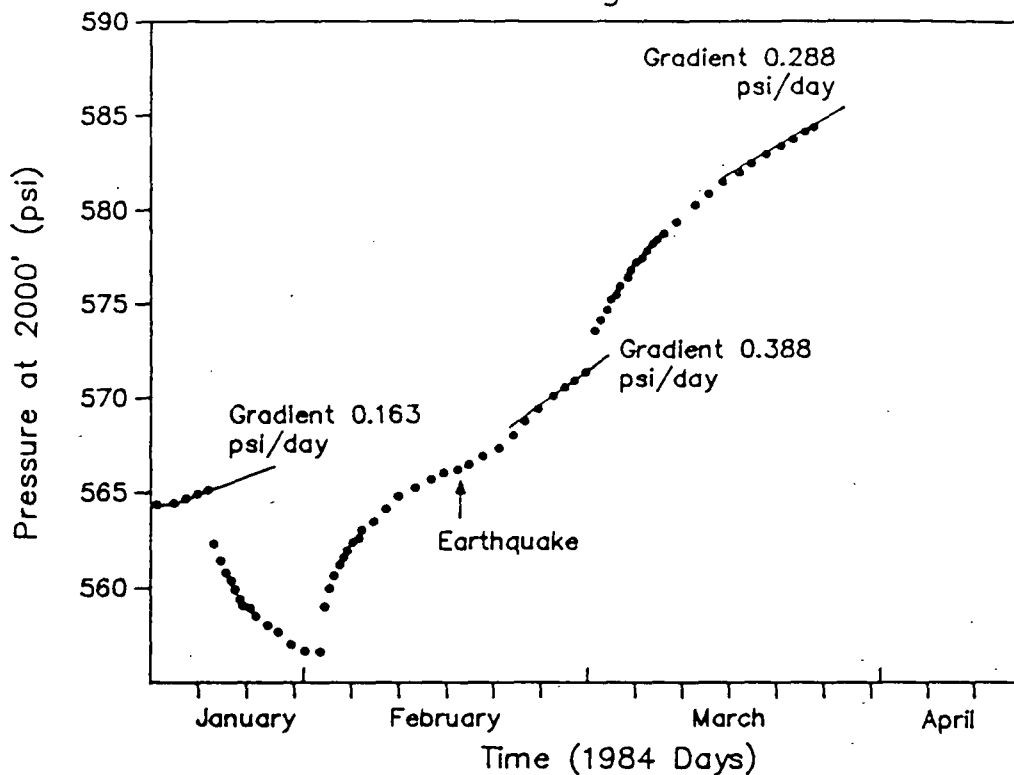


Figure 7.2.2

Pressures in Well 27-33  
While Flowing Well 45-33

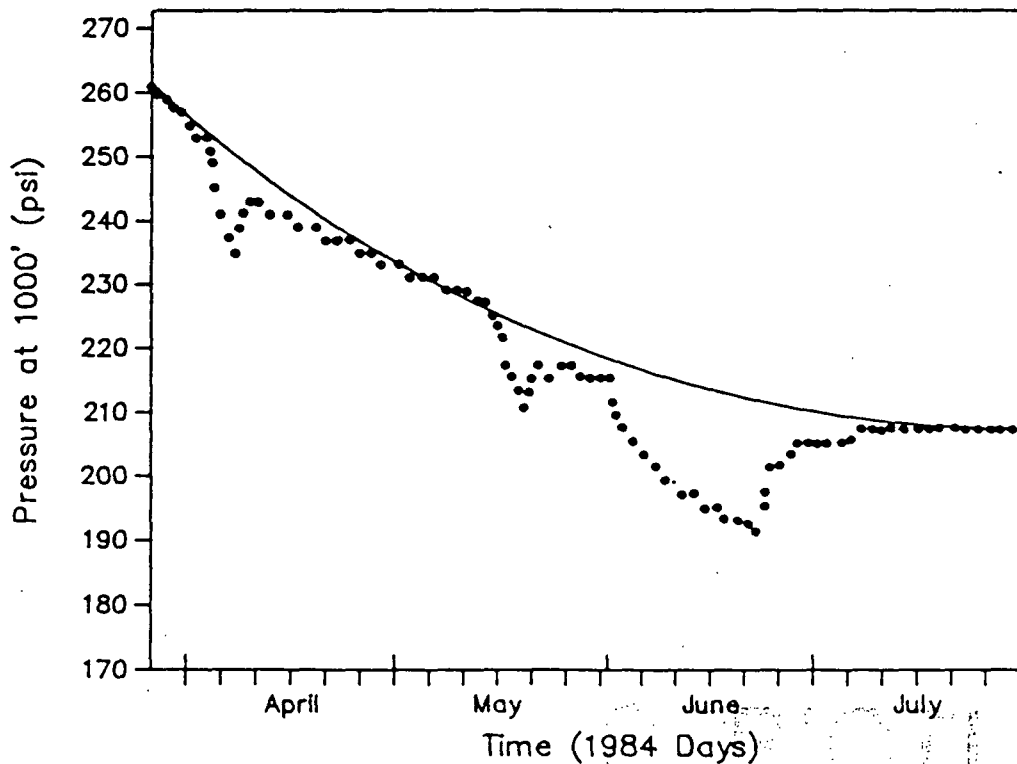


Figure 7.2.3

Pressures In Well 45-33  
While Flowing Well 27-33

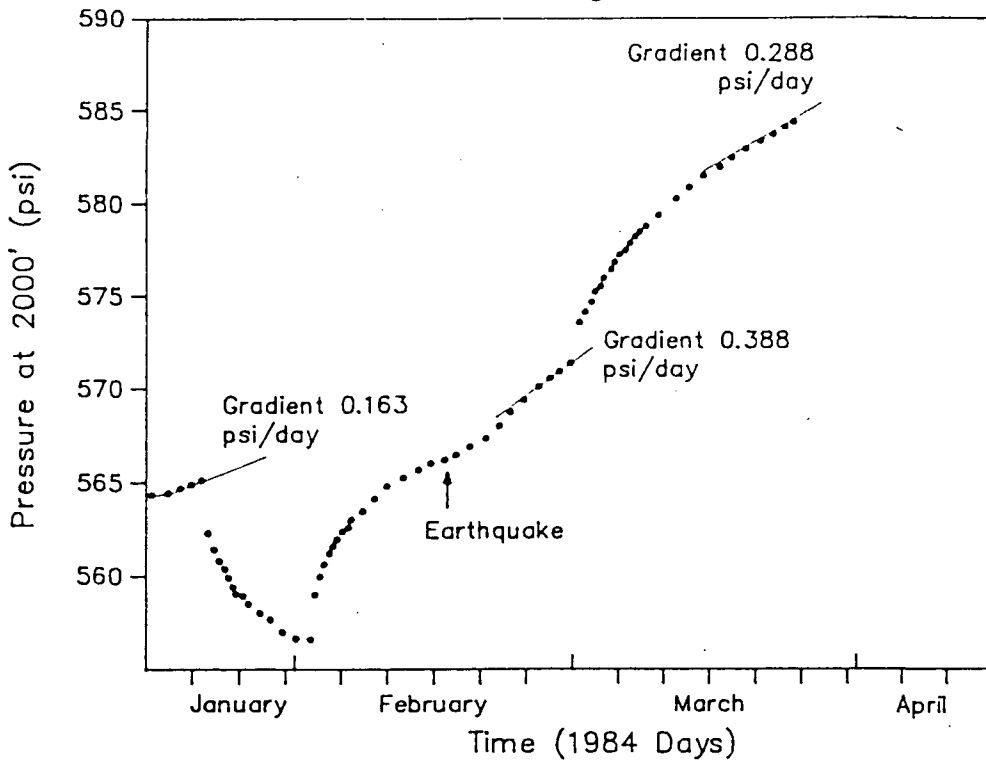


Figure 7.2

Pressures In Well 45-33  
While Flowing Well 27-33

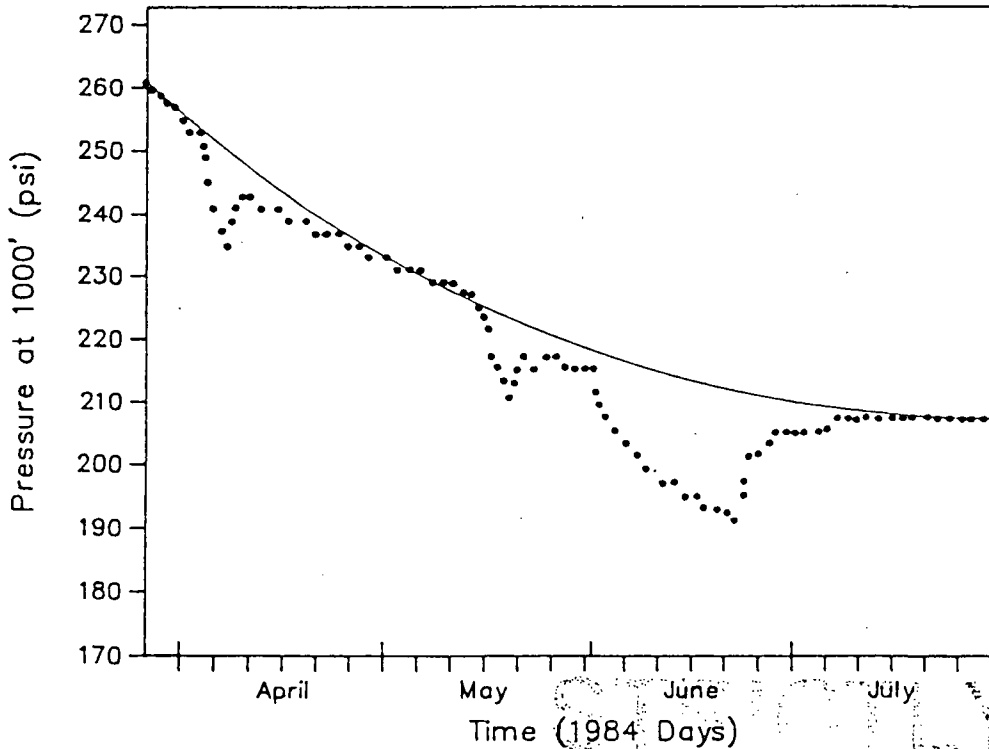


Figure 7.3



# Conceptual Model of Dixie Valley Reservoir Evaluation of Transpacific Geothermal Test Data

Reservoir Properties  
 $kh = 70,000 \text{ md-ft}$   
 $\phi c h x_f^2 = 25,000 \text{ ft}^3/\text{psi}$

Wells



Uniform Flux  
Fracture

STRICTLY  
CONFIDENTIAL

### History Match When 45-33 Was Producing and Subsequent Buildup

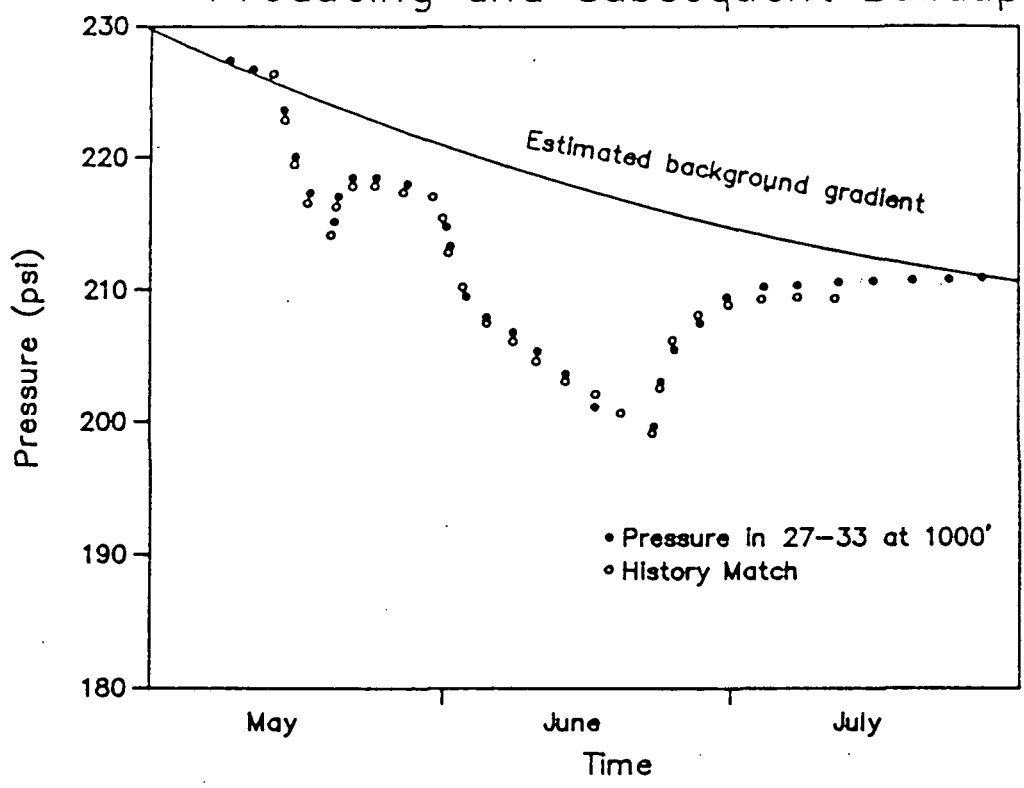


Figure 7.2.5

### Drawdown in Well 45-33 Due to Flow Rate Increase of 27-33

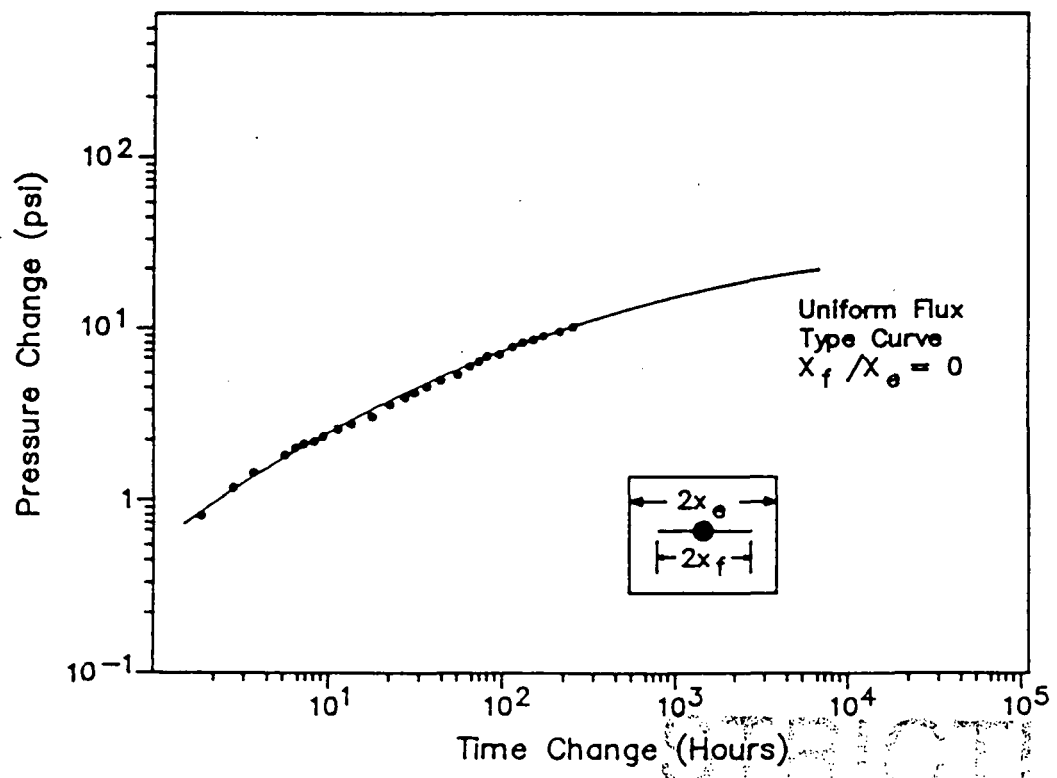


Figure 7.2.6

### History Match When 45-33 Was Producing and Subsequent Buildup

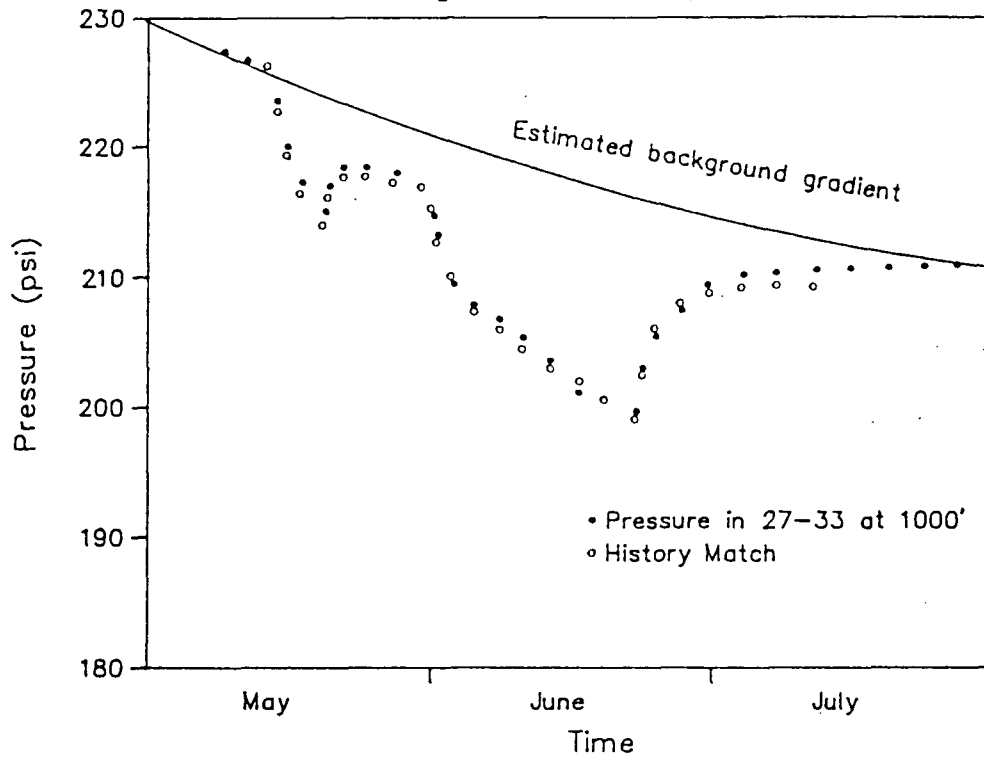


Figure 7.5

### Drawdown In Well 45-33 Due To Flow Rate Increase Of 27-33

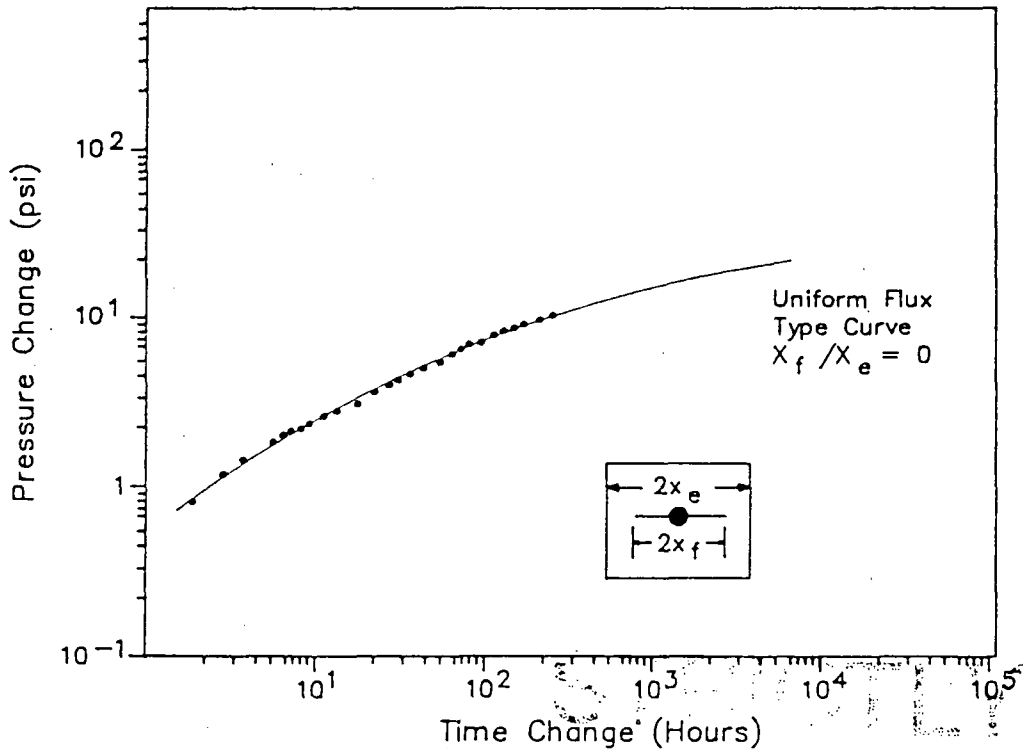


Figure 7.6

### Pressure Response in Well 45-5 Due to Flow in 45-33

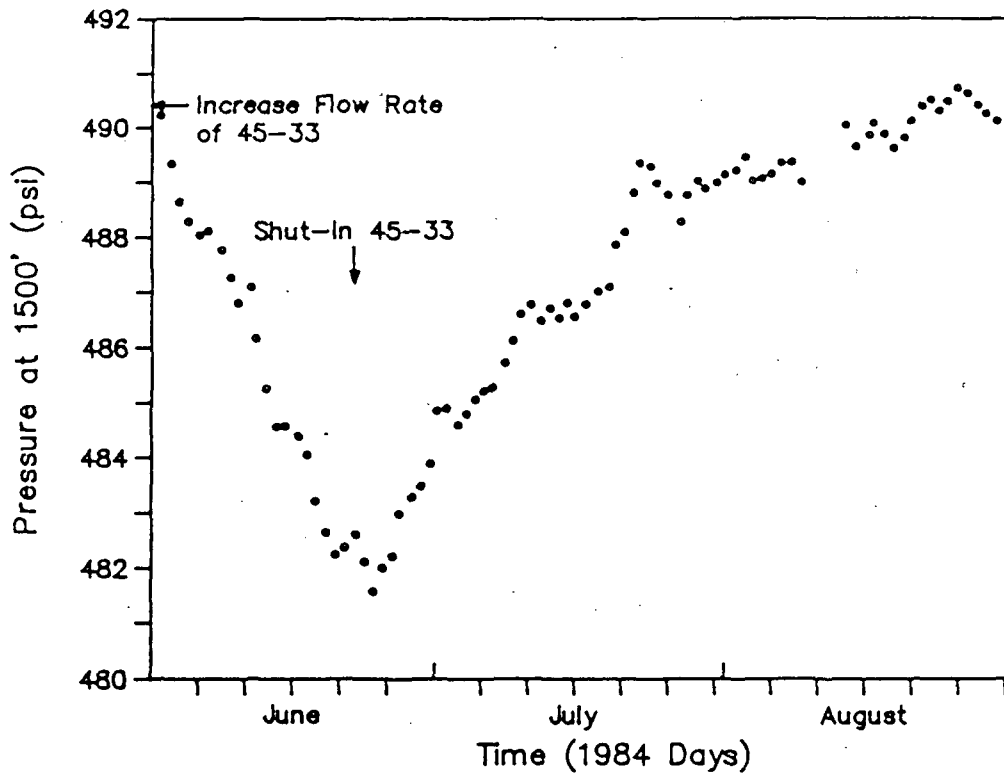


Figure 7.2.7

### Pressure Response in Well 52-18 Due to Flow in 45-33

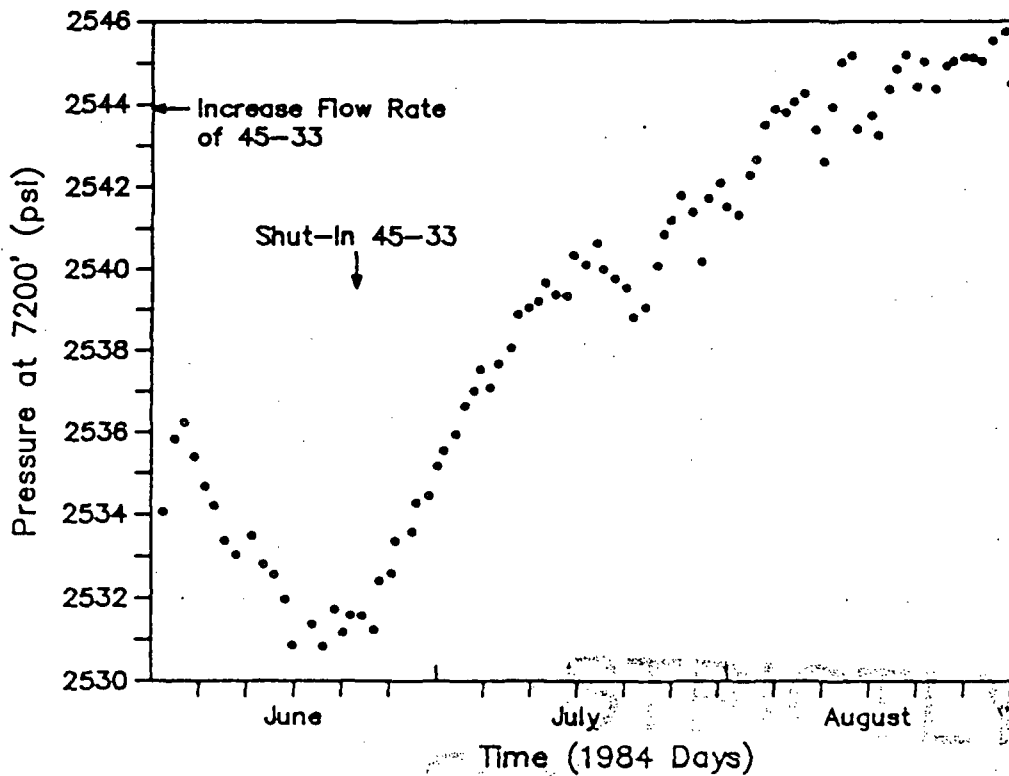


Figure 7.2.8

### Pressure Response In Well 45-5 Due To Flow In 45-33

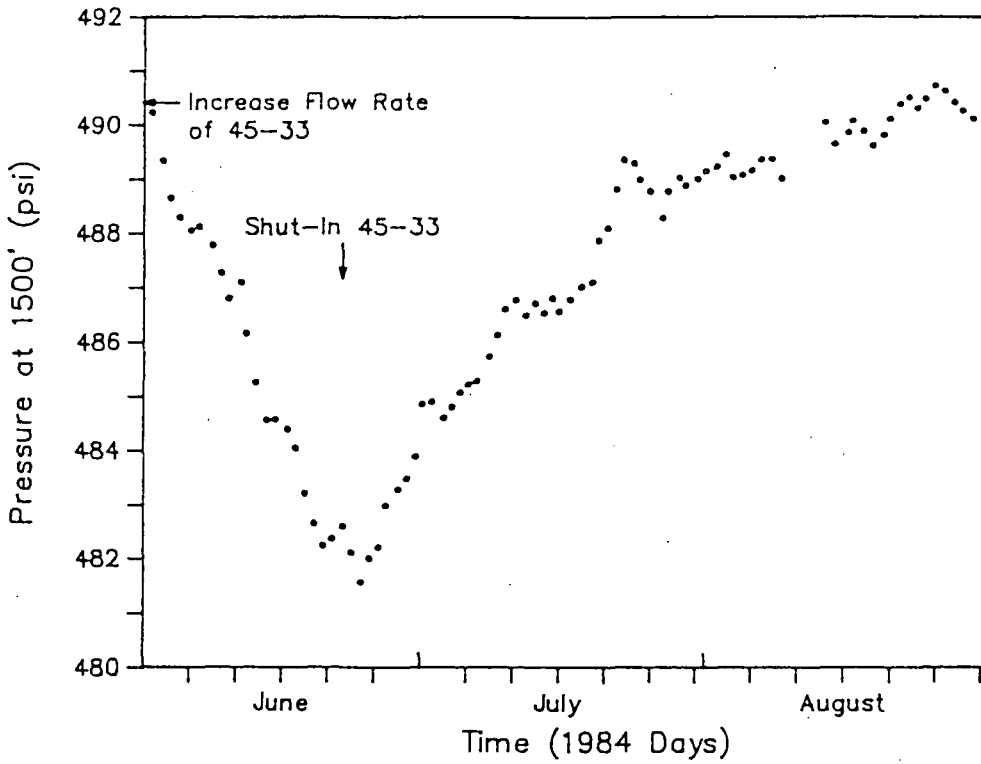


Figure 7.7

### Pressure Response In Well 52-18 Due To Flow In 45-33

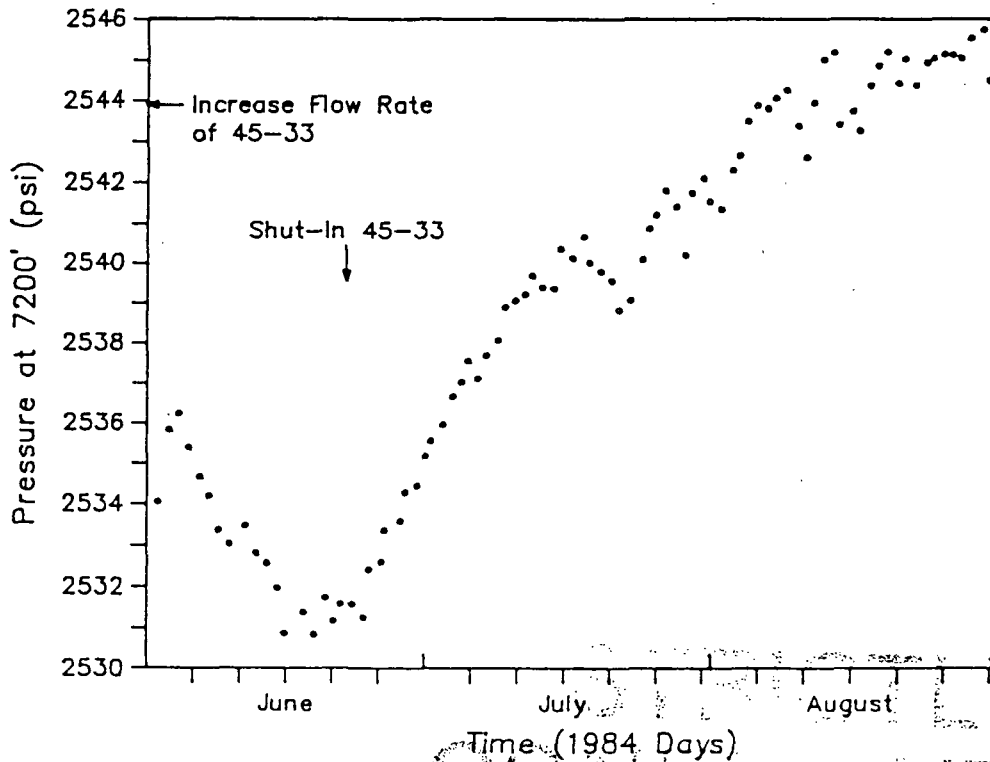


Figure 7.8

CONFIDENTIAL

In summary, the overall character of the pre-1986 data suggests considerable anisotropy in the reservoir and is consistent with the fault-dominated behavior discussed earlier.

### 7.3 Description of Oxbow Reservoir Test

The flow and interference test performed by Oxbow during the first half of 1986 consisted of flowing wells 27-33 and 84-7 for a combined period of 4 months while pressures were monitored in the surrounding nine wells. (For location of wells see Figure 2.2).

In addition, short flow tests were conducted in other wells after completion of drilling or rework operations. The nonflowing wells were instrumented prior to the flow test to provide background reservoir pressure data.

Well 27-33 was kicked-off on December 17, 1985 and produced continuously at 370,000 lbs/hr until March 13, 1986. Well 84-7 was kicked off on January 22, 1986 and produced continuously at 650,000 lbs/hr until April 7, 1986. Various other wells were flowed for periods of between one and seven days. The flow test history is summarized in Table 7.4 and shown graphically in Figure 7.3.

### 7.4 Pressure Monitoring Data

#### 7.4.1 Instrumentation

The observation wells were instrumented using a downhole pressure chamber and capillary tubing system. The system is shown diagrammatically in Figure 7.4. The chamber is hung on capillary tubing below the water level in the well. The chamber and tubing are charged with helium gas from the surface. A quartz pressure transducer or high resolution pressure gage is connected to the tubing at the surface and measures the hydrostatic pressure in the well at the chamber level.

Changes in reservoir pressure produce changes in the hydrostatic column and hence changes in pressure at the chamber. Quartz pressure transducers with a resolution better than 0.01 psi were used during the majority of the test. Pressures were transmitted to a central computerized logging unit where they were logged on disk and printed at regular (usually 20 minute) intervals.

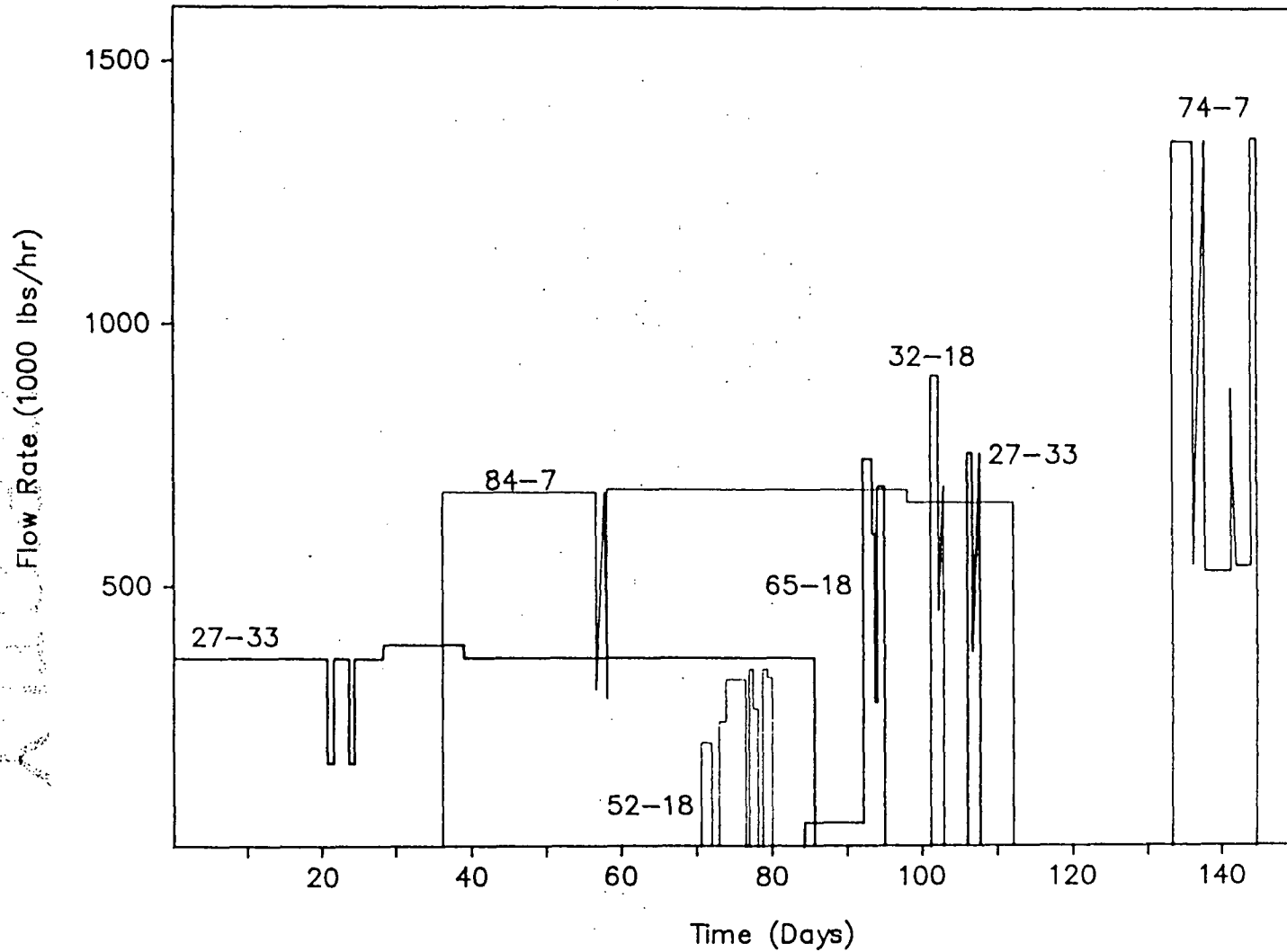
STRICTLY  
CONFIDENTIAL

Table 7.4  
Oxbow Reservoir Test History

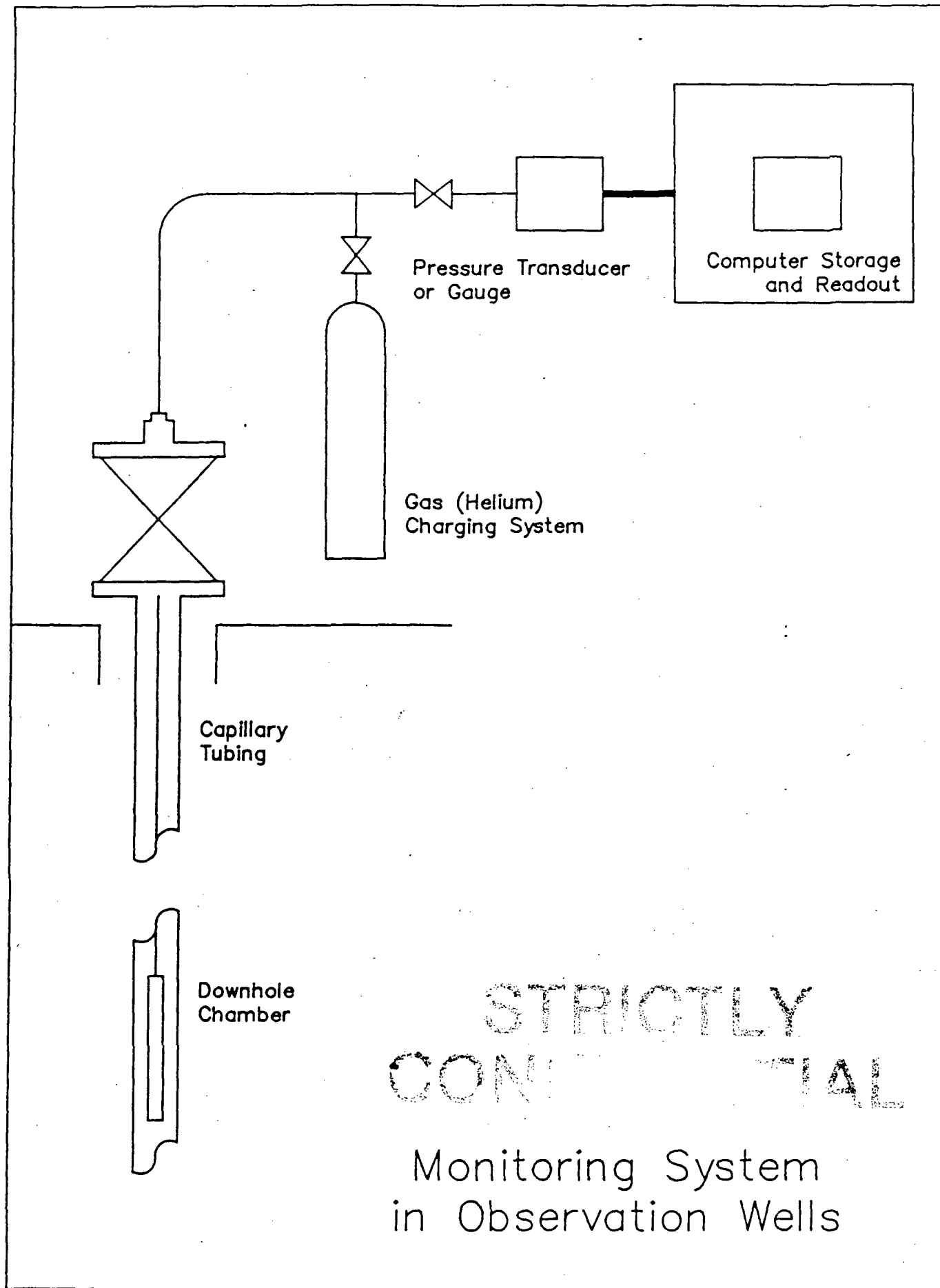
WELL	DATES	TIME FLOWED	PURPOSE
27-33	12/17/85-3/13/86	86 days	Long term test
27-33	4/2/86-4/3/86	31 hours	Test after workover
84-7	1/22/86-4/7/86	75 days	Long term test
52-18	2/25/86-3/5/86 (Intermittent)	139 hours	Test after workover
65-18	3/12/86-3/18/86 (Intermittent)		Air drilling
65-18	3/8/86-3/19/86	25.5 hours	Test after workover
32-18	3/26/86-3/28/86		Air drilling
32-18	3/28/86-3/29/86	24 hours	Initial flow test
SWL-1	3/27/86	7 hours	Test after workover
74-7	3/27/86	1 hour	Rig test
74-7	4/29/86-5/8/86	9 days	Initial flow test
76-7	5/20/86-5/27/86 (Intermittent)		Air drilling
76-7	5/22/86	1 hour	Rig test
45-33	6/29/86-7/3/86 (Intermittent)		Air drilling
45-33	7/3/86	4 hours	Test after workover

STRICTLY  
CONFIDENTIAL

# Reservoir Test Flow Rate History







Toward the end of the test, the quartz transducers were replaced with Heise pressure gages with a resolution of about 0.1 psi. These were logged manually approximately once per day.

#### 7.4.2 Monitor Wells and Monitoring Period

The periods during which monitoring was installed in the various wells is summarized in Table 7.5. The instrumentation was removed from a number of wells in December 1985 in order to conduct logging operations in preparation for rework operations. In some cases the instrumentation was reinstalled and then later removed when the rig was moved on to conduct the rework operations.

Three wells, 45-5, 45-33 and SWL-3, were instrumented during the entire test period and provide the major data base for the reservoir assessment and modeling effort.

Pressure monitoring instrumentation was installed at 6,000 feet in well 27-33 on January 10, 1986 while it was flowing and remained in the well until March 16, 1986, when it was removed in order to conduct a workover.

Well 74-7 was instrumented between April 3 and April 23, 1986 to monitor pressure recovery after nearby well 84-7 was shut in. The instrumentation was subsequently installed in 84-7 between April 23 and May 23, 1986 to monitor the interference during the flowtest of 74-7. The objective in these cases was to evaluate the interference effects between these two closely spaced wells and help determine appropriate well spacing for future wells in Section 7.10.

#### 7.5 Results and Analytical Interpretation of Long Term Interference Test Data

Figures 7.5.1, 7.5.2, 7.5.3, and 7.5.4 show the monitoring data in wells 45-5, 45-33, SWL-1 and SWL-3 respectively. Calculated matches to the data employing a computer model that treats the reservoir as homogeneous and infinite, and has the capability of dealing with multiple flowrates and multiple wells, are shown on the same figures. Good matches were obtained to the drawdown portion of the data when 27-33 and 84-7 were producing. The transmissivities (kh) used to obtain these matches are given in Table 7.6 and ranged between 30,000 and 70,000 md ft. In general, it appears that the transmissivity decreases from north to south. The storage coefficient (0ch) used in the various cases ranged between  $1 \times 10^{-4}$  ft/psi and  $4 \times 10^{-4}$  ft/psi.

STRICTLY

CONFIDENTIAL

CONFIDENTIAL

Table 7.5  
 Periods During Which Pressures  
 Were Monitored in Non-Flowing Wells

WELL	MONITORING PERIOD
45-5	8/31/85 - Present
SWL-3	11/25/85 - Present
45-33	12/19/85 - 6/20/86
62-21	10/10/85 - Present
52-18	8/31/85 - 2/3/86 5/29/86 - Present
SWL-1	12/24/85 - 12/27/85 1/9/86 - 3/20/86 5/12/86 - Present
SWL-2	8/2/86 - 5/20/86 6/17/86 - Present
65-18	12/22/85 - 3/10/86
66-21	10/30/85 - Present Intermittent Monitoring of WHP
74-7	4/4/86-4/24/86
84-7	4/24/86-5/26/86

STRICTLY  
 CONFIDENTIAL

### Downhole Pressure Monitoring Well 45-5

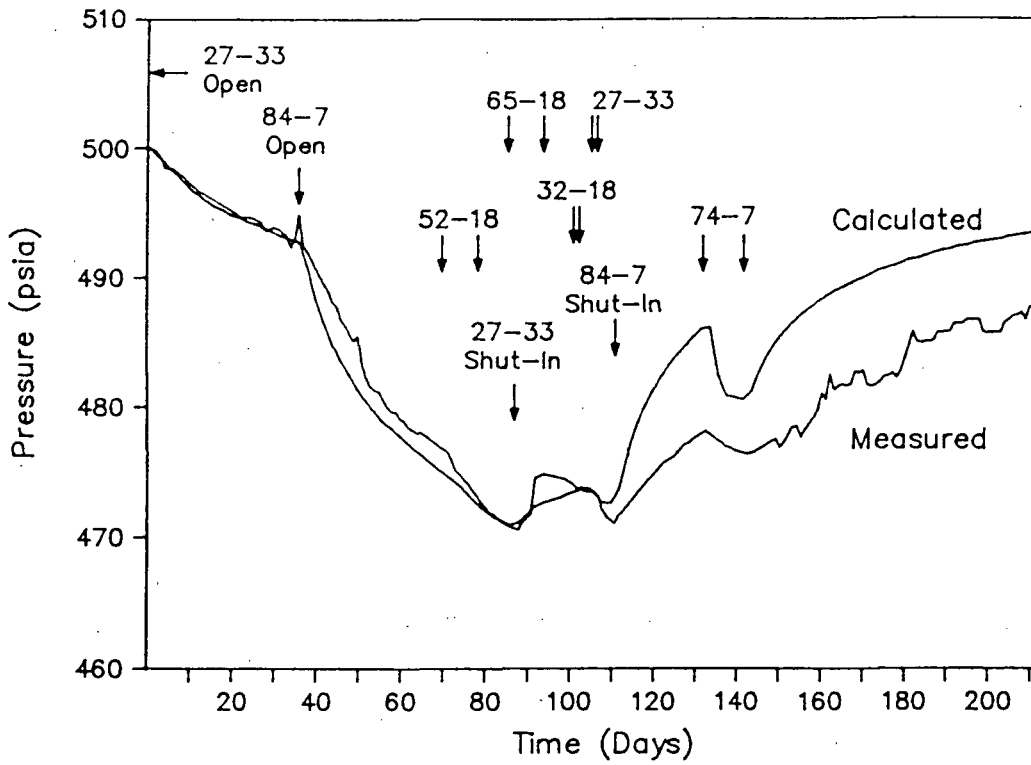


Figure 7.5.1

### Downhole Pressure Monitoring Well 45-33

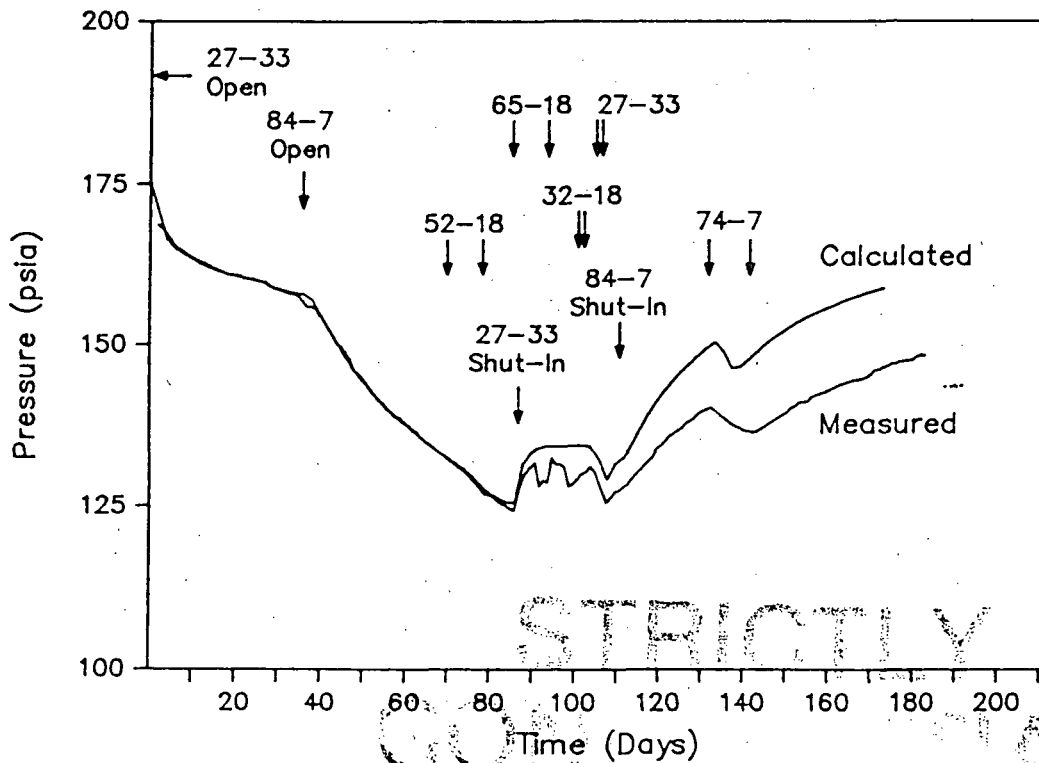


Figure 7.5.2

### Downhole Pressure Monitoring Well SWL-1

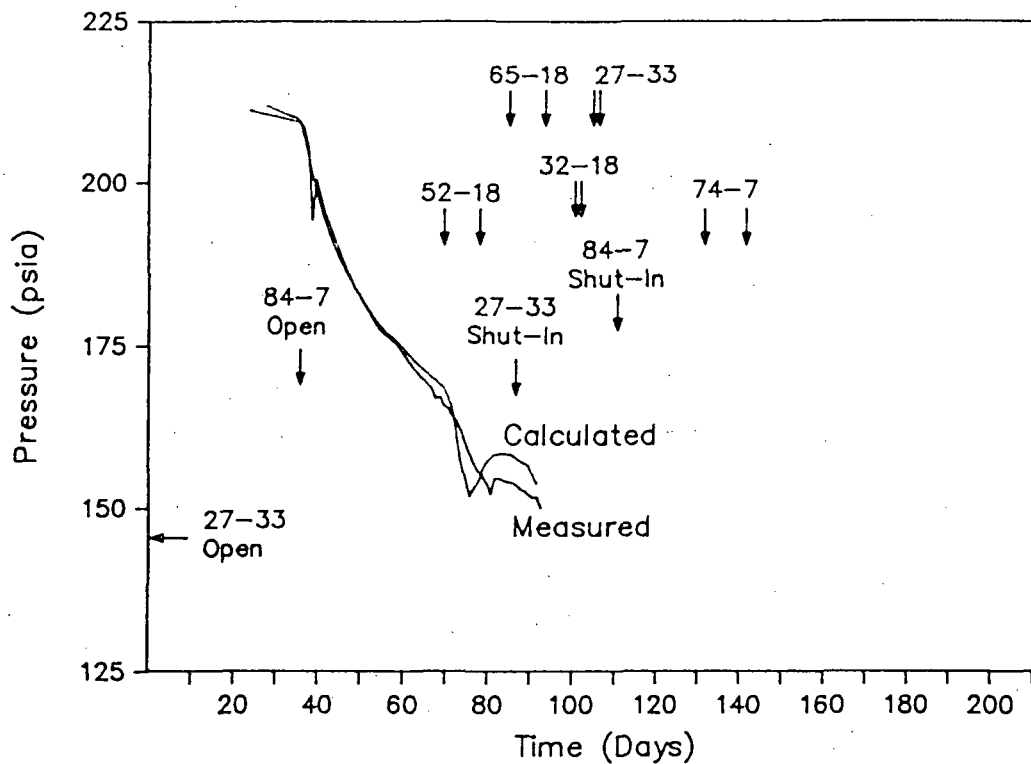


Figure 7.5.3

### Downhole Pressure Monitoring Well SWL-3

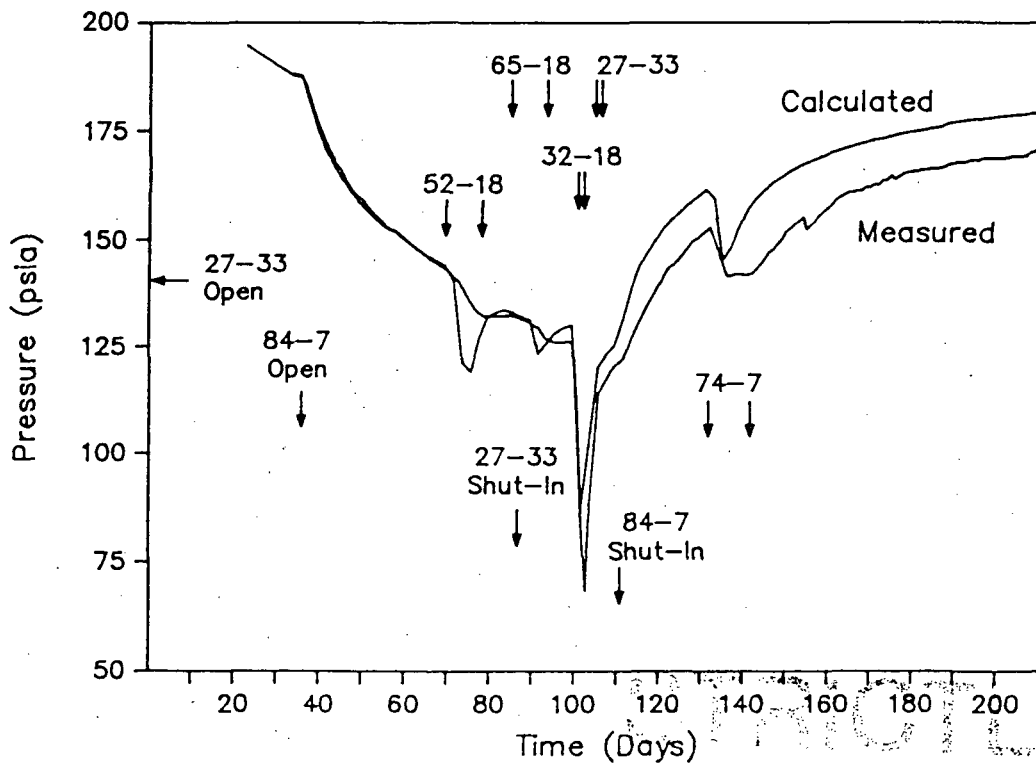


Figure 7.5.4

CONFIDENTIAL

Table 7.6  
 Summaries of Reservoir Properties  
 Used to Match Oxbow Reservoir  
 Test Data

OBSERVATION WELL	TRANSMISSIVITY (MD-FT)	STORAGE COEFFICIENT
45-33	68,000 (27-33) 30,000 (OTHERS)	1X10 exp-3 (27-33) 2X10 exp-4 (OTHERS)
SWL-3	15,000 (32-18) 30,000 (OTHERS)	3,75 X 10 exp-4
45-5	68,000	1X10 exp-3
SWL-1	30,000	4X10 exp-4

STRICTLY  
 CONFIDENTIAL

The interference between closely spaced well-pairs 27-33 and 45-33, and 32-18 and SWL-3 could not be matched using the same regional transmissivity employed between the more widely-spaced wells. Well 27-33 is only 500 feet from 45-33. The next nearest flowing well during the test was 84-7 which is about 12,000 feet from 45-33. Similarly 32-18 is 600 feet from SWL-3. The nearest well that was flowed for any appreciable time during the test is 74-7, which is about 4800 feet from SWL-3.

Interference between closely spaced wells strongly reflects local reservoir conditions (probably the fault zone in this case). Therefore, interference in 45-33 and SWL-3 produced by their near neighbors (27-33 and 32-18 respectively) was calculated separately and added to the interference produced by the more distant flowing wells. Adding effects in this way has little physical justification; however, it is believed reasonable if the relative distance between the nearby and the distant wells is large. It is important to note that these matches do not take into account any structural controls that may produce hydraulic anisotropy in the reservoir.

The same approach employed in matching the drawdown data was used to predict the pressure recovery after the wells were shut in. In all three cases (45-33, SWL-3 and 45-5) the observed pressure recovery was slower than the calculated recovery.

The measured pressures in 45-33 and SWL-3 two months after 84-7 was shut in are about 9 to 11 psi below the calculated pressures for a uniform permeability infinite system. (Figures 7.5.2 and 7.5.4). Pressures in 45-5 (Figure 7.5.1) also show a slower recovery than predicted. In this case, the overall interference effects were less pronounced than those in 45-33 and SWL-3, and the difference between the predicted recovery and observed recovery is about 6 psi.

Monitoring was continued in 45-5 and SWL-3 until the end of July when the six-well flow test was begun. It is interesting to note that in both cases the difference between the observed recovery and the predicted recovery decreases somewhat during July. For SWL-3 the difference was 9.3 psi on June 23 and 8.5 psi on July 17. Similarly, for 45-5 the difference was 6.7 psi on June 23 and 5.7 on July 17. The significance of these observations is discussed in Section 7.6.2.

STRICTLY

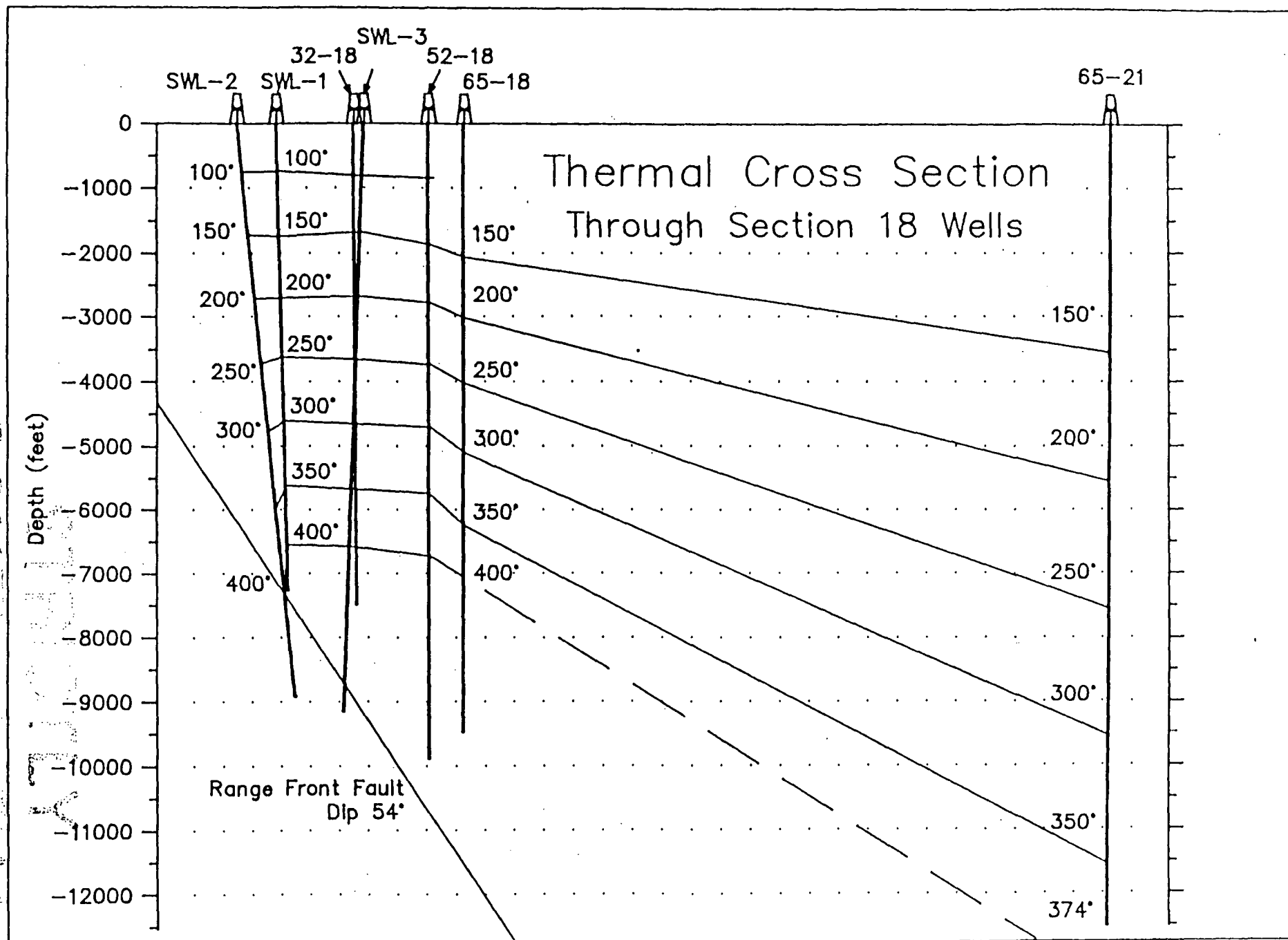
CONFIDENTIAL

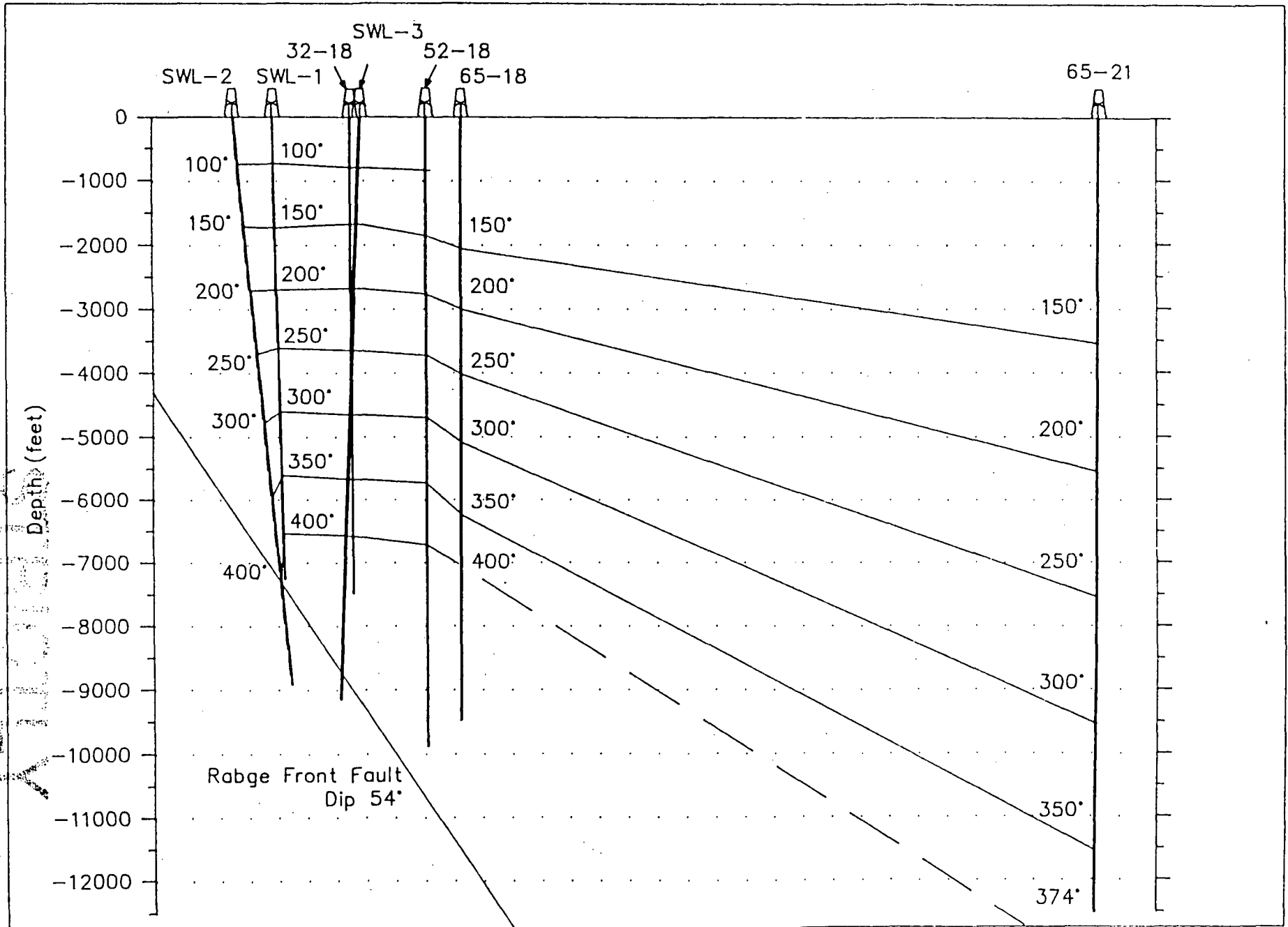
Table 7.3  
 Summary of Short-Term Pressure Data Analysis  
 (Reproduced from GeothermEx Report, November 1984)

WELL	TEST TYPE	DATE	kh					SKIN	PRODUCER
			MEASURED DEPTH (FT)	LOG-LOG	SEMILOG	DYKSTRA			
SWL-1	Interference	11/80-1/81	7242	15,600	18,400	15,600	--	52-18	
SWL-1	Interference	9/81-11/81	3500	--	--	31,000	--	84-7	
SWL-3	Buildup	3/80	--	--	--	5,500	--	SWL-3	
SWL-3	Interference	11/80-1/81	7000	22,000	25,600	22,400	--	52-18	
SWL-3	Interference	9/81	--	--	--	32,400	--	84-7	
52-18	Drawdown	11/80	7050	12,850	--	3,840	+20	52-18	
52-18	Buildup	1/81	7050	10,800	--	--	+20	52-18	
52-18	Interference	9/81	7050	--	--	32,400	--	84-7	
				152,000 (BU)					
52-18	Interference	11/82	7050	32,000 (DD)	14,337	--	--	65-18	
84-7	Drawdown	9/81	7200	94,200	--	67,400	+10	84-7	
84-7	Buildup	10/81	7200	--	17,000	--	--	84-7	
65-18	Drawdown	4/81	7000	22,600	27,400	--	0	65-18	
65-18	Buildup	4/81	7000	--	--	--	--	65-18	
65-18	Interference	9/81	7000	--	4,000	27,000	--	94-7	
65-18	Interference	11/81	7000	29,200	--	--	--	84-7	
45-5	Buildup	7/81	1500	24,500	--	26,400	--	45-5	

CONFIDENTIAL







1000  
 2000  
 3000  
 4000  
 5000  
 6000  
 7000  
 8000  
 9000  
 10000  
 11000  
 12000

TABLE 7.1  
WELL COMPLETION SUMMARY  
FOR PRODUCTION WELLS  
DIXIE VALLEY GEOTHERMAL FIELD

Well No.	Leg No.	Comp. Date	Well Classification	Operator	KB ft.	Grnd. Elev.	MD ft.	TVD ft.	30" Depth ft.	20" depth ft.	13-3/8" depth ft.	9-5/8" Interval ft.	7" Interval ft.	Perf. Interval ft.	Last Workover	Workover type	Last Flowed	Well Status
SML-2	B	25-Aug-79	Non-commercial	Sunedco	25	3469	8588	8456	65	329	2750	2513-4511	4277-7994	6978-8455	11/27/79	Run Liner-Test	01-Feb-80	P Monitoring
45-5	1	24-Jun-81	Non-commercial	Sunedco	25	3451	8261	8238	65	293	2448	5700	5500-6196	None	None	NA	01-Jul-81	P Monitoring
82-5	4	18-Feb-86	Non-commercial	Oxbow	22	3444	9384	9383	52	312	3836	2800-6795	None	None	None	NA		Shut in-Dry
73-7	2	07-Aug-86	Producer	Oxbow	32	3476	8900	8837	122	565	3648	3457-8480	10 3/4 @3457	None	09/04/86	Repr Csg Clapse	18-Sep-86	Flowing
74-7	1	29-Mar-86	Producer	Oxbow	21	3474	8890	8856	59	466	3488	3256-8437	None	None	None	NA	18-Sep-86	Flowing
76-7	2	24-May-86	Producer	Oxbow	29	3463	7498	7463	80	612	4004	377-7143	None	None	None	NA	18-Sep-86	Flowing
84-7	1	17-Jan-81	Producer	Sunedco	25	3473	8142	8140	65	320	2572	6742	6494-7997	None	05/29/82	Scale Removal	07-Apr-86	P Monitoring
32-18	1	31-Mar-86	Producer	Oxbow	32	3467	7461	7429	72	490	3466	3231-6938	None	None	None	NA	12-Sep-86	P Monitoring
52-18	1	08-May-80	Non-commercial	Sunedco	25	3461	9860	9852	65	324	2706	6929	6735-8543	None	02/19/86	Scale Removal	05-Mar-86	P Monitoring
65-18	1	30-Mar-81	Producer	Sunedco	25	3437	9466	9463	65	293	2676	8383	None	None	03/11/86	Clean/Deepen	18-Sep-86	Flowing
SML-1	1	29-Nov-78	Non-commercial	Sunedco	16	3400	7255	7248	56	334	2686	5630	2342-7095	None	03/25/86	P Test Casing	27-Mar-86	P Monitoring
SML-3	1	26-Nov-79	Non-commercial	Sunedco	25	3468	9126	9061	65	328	2655	7420	None	7070-7350	05/12/82	Scale Removal	03-Jun-80	P Monitoring
62-21	1	31-Oct-80	Non-commercial	Sunedco	25	3446	12500	12436	65	319	2599	2479-7417	7165-9718	9040-9440	None	NA		S.I. Non-Comm.
27-33	1	30-Aug-83	Producer	TGI	22	3446	9110	9106		175	2531	7402	None	NA	03/20/86	Clean/Deepen	04-Apr-86	P Monitoring
45-33	3	31-Dec-83	Producer	TGI	22	3448	10266	9495		210	2471	7526	None	NA	06/24/86	Mill Csg/Deepen	18-Sep-86	Flowing
45-33	2	08-Dec-83	Non-commercial	TGI	22	3448	9573	9315		210	2471	7526	None	None	None	NA		Abandoned
45-33	1	18-Nov-83	Non-commercial	TGI	22	3448	10345	10328		210	2471	7526	None	None	None	NA		Abandoned
76-7	1	17-May-86	Non-commercial	Oxbow	29	3463	7926	7889	80	612	4004	None	None	None	None	NA		Abandoned
73-7	1	09-Jun-86	Untested	Oxbow	32	3476	10088	10797	122	565	4026	3784-8707	None	NA	None	NA	04-Jun-86	Abandoned
82-5	3	19-Dec-85	Non-commercial	Oxbow	22	3444	9942	9643	52	312	3836	2800-7018	None	None	None	NA		Abandoned
82-5	2	29-Nov-85	Non-commercial	Oxbow	22	3444	9936	9768	52	312	3836	2800-7018	None	None	None	NA	25-Nov-85	Abandoned
82-5	1	18-Oct-85	Non-commercial	Oxbow	22	3444	9198	9192	52	312	3836	2800-8268	None	None	None	NA		Abandoned
SML-2	A	16-Jul-79	Non-commercial	Sunedco	25	3469	8901	8899	65	329	2750	2513-7303	7247-7500	None	None	NA	14-Jul-79	Abandoned

TABLE 7.2  
GEOLOGIC AND FLOW DATA SUMMARY  
DIXIE VALLEY PRODUCTION WELLS

Well No.	Leg No.	TD ft.	Top TTS ft.	Top TB ft.	Top TS ft.	Top TSV ft.	Top TTF ft.	Top JS ft.	Top JMS ft.	Top JPG ft.	Top JG ft.	Top TRC ft.	Top KGD ft.	Depth to RFF ft.	Prod. Interval ft.	Prod. Lith.	Max. Flowrate lb/hr	WPPMax. Flowrate psig	Enthalpy BTU/lb	Down Hole Flow Temp. deg.F	Stat. Prod. Int. Temp. deg.F	Stat. Pres. @ -5000' MSL
SML-2	B	8588		6210										8290 8850-8290	6570-8290	Tb	50000	38	397	428	410	3848
45-5	1	8261	4390	5330	6200			6500							6020-6200	Tb	609000	65	322	401	404	
82-5	4	9384													None	NA	NA				NA	
73-7	2	8900	5770	7010			7870	8290							8520-8913	Js	1100000	118			Unknown	
74-7	1	8890	6220	7130	7570	8300		8500							8722-8890	Js	1350000	162	450	478	452	3151
76-7	2	7490	6140	7140											7315-7461	Tb	1700000	148				3219
84-7	1	8142	6160	6700	7460			7720							8055-8142	Js	650000	128	443	477	445	3221
32-18	1	7461	6120	6650											7360-7374	Tb	934000	93	395	427	443	3122
52-18	1	9060	6500	6800	7430			7970		9750					9055-9209	Js	263000	90	417	446	443	3149
65-18	1	9466	5250	5730	7650			8220							9265-9417	Js	819000	107	410	438	430	3156
SML-1	1	7255		6150											7191-7255	Tb	252000	56	402	428	429	3143
SML-3	1	9126	6150	6610	7840			8450				8880			7070-7450	Tb	300000	90	395		453	3153
62-21	1	12500	6300								7130	9730			9040-12500	Jg?				356		
27-33	1	9110	4900	5960	7320			8410	9020						8862-9110	Jms	720000	104	443	477	448	3382
45-33	3	10266	5760	6270	7350				8850				10200		10050-10240	Jms	904000	131	446	477		3190
45-33	2	9573	5760	6270	7350				8730				9470		None	NA	NA				NA	
45-33	1	10345	5760	6270	7350				8950				10170	9870-10170	None	NA	NA				NA	
76-7	1	7926	6140	7140											None	NA	NA				NA	
73-7	1	10888	6020	6725	7965			8375					8635	9325-9525?	9195-10036	Js	250000	28			Unknown	
82-5	3	9942													None	NA	NA				NA	
82-5	2	9936													9336-9731	Jms		25		436	Unknown	
82-5	1	9190		6840	7240								9120	9040-9120?	None	NA	NA				NA	
SML-2	A	8901		6170									7410	7340-7410	7500-8901	Kgd	30000	NA			406	